Spring 2019 – Epigenetics and Systems Biology
Discussion Session (Environmental Epigenetics)
Michael K. Skinner – Biol 476/576
Week 12 (March 28)

Environmental Epigenetics

Primary Papers

1. Manikkam M, et al., (2012) Plos One 7(2):e31901.
2. Ben Maamar, et al., (2018) Environmental Epigenetics 26;4(2):dvy010, pp 1-19.
3. Ben Maamar, et al., (2019) Developmental Biology 445: 280-293.

Discussion

Student 32 – Ref #1 above

- What are the transgenerational phenotypes?
- How can the epigenetic biomarkers of exposure be used?
- What does the transgenerational actions of multiple environmental exposures suggest?

Student 33 – Ref #2 above

- What is the experimental design?
- What epigenetic technologies and alterations were investigated?
- What is the primary conclusion of the study?

Student 34 – Ref #3 above

- What is the experimental design?
- What were the developmental origins of the sperm epimutations?
- What conclusions on the development of the sperm epimutations are made?

OPEN ACCESS Freely available online

PLoS one

Transgenerational Actions of Environmental Compounds on Reproductive Disease and Identification of Epigenetic Biomarkers of Ancestral Exposures

Mohan Manikkam[◔], **Carlos Guerrero-Bosagna**[◔], **Rebecca Tracey, Md. M. Haque, Michael K. Skinner***

Center for Reproductive Biology, School of Biological Sciences, Washington State University, Pullman, Washington, United States of America

Abstract

Environmental factors during fetal development can induce a permanent epigenetic change in the germ line (sperm) that then transmits epigenetic transgenerational inheritance of adult-onset disease in the absence of any subsequent exposure. The epigenetic transgenerational actions of various environmental compounds and relevant mixtures were investigated with the use of a pesticide mixture (permethrin and insect repellant DEET), a plastic mixture (bisphenol A and phthalates), dioxin (TCDD) and a hydrocarbon mixture (jet fuel, JP8). After transient exposure of F0 gestating female rats during the period of embryonic gonadal sex determination, the subsequent F1–F3 generations were obtained in the absence of any environmental exposure. The effects on the F1, F2 and F3 generations pubertal onset and gonadal function were assessed. The plastics, dioxin and jet fuel were found to promote early-onset female puberty transgenerationally (F3 generation). Spermatogenic cell apoptosis was affected transgenerationally. Ovarian primordial follicle pool size was significantly decreased with all treatments transgenerationally. Differential DNA methylation of the F3 generation sperm promoter epigenome was examined. Differential DNA methylation regions (DMR) were identified in the sperm of all exposure lineage males and found to be consistent within a specific exposure lineage, but different between the exposures. Several genomic features of the DMR, such as low density CpG content, were identified. Exposure-specific epigenetic biomarkers were identified that may allow for the assessment of ancestral environmental exposures associated with adult onset disease.

Citation: Manikkam M, Guerrero-Bosagna C, Tracey R, Haque MM, Skinner MK (2012) Transgenerational Actions of Environmental Compounds on Reproductive Disease and Identification of Epigenetic Biomarkers of Ancestral Exposures. PLoS ONE 7(2): e31901. doi:10.1371/journal.pone.0031901

Editor: Toshi Shioda, Massachusetts General Hospital, United States of America

Received October 31, 2011; **Accepted** January 15, 2012; **Published** February 28, 2012

Funding: Financial support of the USA Department of Defense and National Institutes of Health (NIEHS ES012974). The funders had no role in the study design, data collection and analysis, decision to publish, or preparation of the manuscript.

Competing Interests: The authors have declared that no competing interests exist.

* E-mail: skinner@wsu.edu

◔ These authors contributed equally to this work.

Introduction

Epigenetic transgenerational inheritance provides an alternative molecular mechanism for germ line transmission of environmentally induced phenotypic change compared to that of classic genetics [1,2]. Most factors do not have the ability to modify DNA sequence, but environmental factors such as nutrition or various toxicants can influence epigenetic processes to mediate alterations in genome activity [1,3]. Environmental epigenetics focuses on how a cell or organism responds to environmental factors or insults to create altered phenotypes or disease. Previous observations have demonstrated that the exposure of a gestating female to the environmental fungicide compound vinclozolin [4] during fetal gonadal sex determination promotes a reprogramming of the male germ line epigenome [2]. The altered DNA methylation profile in the sperm becomes permanently reprogrammed to create an abnormal epigenome in the embryo and all cells and tissues derived from that embryo [5]. Later in life the animals develop adult onset disease states such as mammary tumors, prostate disease, kidney disease, testis abnormalities, and immune abnormalities at high (20–50%) frequencies [6]. Due to the imprinted-like nature of the altered epigenetic DNA methylation sites, the germ line (sperm) transmit this epigenome and adult onset disease phenotype to subsequent generations, which is termed epigenetic transgenerational inheritance [1]. The basic mechanism involves the ability of an environmental factor (compound) to alter the germ line DNA methylation program to promote imprinted-like sites that then transmit an altered epigenome that subsequently promotes adult onset disease phenotypes transgenerationally [1,2]. The vast majority of environmental exposures act on somatic cells at critical windows of development to influence phenotype and/or disease in the individual exposed, but this will not become transgenerational [1,3]. In the event the critical window for the primordial germ cell is affected by environmental exposure, the altered germ line has the ability to promote a transgenerational phenotype for subsequent generations [1]. More recently a number of reports have documented the ability of nutritional factors [7] and environmental toxicants such as bisphenol A (BPA), dioxin, vinclozolin and methoxychlor to promote epigenetic transgenerational inheritance [2,8,9,10].

The current study was designed to investigate the potential epigenetic transgenerational actions of a variety of different toxicants or mixtures of relevant compounds. This was initiated to determine the compound specificity to promote epigenetic transgenerational inheritance and to determine if the epigenetic alterations may provide biomarkers for exposure. The environ-

mental compounds (toxicants) selected have been shown to have biological and health effects [11], and were identified as common suspected exposures of military personnel. In addition, the cellular signal transduction process affected for each exposure is unique. The first compound mixture is termed "plastics" and includes bisphenol A (BPA) and the phthalates DEHP (bis(2-ethylhexyl)phthalate) and DBP (dibutyl phthalate) which are the combined exposures from most plastics that have been shown to promote *in vitro* and *in vivo* toxicologic effects [12]. Epigenetic effects of these compounds after neonatal exposures promotes adult onset disease [13,14]. The second mixture involves the most commonly used human pesticide (permethrin) and insect repellent N,N-Diethyl-meta-toluamide (DEET), and is termed "pesticide" for this study, and has been shown to have some toxicologic effects in either *in vitro* or *in vivo* studies [15,16,17,18,19,20]. The third compound used is dioxin (2,3,7,8-tetrachlorodibenzo-p-dioxin, TCDD), which has been shown to have significant *in vitro* and *in vivo* effects in the promotion of cellular abnormalities and adult onset disease states [21]. Epigenetic parameters have been shown to be influenced by dioxin actions [22]. The fourth exposure is jet fuel (jet propellant 8, JP8) which is a "hydrocarbon" mixture that is a significant environmental exposure due to its use for dust control on road surfaces [23]. Toxicological effects have been shown in *in vitro* and *in vivo* studies with JP8 exposures [24]. The four exposures used are common environmental toxicants which have been generally shown to promote abnormal or disease phenotypes. The objective of this study was to determine the potential ability for these different compounds and mixtures to promote epigenetic transgenerational inheritance of disease and map the potential alterations in the sperm epigenome.

The potential transgenerational diseases investigated focused on pubertal onset parameters and gonadal functions associated with infertility. The incidence of altered pubertal onset has increased over the past several decades in human populations [25,26,27]. Pubertal onset can occur several years early in some women [28]. This early onset of female puberty has been shown to affect brain development, endocrine organ systems and growth, that all potentially increase disease susceptibility later in life [29]. Although environmental exposures to endocrine disrupting compounds have been suggested as a causal factor [28], the basic mechanisms involved are unknown. The other disease parameters examined were associated with testis and ovary functions that influence fertility. In regards to testis function, sperm numbers and motility were examined, as well as spermatogenic cell apoptosis. In the human male population there has been a gradual decline in sperm number in most populations [30]. Estimates of male infertility appears to be over 10% in many human male populations [31]. In regards to ovarian function, the ovarian reserve or primordial follicle pool was assessed. An increasing percentage of the female population is developing premature ovarian failure associated with a loss of the follicle pool which promotes female infertility and affects approximately 15% of many female populations [32]. The causal factors for these gonadal disease phenotypes and increase in infertility are suggested to be due in part to environmental exposures to endocrine disruptor toxicants [33], but the basic molecular mechanisms involved are not known. The potential that the exposures used in the current study may promote the epigenetic transgenerational inheritance of these disease states is investigated.

Results

The current study was designed to investigate the potential ability of various environmental compounds and mixtures to promote epigenetic transgenerational disease with a focus on pubertal and gonadal abnormalities. The alterations in the sperm epigenome were investigated to determine the similarities and differences between the different exposures on differential DNA methylation. The experimental design used pharmacologic doses, Table S1A, based on approximately 1% of the lethal oral dose 50% (LD50) for most of the compounds that previously have been shown *in vivo* to not cause direct toxicological effects. Gestating female outbred Harlan Sprague Dawley rats were given intraperitoneal (IP) injections daily between embryonic days 8–14 of fetal development correlating with gonadal sex determination. No consistent effects were observed on litter size, sex ratios or weaning weights, Figures S1 and S2. The number of litters and male and female animals obtained for each generation is presented in Table S1B and S1C. The F0 generation gestating female was the only animal injected IP. The F1 generation animals at 90 days of age were mated to the same lineage to generate the F2 generation and the F2 generation were mated to generate the F3 generation progeny as previously described [2]. No sibling or cousin breedings were used to avoid any inbreeding artifacts. No major overt toxicity was observed in F1, F2 or F3 generations, Figure S1 and S2. The only treatment that promotes some toxicity in the F1 generation was the high dose plastics, Table S1A, so a lower dose at 50% that shown in Table S1A was also used and termed "Low Dose Plastic" that had no toxicological effects, Figure S1. Anogenital distance was measured as an indicator of exposure to androgenic compounds that promote masculinization during the perinatal period [34,35]. Analysis of anogenital index (AGI) demonstrated some effects of the treatments on the F2 and F3 generation animals, but no effects at the F1 generation animals, Figure S3. These actions on the AGI in the F2 generation are possibly due to the direct exposure of fetal germ cells to the endocrine disruptor activities of several of the exposure compounds (e.g. BPA, DEHP, DBP) [12,13,14], while the increased AGI in the F3 generation appears to be transgenerational. Therefore, classic endocrine disruptor actions [36] are likely not involved in the F2 and F3 generation, but only in the F1 generation. In considering the actions of environmental exposure the direct versus indirect (e.g. epigenetic) actions are critical. The exposure of the F0 generation gestating female directly affects the F0 generation female, the F1 generation embryo and the germ line inside the F1 embryo that will be generating the F2 generation animal [1]. Therefore, phenotypes in the F0, F1 and F2 generations may be due to direct exposures and are not transgenerational effects or phenotypes observed by definition. A transgenerational phenotype or phenomenon requires the lack of direct exposure to promote a generational effect [1,3]. The actions on F0, F1 and F2 are due to a direct multi-generational exposure and only the F3 generation phenotype can be considered a transgenerational effect. Since the mechanisms promoting the F1 or F3 generation effects differ, the phenotypes can be distinct between the generations.

Puberty is a developmental process involving the hypothalamic – pituitary – gonadal axis which initiates during fetal development and matures in adolescence [25]. The onset of puberty was investigated with the different exposure lineages of control (DMSO vehicle), pesticide, low and high dose plastics, dioxin, or hydrocarbons in the F1–F3 generation rats. The analysis was initiated for females at postnatal day 30 and males at postnatal day 35 until puberty (vaginal opening or balano-preputial separation) [37]. In the F1 generation plastics promoted delayed female pubertal onset, while in the F2 generation plastics, dioxin and jet fuel promoted early onset of puberty for females, with plastics and dioxin promoting early onset of puberty in males, Figure S4. In the

transgenerational F3 generation it was demonstrated that plastics, low dose plastics, dioxin and jet fuel promote early onset of puberty in females, while having no effect on males, Figure 1A, 1B. Therefore, several of the exposures were found to promote early onset of puberty in females transgenerationally.

Gonadal function for both testis and ovary were investigated in the F3 generation at postnatal 120 days of age. Previously vinclozolin was shown to promote a transgenerational phenotype of spermatogenic cell apoptosis [2], so potential germ cell apoptosis in the testis was investigated. The jet fuel exposure was found to transgenerationally increase spermatogenetic cell apoptosis in the F3 generation male testis, Figure 1C. Epididymal sperm concentration and motility for the F3 generation were also investigated and did not provide consistent alterations transgenerationally, as previously seen with vinclozolin exposure. The F3 generation ovaries were examined for total follicle number and the individual types of primordial follicles, primary follicles and developing follicles were categorized, Figure 1D and 1E. All the exposures were found to promote a transgenerational effect on the F3 generation ovary with a significant reduction in total follicle number, Figure 1D, and the follicle class primarily affected was the primordial follicle, Figure 1E. Therefore, all the exposures promoted the transgenerational phenotype of a reduction in the primordial follicle pool size. The large developing antral follicles were counted to determine potential effects on later stage follicle development and no differences were observed between the exposures when compared to control, Figure 1F. The transgenerational action of the various exposures on the ovary was a reduction in the primordial follicle pool size. This may promote premature ovarian failure as the animals age. The testis and ovary are hormone regulated and both produce endocrine steroids. Hormone levels were analyzed to determine how the endocrine system was responding transgenerationally. The F3 generation males had a reduction in testosterone levels in the plastics, dioxin and jet fuel exposure lineages, Figure S5A, while the females had no change in progesterone levels, Figure S5B. No change in luteinizing (LH) hormone levels was detected in either male or female F3 generation animals, Figure S5C & D. Therefore, the endocrine system was altered transgenerationally in the males.

The mechanism involved in these transgenerational phenotypes is the reprogramming of the germ line (sperm) during male sex determination [1,3]. This altered sperm epigenome appears to be permanently reprogrammed and escapes the DNA methylation programming at fertilization to allow transgenerational transmission of the altered sperm epigenome, that then promotes all tissues developed from that sperm to have altered cell and tissue transcriptomes that can promote transgenerational disease [1]. Previously, vinclozolin was shown to promote a transgenerational (F3 generation) alteration in DNA methylation [2,5] and a transgenerational transcriptome alteration in tissues like the testis [38]. The F3 generation rat sperm from the control and all exposure groups were collected for genome wide promoter DNA methylation analysis [5]. The procedure involved the use of an antibody to methylcytosine to immunoprecipitate methylated DNA (MeDIP) and then a competitive hybridization tiling array (Chip) for a MeDIP-Chip analysis [5]. Differentially methylated sites were identified for all the different exposure lineages in the F3 generation sperm when compared with vehicle control F3 generation sperm. The complete lists of differential methylation regions (DMR) for each exposure in the F3 generation sperm are provided in Table S2(A–D). The overlap of the DMR sets for each exposure is shown in a Venn diagram in Figure 2A. The number of DMR for hydrocarbons (jet fuel) was 33, dioxin 50, plastics (BPA, DEHP, DBP) 197 and pesticide (permethrin and DEET) 363 with a statistically significant difference ($p<10^{-5}$). Interestingly, the majority of each DMR set was specific to an exposure group and not common with the other exposure DMRs. The only exception was an overlap between plastics and pesticide of 113 DMRs, Figure 2A. Therefore, each exposure had a unique signature of epigenetic alterations in the F3 generation sperm. The chromosomal localizations of these sites are shown in Figure 2B. The DMRs are seen on all autosomes and the X chromosome. Clustering analysis of the DMRs when over represented in specific chromosomal locations identified 35 different clusters (2–5 megabase each) of DMR between the exposures that with z-score analysis have a statistically significant difference ($p<0.05$), Figure 2B. These DMR clusters may represent ''epigenetic control regions'' where different exposure DMRs may commonly regulate genome activity. The functional significance of these DMR clusters remains to be elucidated and are identified for individual DMR in Table S2. In considering the combined DMR and associated gene promoters for all exposures, the potential cellular signaling processes affected demonstrated similar pathways are predominant, as shown in Table S3. A gene network analysis for direct connections within the total gene set associated with the DMR is shown in Figure 3 and demonstrates extracellular, membrane, cytoplasmic and nuclear associated genes are all associated with the DMR identified. Common cellular signaling pathways and processes appear to be involved from the gene network identified. Therefore, common cellular pathways and gene networks may be influenced by the different exposures and transgenerational sperm epigenomes. Although exposure specific transgenerational differential DNA methylation regions (DMR) are predominant, the common cellular processes and gene networks effected may explain the similar disease phenotypes observed.

The identification of epigenetic alterations in specific regions of the F3 generation sperm support a role for epigenetic transgenerational inheritance of the disease phenotypes observed. Several of the top exposure specific DMRs for each exposure with the highest statistical significance were selected for confirmation with quantitative PCR of the MeDIP samples. A list of the confirmed exposure specific signatures are presented in Figure 4. In addition, several of the top overlapped (common) DMR were also selected and shown. The MeDIP qPCR analysis demonstrated both increases and decreases for the exposure specific and common DMR, Figure 4B. These exposure specific DMR are considered potential epigenetic biomarkers for exposure and the transmission of transgenerational phenotypes. Further analysis of the epigenetic sites identified considered two genomic features associated with the DMRs. The first one was a DNA sequence motif termed ''Environmentally Induced DNA Methylation Region 1'' (EDM1) that was previously identified and shown to be associated with a high percentage of the vinclozolin induced sperm DMRs [5]. This motif may not be at the specific altered DNA methylation site, but is within the 400–500 bp region. A DNA sequence motif such as EDM1 may promote a region of sensitivity for these DMR's to be programmed transgenerationally. The potential presence of this EDM1 motif in the epigenetic sites (DMR) identified in the current study for all the exposures was determined. An evaluation of the presence of EDM1 using the MCAST online software revealed a statistically significant higher EDM1 presence in promoter regions of the jet fuel and dioxin exposure groups (74.19% and 57.63%, respectively) compared to a computer generated random set of 144 promoters (20.83%). The presence of EDM1 in the promoter regions of the plastics (20.47%) and pesticides (7.36%) was similar or below its presence in the random set of promoters. This suggests that the molecular

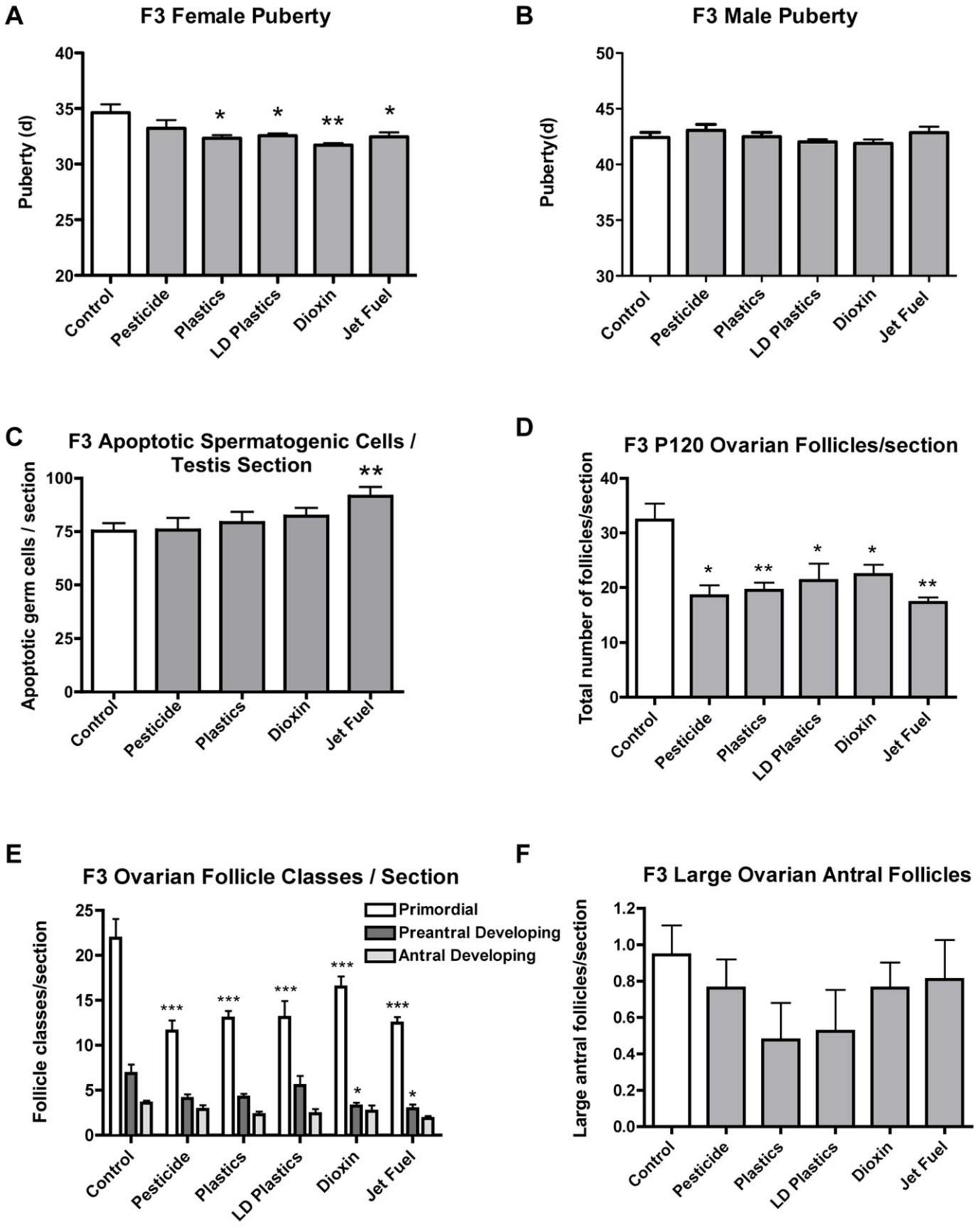

Figure 1. Ancestral (F0 generation female) exposures to environmental compounds promote transgenerational diseases, altering onset of puberty, testicular spermatogenic function and ovarian follicular development in F3 generation rat progeny. (A) Onset of female puberty was advanced from exposures to plastics, dioxin and jet fuel. (B) Onset of male puberty was unaffected from these exposures. (C) Increased apoptotic spermatogenic cells per testis section were observed from jet fuel exposure. (D) Total numbers of ovarian follicles per section

were reduced in individuals from all exposures, (E) Total numbers of primordial follicles per section declined. (F) Total numbers of large ovarian antral follicles were unaffected. The animal n value is presented in Table S1C (*p<0.05; **p<0.01, ***p<0.001).
doi:10.1371/journal.pone.0031901.g001

mechanisms involved in the targeting of these regions to produce a transgenerational change in DNA methylation may differ among the exposure groups. Another genomic feature investigated was the CpG density within the DMR identified. The frequency of CpG number per 100 bp for the DMR demonstrates the DMR identified for all exposures have an average CpG content of 4.9 CpG/100 bp with none above 15 CpG/100 bp, Figure 5. A small CpG cluster in a CpG desert appears to be a primary feature of the transgenerational DMR identified, and not shores or islands of CpG. Therefore, specific genomic features such as low CpG density, isolated CpG clusters, and the presence of a unique DNA sequence motif may be involved in facilitating the programming of these epigenetic sites (DMR) in the male germ line.

Discussion

The current study used pharmacologic doses of all the compounds and mixtures based on approximately 1% of the oral LD50 dose for most exposures (compounds), Table S1A. The objective was to determine if these exposures have the capacity to promote epigenetic transgenerational inheritance of a disease phenotype, and not to do risk assessment of the exposures. Now that the current study has established the transgenerational actions of these compounds, risk assessment toxicological studies involving dose curves of relevant environmental doses are needed. The phenotypes observed may vary with the dose as shown with the plastics in the current study. Since the F1 generation involves direct exposure and the F3 generation is germ line mediated transgenerationally, the phenotypes can differ between the generations. In addition to considering the mode of administration and dose, the critical window of exposure to promote the epigenetic transgenerational phenotype is gonadal sex determination, which for the human is 6–18 weeks of gestation. The gestating women in the first half of pregnancy would be the population most sensitive to exposures of environmentally induced epigenetic transgenerational inheritance.

The transgenerational disease phenotype investigated focused on pubertal onset and gonadal function. It was previously observed with vinclozolin induced transgenerational adult onset rat disease [2], the majority of disease developed between 6–12 months of age [6]. Therefore, additional adult onset diseases are anticipated as the animals age, but remain to be investigated. In regards to pubertal onset the plastics, low dose plastics, dioxin and hydrocarbon (jet fuel) exposures promoted an early (precocious) pubertal onset, Figure 1, with no transgenerational effects on male pubertal onset, Figure S6. In the majority of developed countries early pubertal onset in girls has increased significantly in the past several decades [25,28]. This precocious puberty can promote behavioral, mental and endocrine physiological effects in the female and increase the incidence of adult onset disease [28]. Previous studies have suggested environmental exposures of estrogenic endocrine disruptors may be in part the causal factor for this pubertal onset condition. The current study extends this hypothesis to not only consider the direct exposures of the female, but ancestral exposures of the previous generations. The potential that early pubertal onset may in part involve epigenetic transgenerational inheritance mechanisms now needs to be considered.

In considering gonadal function and fertility both the testis and ovary were investigated. The testis was found to have an increased spermatogenic cell apoptosis in the jet fuel hydrocarbon F3 lineage males, Figure 1. Previous observations with vinclozolin also showed a transgenerational spermatogenic cell apoptosis phenotype [2]. In many regions of the world human sperm numbers have declined [30] and male infertility has increased [31]. The potential that environmentally induced epigenetic transgenerational inheritance may be a factor in these disease conditions needs to be considered. In regards to ovarian function all the environmental exposures were found to promote a decline in total follicle numbers and specifically the primordial follicle pool size, Figure 1. The primordial follicle pool size is the ovarian reserve for oocyte (egg) production throughout reproductive life [39]. The primordial follicle pool develops early in fetal (human) or early postnatal (rodent) life and then can not increase, but declines with age. Human females enter menopause when the primordial follicle pool is exhausted. A premature loss of follicles promotes infertility and is termed premature ovarian failure (POF), which is associated in part with the dramatic increase in female infertility in many parts of the world [32]. Previously it was hypothesized that POF was primarily of genetic origin, but the current study suggests environmental exposures and epigenetic transgenerational inheritance may also be a significant factor in the disease etiology to increase female infertility and premature onset of menopause. The environmental induction of the pubertal, testis and ovarian transgenerational disease phenotypes suggests that environmental epigenetics and epigenetic transgenerational inheritance will be molecular factors to consider in these and other disease etiologies.

The environmental compounds and mixtures used in the current study are all reported to be major exposures for the general population and military personnel. The ability of epigenetics to be involved in the long term and transgenerational actions of these exposures needs to be further investigated. The current study documents the distinct actions of each exposure to promote a unique sperm epigenome alteration, Figure 2. Interestingly, these environmentally induced distinct epigenetic changes in differential DNA methylation regions (DMR) provide epigenetic biomarkers for ancestral environmental exposures. Each exposure had a distinct epigenetic signature that can be used as a biomarker. Although further research on individual animal variation, alterations in DMR in different cell types, and developmental effects on DMR are needed, the current study provides the proof of concept that epigenetic biomarkers for environmental exposures exist.

In addition to the identification of these ancestral epigenetic biomarkers in sperm, genomic features were identified that provide insight into why these sites may become permanently reprogrammed. A DNA sequence motif previously identified and termed "Environmentally Induced DNA Methylation Region 1 (EDM1)" [5] was found to be associated with a high percentage of the promoter regions of the hydrocarbon and dioxin exposure groups. Similar observations were previously made in examining the vinclozolin induced DMR in transgenerational sperm [5]. Interestingly, the plastics and pesticide exposure groups DMR did not have the presence of the EDM1 motif above background random promoter levels. Therefore, distinct molecular mechanisms may be involved in promoting the sensitivity of transgenerationally programmed DMR. This may include an alternate DNA sequence motif to be elucidated, or a more stochastic mechanism to be considered. The other genomic feature identified involved

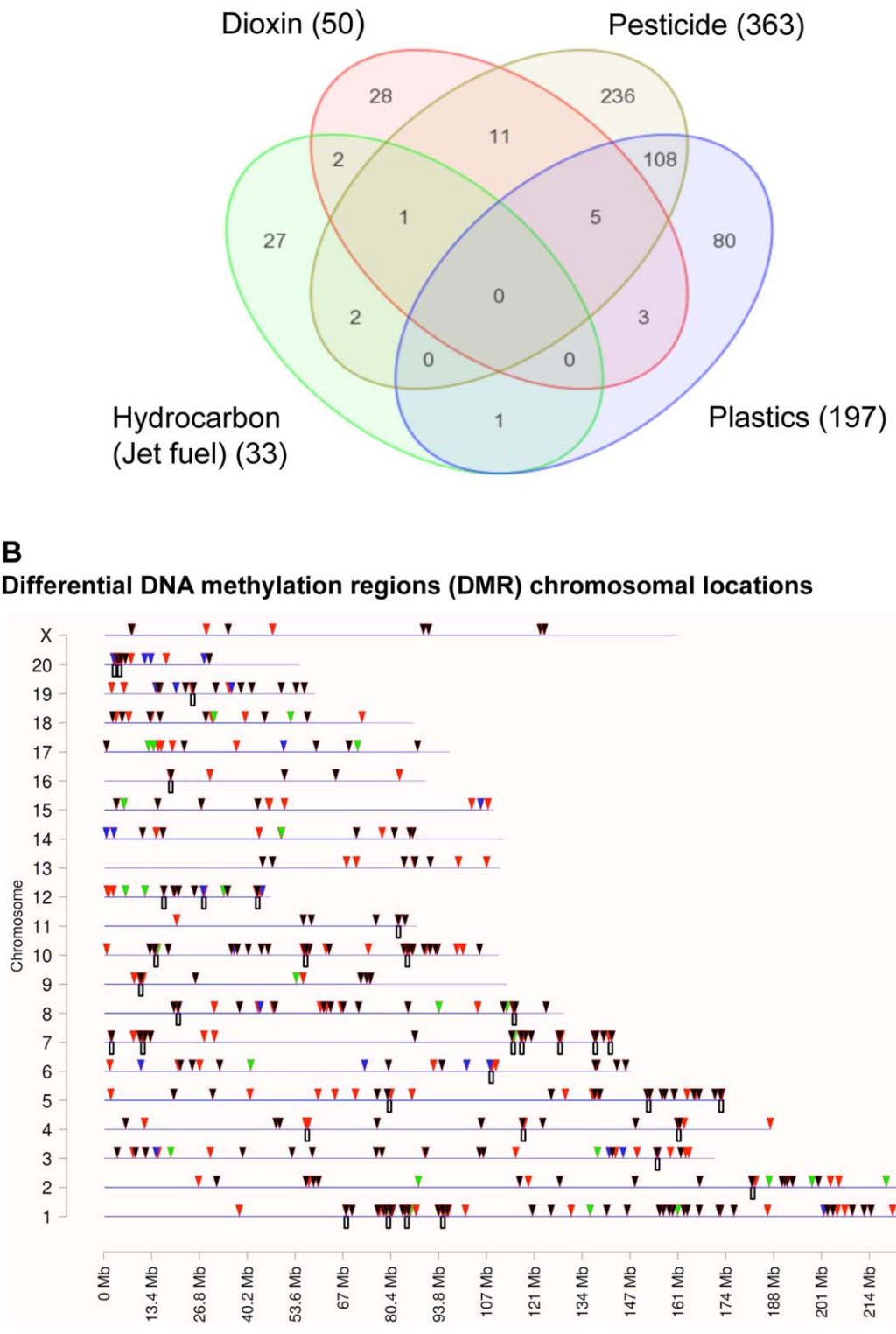

Figure 2. The transgenerational DMR associated with each exposure group identified. (A) Venn diagram of exposure DMR lists of F3 generation rat genes with differential DNA methylation due to *in vivo* exposure of F0-generation gestating female with Dioxin, Pesticide, Plastics or Hydrocarbons/Jet fuel. (B) Chromosomal location of each exposure group DMR are indicated with red arrow (plastics), green arrow (dioxin), blue arrow (hydrocarbon) and black arrow (pesticide). The chromosome number and size are indicated. The box below the line indicates DMR cluster in 2–5 megabase regions with statistical significance ($p<0.05$).
doi:10.1371/journal.pone.0031901.g002

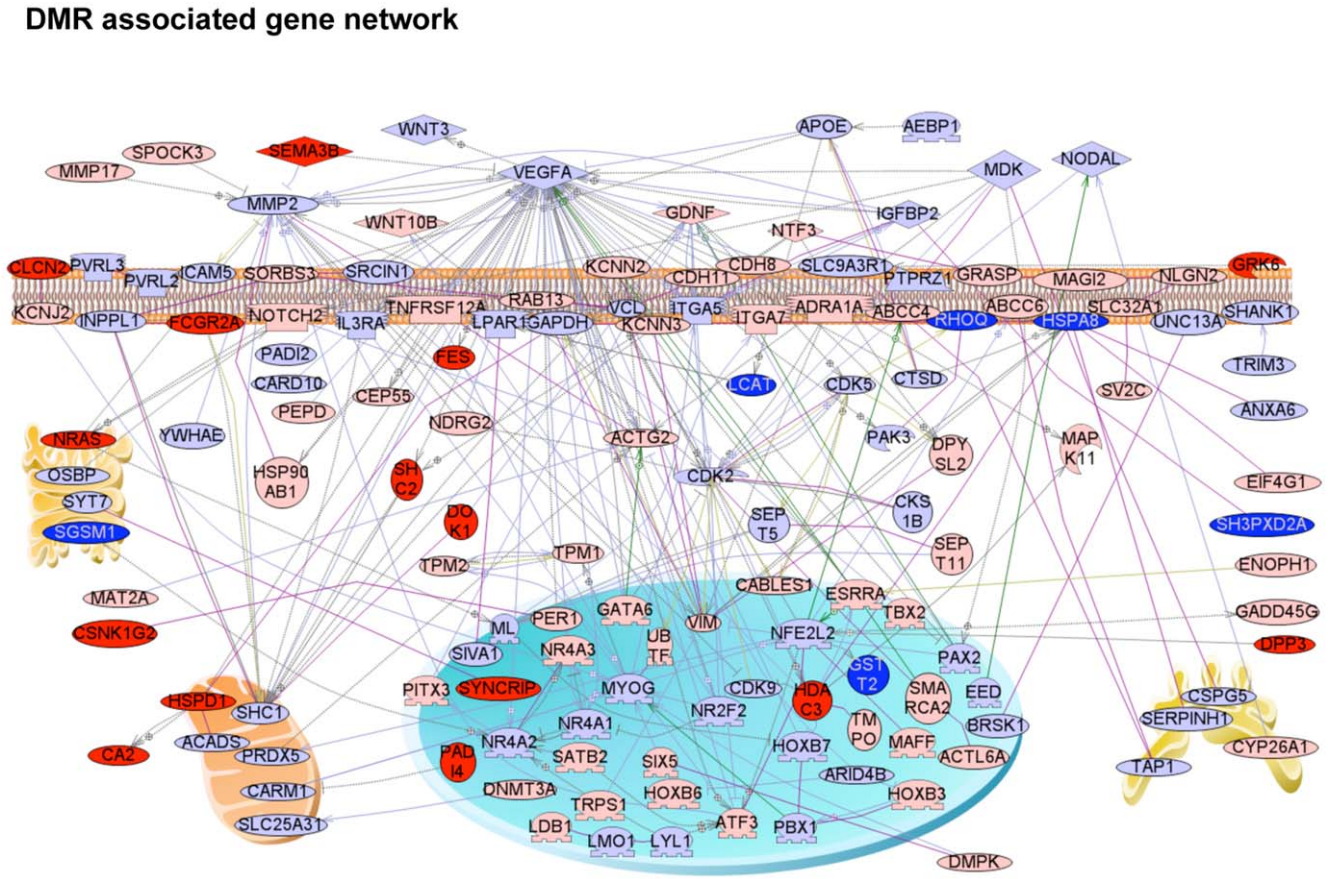

Figure 3. Direct connection gene sub-network for combined genes with transgenerational DMR associated exposures for Dioxin (red shapes), Pesticide (light blue shapes), Plastics (pink shapes) or Hydrocarbons/Jet fuel (dark blue shapes) indicated. Only 140 directly connected genes out of 499 unique genes associated with the combined lists are shown. Node shapes code: oval and circle – protein; diamond – ligand; circle/oval on tripod platform – transcription factor; ice cream cone – receptor; crescent – kinase or protein kinase; irregular polygon – phosphatase. Arrows with plus sign show positive regulation/activation, arrows with minus sign – negative regulation/inhibition; grey arrows represent regulation, lilac – expression, purple – binding, green – promoter binding, and yellow/olive – protein modification.
doi:10.1371/journal.pone.0031901.g003

the CpG content or density associated with all the DMRs identified for all exposures. The previous dogma is that epigenetic modifications in CpG islands or shores with highest CpG density are critical. The DMRs identified had what is considered a low range CpG density [40] with an average of 8 CpG/100 bp content and no DMR with a CpG density greater than 15 CpG/100 bp, Figure 5. Therefore, the DMR appear to have small clusters of CpG in a CpG desert, as previously described [41]. Evolutionarily CpG deserts develop due to the high mutation rate of CpG sites. The maintenance of small CpG clusters in these deserts may suggest a conserved critical epigenetic regulatory site. These genomic features are speculated to have a role in how the DMR become permanently programmed and promote epigenetic transgenerational inheritance. The current study focuses on a genome wide analysis of promoters. Further investigation of genome wide effects and the role of these genomic features is now needed to provide further insights into the molecular elements of epigenetic transgenerational inheritance.

The transmission of epigenetic information between generations in the absence of any direct environmental exposures is defined as epigenetic transgenerational inheritance [1,2,3]. Therefore, in the case of exposure of a gestating female, only after the F3 generation can epigenetic transgenerational inheritance be considered [1]. The previous observations that vinclozolin and methyoxychlor induced epigenetic transgenerational inheritance [2] developed the question of compound specificity. The current study indicates different environmental compounds and mixtures with very different effects on signal transduction processes involved can all promote epigenetic transgenerational phenotypes. Therefore, the specific compound or signaling event does not appear critical, but instead any agent that can modify the normal development and differentiation of the primordial germ cell during gonadal sex determination [1,3] can impact epigenetic programming and promote transgenerational inheritance. Although the majority of exposures will influence somatic cells and disease or phenotypes in the individual exposed, those actions that promote epigenetic transgenerational inheritance may have additional significant biological impacts. This includes providing a molecular mechanism for environmental toxicology, disease etiology, early life basis of adult onset disease [1,3] and evolutionary biology [42]. The availability of ancestral environmental epigenetic biomarkers is anticipated to significantly facilitate the research in these areas of science.

Materials and Methods

Animal studies

All experimental protocols for the procedures with rats were pre-approved by the Washington State University Animal Care

A

Gene Symbol	Gene name	Gene ID	Region changed	MeDIP-qPCR exposure/control ratio			
				Plastics	Dioxin	Pesticide	Jet Fuel
Carm1	Coactivator-associated arginine methyltransferase 1	363026	chr8:20650587-20651612			3.491126	
Dmpk or Six5	Dystrophia myotonica-protein kinase or SIX homeobox 5	308405 or 308406	chr1:78450272-78451687	3.710558		2.519094	
Fgf15	Fibroblast growth factor 15	170582	chr1:205323456-205324556	25.69776			
Flg	Filaggrin	24641	chr2:186309317-186310200		3.096977	4.735184	
Hoxb6	Homeo box B6	497986	chr10:85032294-85033194	2.108708			
Hspd1	Heat shock protein 1 (chaperonin)	63868	chr9:53896237-53896837		0.695904		
Irx2	Iroquois homeobox 2	306657	chr17:746309-746989			2.053513	
Nras	Neuroblastoma ras oncogene	24605	chr2:198292829-198293429		7.986455	11.12386	
Ntng1	Netrin G1	295382	chr2:205805922-205806522	0.148596			
Prrt1	Proline-rich transmembrane protein 1	406167	chr20:4220107-4221198			3.885713	
Rhoq	Ras homolog gene family, member Q	85428	chr6:10413845-10414445				3.141808
Satb2	SATB homeobox 2	501145	chr9:55824749-55825838			0.132503	
Sema3b	Sema domain, immunoglobulin domain (Ig), short basic domain, secreted, (semaphorin) 3B	363142	chr8:112852022-112852622		2.477172		2.480198
Shc2	SHC (Src homology 2 domain containing) transforming protein 2	314612	chr7:11584014-11584614		2.080849		
Tbx2	T-box 2	303398	chr10:74084425-74085225	7.887618			
Vom2r69	Vomeronasal 2 receptor, 69	289433	chr14:740492-741794				0.517274

B

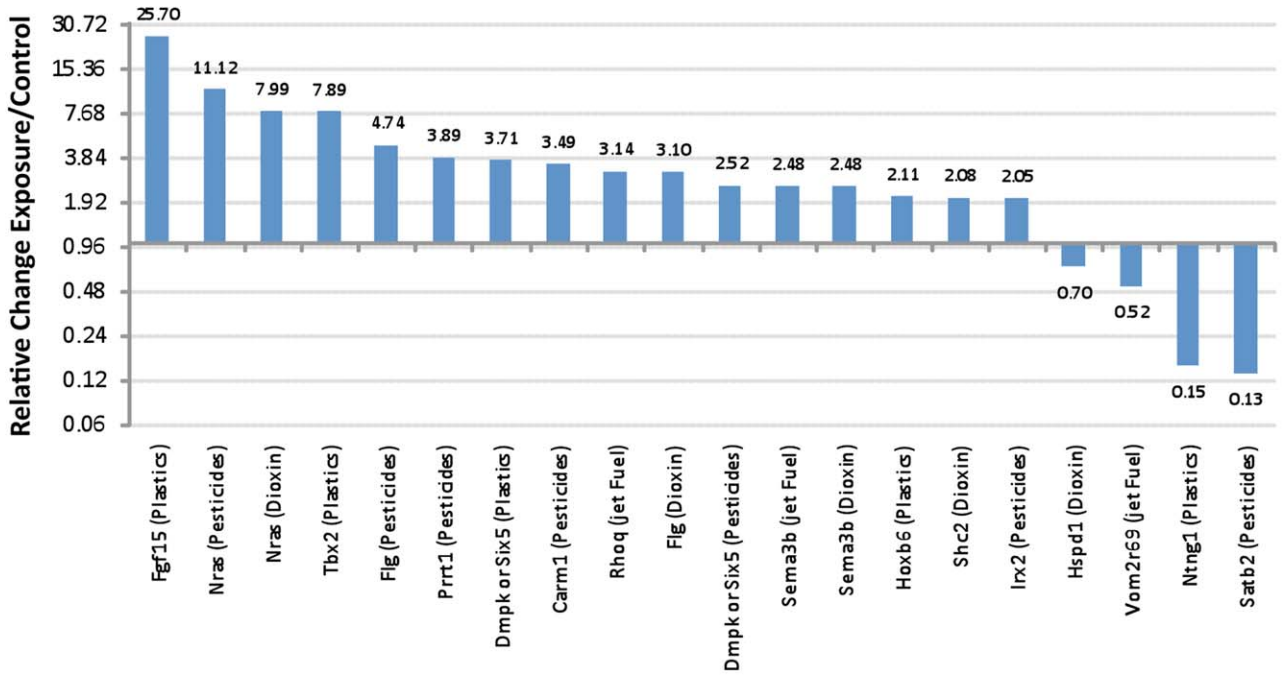

Figure 4. The MeDIP-qPCR analysis of (A) selected DMR for each exposure was used to confirm MeDIP-Chip analysis and (B) relative change (exposure/control) ratio presented for each DMR. All changes shown are statistically significant between control and exposure ($p<0.05$).
doi:10.1371/journal.pone.0031901.g004

and Use Committee (IACUC approval # 02568-026). The University Department of Environmental Health and Safety approved all the protocols for the use of hazardous chemicals in this experiment. Sprague Dawley SD female and male rats of an outbred strain (Harlan) at about 70 and 100 days of age were maintained in ventilated (up to 50 air exchanges/hour) isolator

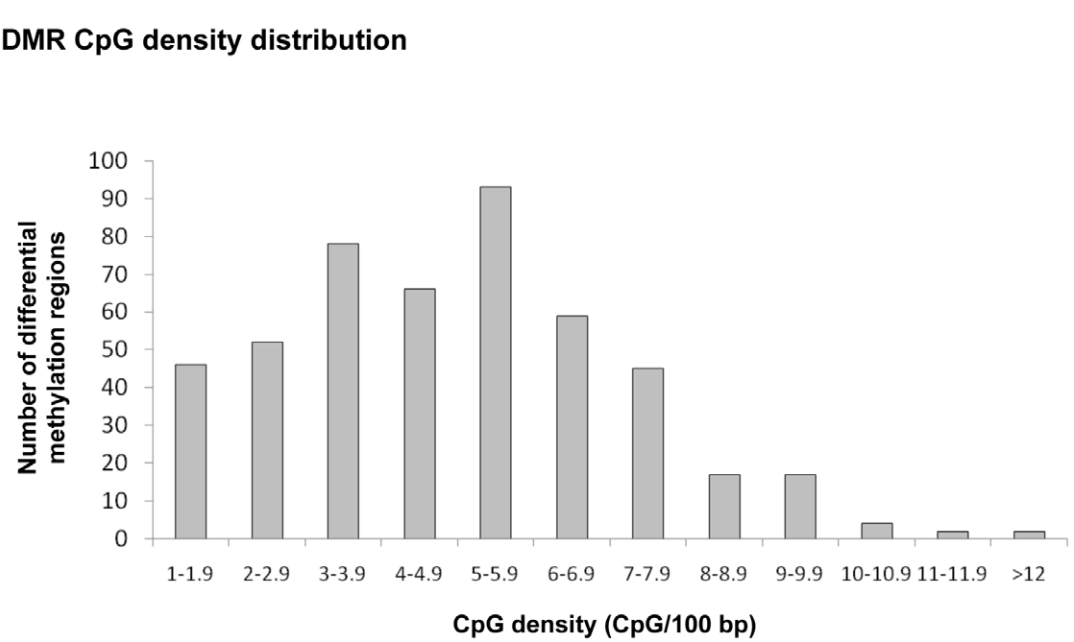

Figure 5. Differential DNA methylated region (DMR) CPG density distribution. The CpG density (CpG/100 bp) associated with all exposure DMR are presented with number of DMR on y axis and density (CpG per 100 bp) on x axis.
doi:10.1371/journal.pone.0031901.g005

cages (cages with dimensions of 10 ¾″ W×19 ¼″ D×10 ¾″ H, 143 square inch floor space, fitted in Micro-vent 36-cage rat racks; Allentown Inc., Allentown, NJ) containing Aspen Sani chips (pinewood shavings from Harlan) as bedding, and a 14 h light: 10 h dark regimen, at a temperature of 70 F and humidity of 25% to 35%. The mean light intensity in the animal rooms ranged from 22 to 26 ft-candles. Rats were fed ad lib with standard rat diet (8640 Teklad 22/5 Rodent Diet; Harlan) and ad lib tap water for drinking. During the procedures, rats were held in an animal transfer station (AniGard 6VF, The Baker Company, Sanford, ME) that provided an air velocity of about 0.5 inch.

At proestrus as determined by daily vaginal smears, the female rats, (90 days) were pair-mated with male rats (120 days). On the next day, the females were separated and their vaginal smears were examined microscopically and if they were sperm-positive (day 0) the rats were tentatively considered pregnant and then weighed with a digital animal weighing balance to monitor increases in body weight. Vaginal smears were continued for monitoring diestrus status in these rats until day 7. On embryonic day 7 (E-7) these females were weighed to determine if there was a significant increase in (greater than about 10 g) body weight, to confirm pregnancy in sperm-positive females. These pregnant rats were then given daily intraperitoneal injections of any one of the following single chemicals or mixtures with an equal volume of sesame oil (Sigma) on days E-8 through E-14 of gestation [43]. Treatment groups were Control, Pesticide (Permethrin+DEET), Plastics (Bisphenol-A, DBP and DEHP), Dioxin (TCDD), and Jet Fuel (JP8 hydrocarbon). The pregnant female rats treated with various mixtures were designated as the F0 generation. When there was a drop in the litter size and the sex ratio of pups in F1 generation of Plastics group, another treatment group was included with only half the dose of Bisphenol-A, DBP and DEHP and this group was designated 'Low Dose Plastics' group. Doses, percent of oral LD50, and sources of chemicals for the compounds are given in Table S1A.

Breeding for F1, F2, and F3 generations, weaning measures and puberty checks

The offspring of the F0 generation were the F1 generation. Likewise F2 and F3 generation offspring were generated. The breeding used males and females from the same lineage (control or exposure), but did not use any sibling or cousin crosses to avoid inbreeding artifacts. These rats were weaned from their mothers at 21 days of age. At weaning, the following weaning traits were measured; litter size, sex ratio, weaning weight (in grams), and anogenital index (AGI). Anogenital distance (AGD), was measured with a caliper that had an accuracy of $1/100^{th}$ of a mm. Males have a significantly higher AGD than that of females. Weaning weights of rats were measured by a digital balance. AGI was computed as the AGD in mm (from the ventral edge of the anal opening to the caudal edge of the genital opening) per gram of body weight at weaning. Starting at the age of 30 days for females and 35 days for males, puberty checks were performed. These checks were performed on a daily basis until puberty in each rat was confirmed. Onset of puberty for females was indicated by a clear vaginal opening, and for males it was indicated when the glans penis was able to fully extend free of the preputial fold (balano-preputial separation) [37] (Figure S6).

Dissection of rats for tissue collection

Both female and male rats of F1, F2 and F3 generation at 90–120 days of age were euthanized by CO_2 inhalation and cervical dislocation for dissection, collection and examination of tissues including testis, epididymis, and ovary. Body and tissue weights were measured at dissections. Blood samples were collected, allowed to clot, centrifuged and serum samples stored for hormone assays. Tissues were fixed in Bouin's solution (Sigma) and 70% ethanol, then processed for paraffin embedding by standard procedures for histopathology examination. Five-micrometer sections were made and were either unstained or stained with H & E stain.

TUNEL cell death assay

Testis sections were examined by Terminal deoxynucleotidyl transferase-mediated dUTP nick end labeling (TUNEL) assay (In situ cell death detection kit, Fluorescein, Roche Diagnostics, Mannheim, Germany) as per the manufacturer's protocols. The sections were deparaffinized in xylene, rehydrated through descending series of ethyl alcohols, deionized water and 1× PBS buffer. The sections were deproteinized by incubation at 37°C in 250 ml of 1× PBS buffer containing 150 µl of Fungal Proteinase K (20 mg/ml; Invitrogen, Carlsbad, CA) and washed in 1× PBS buffer. About 20–25 µl of the enzyme-label solution mix was applied to testis sections. Slides were incubated at 37°C for 90 min, washed in fresh 1× PBS buffer for 10 min, mounted with GVA mount and kept at 4°C until examination. Testis sections were examined in a fluorescent microscope in dark to count the number of brightly fluorescing germ cells that are apoptotic.

Ovarian analysis

Evaluation of adult ovaries: Ovaries taken from rats at the time of sacrifice were fixed, paraffin embedded and sectioned at 5 µm thickness. Every 30th section was collected and hematoxylin/eosin stained. The three stained sections (150 µm apart) through the central portion of the ovary with the largest cross-section were evaluated for number of primordial follicles, developing pre-antral follicles, small antral follicles, large antral follicles, small cystic structures and large cysts. The mean number of each evaluated structure per section was calculated across the three sections. Follicles had to be non-atretic and have the oocyte nucleus visible in the section in order to be counted. Primordial follicles had an oocyte surrounded by a single layer of either squamous or both squamous and cuboidal granulosa cells [44]. Developing pre-antral follicles had one or more complete layers of cuboidal granulosa cells. Small antral follicles had a fluid-filled antrum and a maximum diameter of 51 µm measured across the outermost granulosa cell layer. Large antral follicles had a diameter greater than 51 µm.

Sperm DNA isolation and methylated DNA immunoprecipitation (MeDIP)

Sperm heads were separated from tails through sonication following previously described protocol (without protease inhibitors) [45] and then purified using a series of washes and centrifugations [46] from a total of nine F3 generation rats per treatment lineage that were 120 days of age. DNA extraction on the purified sperm heads was performed as previously described [5]. Equal concentrations of DNA from individual sperm samples were then used to produce pools of DNA material. Three DNA pools were produced in total per treatment, which contained the same amount of sperm DNA from three animals. Therefore a total of 45 animals were used for building three DNA pools per treatment for the 4 experimental groups plus controls. These DNA pools were then used for methylated DNA immunoprecipitation (MeDIP). MeDIP was performed as follows: 6 µg of genomic DNA was subjected to series of three 20 pulse sonications at 20% amplitude and the appropriate fragment size (200–1000 ng) was verified through 2% agarose gels; the sonicated genomic DNA was resuspended in 350 ul TE and denaturated for 10 min at 95°C and then immediately placed on ice for 5 min; 100 ul of 5× IP buffer (50 mM Na-phosphate pH 7, 700 mM NaCl, 0.25% Triton X-100) was added to the sonicated and denatured DNA. An overnight incubation of the DNA was performed with 5 ug of antibody anti-5-methylCytidine monoclonal from Diagenode S.A (Denville, NJ) at 4°C on a rotating platform. Protein A/G beads from Santa Cruz (Santa Cruz, CA) were prewashed on PBS-BSA 0.1% and resuspended in 40 ul 1× IP buffer. Beads were then added to the DNA-antibody complex and incubated 2 h at 4°C on a rotating platform. Beads bound to DNA-antibody complex were washed 3 times with 1 ml 1× IP buffer; washes included incubation for 5 min at 4°C on a rotating platform and then centrifugation at 6000 rpm for 2 min. Beads-DNA-antibody complex were then resuspended in 250 ul digestion buffer (50 mM Tris HCl pH 8, 10 mM EDTA, 0.5% SDS) and 3.5 ul of proteinase K (20 mg/ml) was added to each sample and then incubated overnight at 55°C on a rotating platform. DNA purification was performed first with phenol and then with chloroform:isoamyl alcohol. Two washes were then performed with 70% ethanol, 1 M NaCl and glycogen. MeDIP selected DNA was then resuspended in 30 ul TE buffer.

Tilling array MeDIP-Chip analysis

Roche Nimblegen's Rat DNA Methylation 3×720 K CpG Island Plus RefSeq Promoter Array was used, which contains three identical sub-arrays, with 720,000 probes per sub-array, scanning a total of 15,287 promoters (3,880 bp upstream and 970 bp downstream from transcription start site). Probe sizes range from 50–75 mer in length with the median probe spacing of 100 bp. Three different comparative (MeDIP vs MeDIP) hybridizations experiments were performed for each experimental group versus control, each encompassing DNA samples from 6 animals (3 treatment and 3 control groups) and 3 sub-arrays. MeDIP DNA samples from experimental groups were labeled with Cy3 and MeDIP DNA samples from the control group were labeled with Cy5.

Bioinformatic and statistic analyses of Chip data

For each comparative hybridization experiment, raw data from both the Cy3 and Cy5 channels were imported into R (R Development Core Team (2010), R: A language for statistical computing, R Foundation for Statistical Computing, Vienna, Austria. ISBN 3-900051-07-0, URL http://www.R-project.org), checked for quality and converted to MA values (M = Cy5-Cy3; A = (Cy5+Cy3)/2). The following normalization procedure was conducted. Within each array, probes were separated into groups by GC content and each group was separately normalized, between Cy3 and Cy5 using the loess normalization procedure. This allowed for GC groups to receive a normalization curve specific to that group. After each array was normalized within array, the arrays were then normalized across arrays using the A quantile normalization procedure.

Following normalization each probe within each array was subjected to a smoothing procedure, whereby the probe's normalized M values were replaced with the median value of all probe normalized M values across all arrays within a 600 bp window. If the number of probes present in the window was less than 3, no value was assigned to that probe. Each probe's A values were likewise smoothed using the same procedure. Following normalization and smoothing each probe's M value represents the median intensity difference between vinclozolin lineage and control lineage of a 600 bp window. Significance was assigned to probe differences between lineage and generation samples by calculating the median value of the intensity differences as compared to a normal distribution scaled to the experimental mean and standard deviation of the normalized M. A Z-score and P-value were computed for each probe from that distribution. The statistical analysis was performed in pairs of comparative IP hybridizations between treatment lineage (T) and control lineage (C) (e.g. T1-C1 and T2-C2; T1-C1 and T3-C3; T2-C2 and T3-C3). In order to assure the reproducibility of the candidates

obtained, only the candidates showing significant changes in every one of the paired comparisons were chosen as having a significant change in DNA methylation between each of the experimental group and controls. This is a very stringent approach to select for changes, since it only considers repeated changes in all paired analysis.

Clustered Regions of interest were then determined by combining consecutive probes within 600 bases of each other, and based on whether their mean M values were positive or negative, with significance p-values less than 10^{-5}. The statistically significant differential DNA methylated regions were identified and P-value associated with each region presented. Each region of interest was then annotated for gene and CpG content. This list was further reduced to those regions with an average intensity value exceeding 9.5 (log scale) and a CpG density $\geq$1 CpG/100 bp.

MeDIP-qPCR confirmation

The MeDIP-Chip differential DNA methylation sites identified were further tested with a quantitative PCR analysis [47,48]. Real time qPCR quantification of each significant region obtained from the array was performed on MeDIP samples and the values were normalized to the DNA concentration of MeDIP samples measured by picogreen. These qPCR assays were optimized and performed by the Genomics Core Laboratory at the University of Arizona, Tucson, AZ. Three technical replicates of Real Time qPCR reactions were performed for each one of three different MeDIPs per experimental group. Each MeDIP was from pools of sperm DNA samples from three animals. Ct values were obtained and the relative presence of specific DNA amplicons was calculated between control and exposure groups through the equation 'relative change = $2^{-\Delta Ct}$'. Statistical analysis between control and exposure groups was performed with student's t-test and changes with $p<0.05$ were considered significant. The level of DNA in the pool is a weighted average of all individuals, as previously described, [49].

Statistical analysis

For statistical analysis, all the data on weaning traits and onset of puberty were averaged for each litter. These averages were used as input in the program GraphPad© Prism 5 statistical analysis program. One-way ANOVA or t-test were used to determine if the data on puberty, number of apoptotic germ cells, number of ovarian follicles from the individual treatment groups differ from those of Control groups with a probability of significance, $p = 0.05$.

Supporting Information

Figure S1 Weaning traits including litter size and sex ratio were measured in three generations of rat progeny derived from pregnant F0 females exposed to environmental compounds (Pesticide, Plastics, Dioxin and Jet Fuel). Litter size and sex ratio were reduced only in Plastics group in F1 generation rats (* $p<0.05$; ** $p<0.01$).
(PDF)

Figure S2 Weaning weight measured in three generations of rat offspring derived from pregnant F0 females exposed to environmental compounds (Pesticide, Plastics, Dioxin and Jet Fuel). Weaning weight increased only in Pesticide group in F2 generation rats.
(PDF)

Figure S3 Anogenital indexes (AGI) were computed based on anogenital distance and weaning weights in three generations of rat offspring derived from pregnant F0 females exposed to environmental compounds (Pesticide, Plastics, Dioxin and Jet Fuel). AGI was unaffected in both female and male rats of F1 generations. AGI was reduced in Pesticide and Plastics groups of F2 female rats while it increased in LD Plastics F2 female rats. AGI declined in Pesticide group of F2 male rats while it increased in LD Plastics F2 male rats (* $p<0.05$; ** $p<0.01$).
(PDF)

Figure S4 Onset of puberty in female and male rats were investigated in three generations of rat offspring derived from pregnant F0 females exposed to environmental compounds (Pesticide, Plastics, Dioxin and Jet Fuel). Data from the first two generations are shown. (Puberty data of F3 generation rats are presented in Fig. 1). In the F1 generation, a delayed onset of puberty was recorded in female rats of Plastics group, and male rats of Plastics and Jet Fuel groups. In the F2 generation, an early onset of puberty was found for females rats of Plastics, LD Plastics, Dioxin and Jet Fuel groups and for the male rats of Plastics and Dioxin groups (* $p<0.05$; ** $p<0.01$; *** $p<0.001$).
(PDF)

Figure S5 Serum hormone concentrations were measured in the third generation rat offspring derived from pregnant F0 females exposed to environmental compounds (Pesticide, Plastics, Dioxin and Jet Fuel)(* $p<0.05$; ** $p<0.01$). (A) Serum testosterone concentrations in male rats were severely reduced in Plastics, Dioxin and Jet Fuel groups. (B) Serum progesterone concentrations were unaffected in female rats (C) Serum LH concentrations were unaltered in male rats (D) Serum LH concentrations were not changed in female rats.
(PDF)

Figure S6 Onset of puberty was identified by (A) the opening of vaginal orifice in female rats and (B) the separation of glans penis from the prepuce in male rats.
(PDF)

Table S1 Doses and Sources of Chemicals used.
(PDF)

Table S2 List of rat sperm differential methylation regions (DMR).
(PDF)

Table S3 Pathways influenced by genes associated with DMR.
(PDF)

Acknowledgments

We thank the expert technical assistance of Dr. Eric Nilsson, Dr. Marina Savenkova, Ms. Renee Espinosa Najera, Ms. Jessica Shiflett, Ms. Ginger Beiro, Ms. Chrystal Bailey, Ms. Colleen Johns, Mr. Trevor Covert and Ms. Sean Leonard, as well as the assistance of Ms. Heather Johnson in preparation of the manuscript. We acknowledge the helpful advice of Dr. David Jackson and Dr. John Lewis, US Army Center for Environmental Health Research, Department of Defense (DOD), and the leadership at the DOD TATRC.

Author Contributions

Conceived and designed the experiments: MKS. Performed the experiments: MM CG RT MMH. Analyzed the data: MKS MM CG RT MMH. Wrote the paper: MKS MM CG.

References

1. Skinner MK, Manikkam M, Guerrero-Bosagna C (2010) Epigenetic transgenerational actions of environmental factors in disease etiology. Trends Endocrinol Metab 21: 214–222.
2. Anway MD, Cupp AS, Uzumcu M, Skinner MK (2005) Epigenetic transgenerational actions of endocrine disruptors and male fertility. Science 308: 1466–1469.
3. Jirtle RL, Skinner MK (2007) Environmental epigenomics and disease susceptibility. Nat Rev Genet 8: 253–262.
4. Kavlock R, Cummings A (2005) Mode of action: inhibition of androgen receptor function–vinclozolin-induced malformations in reproductive development. Crit Rev Toxicol 35: 721–726.
5. Guerrero-Bosagna C, Settles M, Lucker BJ, Skinner MK (2010) Epigenetic transgenerational actions of vinclozolin on promoter regions of the sperm epigenome. PLoS ONE 5: e13100.
6. Anway MD, Leathers C, Skinner MK (2006) Endocrine disruptor vinclozolin induced epigenetic transgenerational adult-onset disease. Endocrinology 147: 5515–5523.
7. Waterland RA (2009) Is epigenetics an important link between early life events and adult disease? Horm Res 71 Suppl 1: 13–16.
8. Bruner-Tran KL, Osteen KG (2011) Developmental exposure to TCDD reduces fertility and negatively affects pregnancy outcomes across multiple generations. Reprod Toxicol 31: 344–350.
9. Salian S, Doshi T, Vanage G (2009) Impairment in protein expression profile of testicular steroid receptor coregulators in male rat offspring perinatally exposed to Bisphenol A. Life Sci 85: 11–18.
10. Stouder C, Paoloni-Giacobino A (2010) Transgenerational effects of the endocrine disruptor vinclozolin on the methylation pattern of imprinted genes in the mouse sperm. Reproduction 139: 373–379.
11. Pimentel D, Cooperstein S, Randell H, Filiberto D, Sorrentino S, et al. (2007) Ecology of Increasing Diseases: Population Growth and Environmental Degradation. Human Ecology 35: 653–668.
12. Talsness CE, Andrade AJ, Kuriyama SN, Taylor JA, vom Saal FS (2009) Components of plastic: experimental studies in animals and relevance for human health. Philos Trans R Soc Lond B Biol Sci 364: 2079–2096.
13. Bernal AJ, Jirtle RL (2010) Epigenomic disruption: the effects of early developmental exposures. Birth Defects Res A Clin Mol Teratol 88: 938–944.
14. Hunt PA, Susiarjo M, Rubio C, Hassold TJ (2009) The bisphenol A experience: a primer for the analysis of environmental effects on mammalian reproduction. Biol Reprod 81: 807–813.
15. Kitchen LW, Lawrence KL, Coleman RE (2009) The role of the United States military in the development of vector control products, including insect repellents, insecticides, and bed nets. J Vector Ecol 34: 50–61.
16. Das PC, Cao Y, Rose RL, Cherrington N, Hodgson E (2008) Enzyme induction and cytotoxicity in human hepatocytes by chlorpyrifos and N,N-diethyl-m-toluamide (DEET). Drug Metabol Drug Interact 23: 237–260.
17. Corbel V, Stankiewicz M, Pennetier C, Fournier D, Stojan J, et al. (2009) Evidence for inhibition of cholinesterases in insect and mammalian nervous systems by the insect repellent deet. BMC Biol 7: 47.
18. Torres-Altoro MI, Mathur BN, Drerup JM, Thomas R, Lovinger DM, et al. (2011) Organophosphates dysregulate dopamine signaling, glutamatergic neurotransmission, and induce neuronal injury markers in striatum. J Neurochem 119: 303–313.
19. Heder AF, Hirsch-Ernst KI, Bauer D, Kahl GF, Desel H (2001) Induction of cytochrome P450 2B1 by pyrethroids in primary rat hepatocyte cultures. Biochem Pharmacol 62: 71–79.
20. Olgun S, Gogal RM, Jr., Adeshina F, Choudhury H, Misra HP (2004) Pesticide mixtures potentiate the toxicity in murine thymocytes. Toxicology 196: 181–195.
21. Birnbaum LS, Fenton SE (2003) Cancer and developmental exposure to endocrine disruptors. Environ Health Perspect 111: 389–394.
22. Baccarelli A, Bollati V (2009) Epigenetics and environmental chemicals. Curr Opin Pediatr 21: 243–251.
23. Ritchie G, Still K, Rossi J, 3rd, Bekkedal M, Bobb A, et al. (2003) Biological and health effects of exposure to kerosene-based jet fuels and performance additives. J Toxicol Environ Health B Crit Rev 6: 357–451.
24. Wong SS, Vargas J, Thomas A, Fastje C, McLaughlin M, et al. (2008) In vivo comparison of epithelial responses for S-8 versus JP-8 jet fuels below permissible exposure limit. Toxicology 254: 106–111.
25. DiVall SA, Radovick S (2009) Endocrinology of female puberty. Curr Opin Endocrinol Diabetes Obes 16: 1–4.
26. Biro FM, Galvez MP, Greenspan LC, Succop PA, Vangeepuram N, et al. (2010) Pubertal assessment method and baseline characteristics in a mixed longitudinal study of girls. Pediatrics 126: e583–590.
27. Cesario SK, Hughes LA (2007) Precocious puberty: a comprehensive review of literature. J Obstet Gynecol Neonatal Nurs 36: 263–274.
28. Traggiai C, Stanhope R (2003) Disorders of pubertal development. Best Pract Res Clin Obstet Gynaecol 17: 41–56.
29. Rockett JC, Lynch CD, Buck GM (2004) Biomarkers for assessing reproductive development and health: Part 1–Pubertal development. Environ Health Perspect 112: 105–112.
30. Fisher JS (2004) Environmental anti-androgens and male reproductive health: focus on phthalates and testicular dysgenesis syndrome. Reproduction 127: 305–315.
31. Hauser R, Sokol R (2008) Science linking environmental contaminant exposures with fertility and reproductive health impacts in the adult male. Fertil Steril 89: e59–65.
32. Vujovic S (2009) Aetiology of premature ovarian failure. Menopause Int 15: 72–75.
33. Kumar S (2004) Occupational exposure associated with reproductive dysfunction. J Occup Health 46: 1–19.
34. Hotchkiss AK, Lambright CS, Ostby JS, Parks-Saldutti L, Vandenbergh JG, et al. (2007) Prenatal testosterone exposure permanently masculinizes anogenital distance, nipple development, and reproductive tract morphology in female Sprague-Dawley rats. Toxicol Sci 96: 335–345.
35. Watanabe N, Kurita M (2001) The masculinization of the fetus during pregnancy due to inhalation of diesel exhaust. Environ Health Perspect 109: 111–119.
36. Honma S, Suzuki A, Buchanan DL, Katsu Y, Watanabe H, et al. (2002) Low dose effect of in utero exposure to bisphenol A and diethylstilbestrol on female mouse reproduction. Reprod Toxicol 16: 117–122.
37. Engelbregt MJ, Houdijk ME, Popp-Snijders C, Delemarre-van de Waal HA (2000) The effects of intra-uterine growth retardation and postnatal undernutrition on onset of puberty in male and female rats. Pediatr Res 48: 803–807.
38. Anway MD, Rekow SS, Skinner MK (2008) Transgenerational epigenetic programming of the embryonic testis transcriptome. Genomics 91: 30–40.
39. Skinner MK (2005) Regulation of primordial follicle assembly and development. Hum Reprod Update 11: 461–471.
40. Brinkman AB, Simmer F, Ma K, Kaan A, Zhu J, et al. (2010) Whole-genome DNA methylation profiling using MethylCap-seq. Methods 52: 232–236.
41. Guerrero-Bosagna C, Covert T, Haque MM, Settles M, Nilsson E, et al. (2011) Epigenetic Transgenerational Inheritance of Vinclozolin Induced Mouse Adult Onset Disease and Associated Sperm Epigenome Biomarkers. (Submitted).
42. Crews D, Gore AC, Hsu TS, Dangleben NL, Spinetta M, et al. (2007) Transgenerational epigenetic imprints on mate preference. Proc Natl Acad Sci U S A 104: 5942–5946.
43. Nilsson EE, Anway MD, Stanfield J, Skinner MK (2008) Transgenerational epigenetic effects of the endocrine disruptor vinclozolin on pregnancies and female adult onset disease. Reproduction 135: 713–721.
44. Meredith S, Dudenhoeffer G, Jackson K (2000) Classification of small type B/C follicles as primordial follicles in mature rats. J Reprod Fertil 119: 43–48.
45. Tateno H, Kimura Y, Yanagimachi R (2000) Sonication per se is not as deleterious to sperm chromosomes as previously inferred. Biol Reprod 63: 341–346.
46. Ward WS, Kimura Y, Yanagimachi R (1999) An intact sperm nuclear matrix may be necessary for the mouse paternal genome to participate in embryonic development. Biol Reprod 60: 702–706.
47. Martinato F, Cesaroni M, Amati B, Guccione E (2008) Analysis of Myc-induced histone modifications on target chromatin. PLoS ONE 3: e3650.
48. Sadikovic B, Yoshimoto M, Al-Romaih K, Maire G, Zielenska M, et al. (2008) In vitro analysis of integrated global high-resolution DNA methylation profiling with genomic imbalance and gene expression in osteosarcoma. PLoS ONE 3: e2834.
49. Zhang W, Carriquiry A, Nettleton D, Dekkers JC (2007) Pooling mRNA in microarray experiments and its effect on power. Bioinformatics 23: 1217–1224.

Environmental Epigenetics, 2018, 1–19

doi: 10.1093/eep/dvy010
Research article

RESEARCH ARTICLE

Alterations in sperm DNA methylation, non-coding RNA expression, and histone retention mediate vinclozolin-induced epigenetic transgenerational inheritance of disease

Millissia Ben Maamar[1], Ingrid Sadler-Riggleman[1], Daniel Beck[1], Margaux McBirney[1], Eric Nilsson[1], Rachel Klukovich[2], Yeming Xie[2], Chong Tang[2], Wei Yan[2,‡] and Michael K. Skinner[1,*,‡]

[1]Center for Reproductive Biology, School of Biological Sciences, Washington State University, Pullman, WA 99164-4236, USA and [2]Department of Physiology and Cell Biology, University of Nevada, Reno School of Medicine, 1664 North Virginia Street, MS557, Reno, NV 89557, USA

*Correspondence address. Center for Reproductive Biology, School of Biological Sciences, Washington State University, Pullman, WA 99164-4236, USA. Tel: +1-509-335-1524; Fax: +1-509-335-2176; E-mail: skinner@wsu.edu

‡Both authors contributed equally to this study.

Managing Editor: Christopher Faulk

Abstract

Epigenetic transgenerational inheritance of disease and phenotypic variation can be induced by several toxicants, such as vinclozolin. This phenomenon can involve DNA methylation, non-coding RNA (ncRNA) and histone retention, and/or modification in the germline (e.g. sperm). These different epigenetic marks are called epimutations and can transmit in part the transgenerational phenotypes. This study was designed to investigate the vinclozolin-induced concurrent alterations of a number of different epigenetic factors, including DNA methylation, ncRNA, and histone retention in rat sperm. Gestating females (F0 generation) were exposed transiently to vinclozolin during fetal gonadal development. The directly exposed F1 generation fetus, the directly exposed germline within the fetus that will generate the F2 generation, and the transgenerational F3 generation sperm were studied. DNA methylation and ncRNA were altered in each generation rat sperm with the direct exposure F1 and F2 generations being distinct from the F3 generation epimutations. Interestingly, an increased number of differential histone retention sites were found in the F3 generation vinclozolin sperm, but not in the F1 or F2 generations. All three different epimutation types were affected in the vinclozolin lineage transgenerational sperm (F3 generation). The direct exposure generations (F1 and F2) epigenetic alterations were distinct from the transgenerational sperm epimutations. The genomic features and gene pathways associated with the epimutations were investigated to help elucidate the integration of these different epigenetic processes. Our results show that the three different types of epimutations are involved and integrated in the mediation of the epigenetic transgenerational inheritance phenomenon.

Received 30 January 2018; **revised** 20 March 2018; **accepted** 22 March 2018

Key words: epigenetics; sperm; spermatogenesis; transgenerational; inheritance; DNA methylation

Introduction

Environmentally induced epigenetic transgenerational inheritance is defined as "germline (sperm or egg) transmission of epigenetic information between generations in the absence of any continued exposure or genetic manipulation." In 1987 the word epimutation was introduced to describe heritable changes in genes which were not due to changes in DNA sequence [1]. A number of different epigenetic factors have been described and are critical in regulating gene expression including chromatin structure and non-coding RNA (ncRNA) methylation which have become an intensively active field of research. The modification of histones, particularly acetylation and methylation, play a crucial role in regulating genome activity [2]. DNA methylation can provide a primary switch where methylation triggers the changes that lead to a closed (not allowing gene transcription) or opened chromatin configuration (allowing gene transcription) [3]. The role of ncRNA in epigenetic events has become increasingly important [4–6]. All these epigenetic processes can be altered by numerous environmental exposures [7]. These environmental exposures can alter the early development of various organ systems that result in later life adult individuals with greater susceptibilities to develop disease when they encounter a second disease-promoting stimulus [8].

Epigenetic alterations in the germline mediate the heritable molecular relationship between the environment and gene expression [9, 10]. Studies have observed epigenetic transgenerational inheritance effects in different species, including plants [11], flies [12], worms [13], fish [14], birds [15] rodents [16–18], pigs [19], and humans [20]. This phenomenon has been observed in a large number of organisms showing that epigenetic transgenerational mechanisms are conserved and induced by environmental factors [21]. Many studies on environmental toxicants have been conducted, such as 2, 3, 7, 8-tetrachlorodibenzo [p]dioxin [22], permethrin and *N*, *N*-diethyl-meta-toluamide mixture [23], jet fuel JP-8 [24], plastics mixture [bisphenol-A, bis (2-ethylhexyl)phthalate, dibutyl phthalate] [25], dichlorodiphenyltrichloroethane (DDT) [26], methoxychlor [27], and atrazine [28]. For each exposure, alterations in DNA methylation have been observed in F3 generation rat sperm.

The first compound showing a transgenerational effect was vinclozolin. Vinclozolin [3-(3, 5-dichlorophenyl)-5methyl-5-vinyl-1, 3-oxazolidine-2, 4-dione] is a fungicide used on fruits and vegetables crops. This chemical was found to exert significant antiandrogenic effects [29, 30]. Vinclozolin administration to pregnant female mice during the gestation period of embryonic days E13–E17 (which corresponds to fetal gonadal sex determination) was found to affect the offspring [16, 31]. This chemical also demonstrated transgenerational (F1 through F4 generations) effects on male fertility and altered the DNA methylation patterns in the F2 and F3 generation sperm [16]. This suggested that environment can induce epigenetic changes in the germline and be inherited to contribute to disease. Other exposures since then have been shown to promote epigenetic transgenerational phenotypes [21]. One of the proposed mechanisms is that "epimutations" induced in the germline become "imprinted-like" and therefore escape the post-fertilization DNA methylation erasure. The altered epigenome leads to modified transcriptomes in somatic cells resulting in adult-onset disease susceptibility [27, 32, 33]. Anway and collaborators revealed that following transient gestational exposure to F0 generation females between E8 and E15 (corresponding to the epigenetic reprogramming of germ cells and gonadal sex determination) the F1, F2, F3, and F4 generation adult males showed increased spermatogenic apoptosis and a decreased sperm number and motility [16]. Altered DNA methylation patterns in F2 and F3 generation vinclozolin lineages were also observed [34]. Prostate abnormalities were noted in F1–F4 generation males [35], severe anemia during pregnancy in F1–F3 generation females [36] and also sexually dimorphic changes in anxiety behaviors [37]. The mRNA expression of 196 genes was found to be consistently different in testis among the F1–F3 generation vinclozolin animals compared to the F1–F3 generation controls [35]. Transcription alterations in prostate from F3 males [35], hippocampus and amygdala in F3 males and females [37], and Sertoli cells [38] were also reported. These studies demonstrate the effects of vinclozolin transgenerationally on somatic gene expression.

The involvement of sperm small non-coding RNA (sncRNA) in the impact of traumatic stress in early life across generations was also investigated. Sperm RNAs from traumatized males were injected into fertilized wild-type oocytes which reproduced the behavioral and metabolic alterations in their offspring [39]. This suggests that sncRNAs are sensitive to environmental factors in early life which can be passed to the next generation and contribute to the inheritance of trauma-induced phenotypes [39]. Subsequently vinclozolin has also been shown to alter transgenerationally the sncRNA in sperm [40]. Previous studies have revealed that ncRNA can modulate gene expressions and many of them have been identified to participate in the epigenetic control by affecting DNA methylation [41, 42] or by interacting with various types of proteins involved in histone modification or chromatin remodeling [43–46]. Therefore, long ncRNA (lncRNA) is an ideal mediator to regulate local and sequence-specific DNA methylation or demethylation which may also trigger epigenetic disorders and transgenerational effects [43].

The lncRNAs have been hypothesized to maintain epigenetic memory and a recent study has correlated lncRNA differential expression to DDT-induced epigenetic transgenerational inheritance [7]. The sncRNAs were also implicated when the effects of starvation were found to induce the production of sncRNAs that persisted for multiple generations and resulted in a longer lifespan for the F3 generation [47]. Total estimates for both lncRNA and sncRNA in a single spermatozoa have exceeded 20 000 [48, 49]. As such, there are various different kinds of small RNAs found in spermatozoa including: micro-RNA (miRNAs) and siRNAs involved in regulating spermatogenesis via translation; piwi-interacting RNAs (piRNAs) believed to regulate transcript stability in the germline; and many smaller classes of sncRNA such as tRNA-derived sncRNAs and mitosRNAs have also been discovered in spermatozoa [50, 51]. The expression of ncRNAs throughout spermatogenesis has been shown to be differential [51], suggesting an environmentally induced disruption of ncRNA expression in spermatogenic cells can have lasting effects for generations. Both DNA methylation and ncRNA transgenerational alterations have been reported to be altered in the epigenetic transgenerational inheritance phenomenon, but to the best of our knowledge no studies have examined histone modifications until recently [52]. Several studies have

observed conserved genes associated with histone retention sites and modifications [53] indicating modifications of histones may have an impact transgenerationally.

This study was designed to investigate concomitantly the epigenetic modifications of DNA methylation, ncRNA, and histones retention in sperm. The transgenerational model used for this study involves epigenetic transgenerational inheritance of sperm epigenetic alterations and disease triggered by vinclozolin exposure. This study will use this vinclozolin-induced epigenetic transgenerational inheritance of disease in rats to investigate the epigenetic changes in the F1, F2, and F3 generation sperm. This information combined with associated genes will be useful in the elucidation of the molecular processes implicated in the epigenetic transgenerational inheritance phenomenon. Observations demonstrate all three epigenetic processes are potentially involved and reflect transgenerational epimutations, including a novel role of new induced transgenerational differential histone retention sites (DHRs), and distinct transgenerational DNA methylation and ncRNA epimutations.

Results

The experimental design (Fig. 1A) involved a daily transient exposure of gestating female F0 generation rats during embryonic days E8–E14 to 100 mg/kg per day of vinclozolin in dimethylsulfoxide (DMSO) using intraperitoneal injection as previously described [16]. A separate control generation lineage was exposed during Days E8–E14 of gestation to vehicle DMSO alone. Six different gestating females from different litters for each control and vinclozolin lineage were used. The F1 generation offspring were obtained and aged to 90-day postnatal age and selected males and females bred within the control or vinclozolin lineage. The F2 generation offspring were obtained and aged to 90 days and selected males and females from different litters bred to generate the F3 generation. No sibling or cousin breeding was used to avoid any inbreeding artifacts. All the males were sacrificed at 120 days of age for epididymal sperm collection. In previous studies, onset of disease was primarily observed between 6 and 12 months of age [54], hence the postnatal 120-day (P120) males were used to avoid any disease artifacts. The only disease detectable at P120 is testis spermatogenic cell apoptosis [16]. Selected male testis at each generation for both the control and vinclozolin lineages was used for spermatogenic cell apoptosis analysis. A significant level of apoptosis was observed in the F3 generation vinclozolin lineage (Fig. 1B) supporting the transgenerational phenotype of the vinclozolin model used. The sperm collected was then used for epigenetic analysis.

Sperm DNA Methylation Alterations

Methylated DNA immunoprecipitation (MeDIP) followed by DNA next-generation sequencing (NGS) for a MeDIP-Seq analysis was used to identify the differential DNA-methylated regions (DMRs) between the control versus vinclozolin lineage male sperm. Initially the sperm DNA was sonicated to produce DNA fragments of 200–500 bp. A methylcytosine antibody was used to immunoprecipitate the methylated DNA fragments. Libraries were generated for sequencing 50-bp paired-end reads to assess differential levels (read depths) of DNA methylation. The DMRs for the F1, F2, and F3 generation sperm were determined and different threshold p values are shown in Fig. 2. A *P*-value of $P < 1e\text{-}06$ was chosen for comparison of all single 100-bp windows, as well as DMRs with multiple (≥ 2) adjacent windows. The direct exposure F1 generation sperm had the lowest number of DMRs (Fig. 2A), the F2 generation an increased number of DMRs (Fig. 2B), and the F3 generation the highest number of DMRs (Fig. 2C). The DMR lists are presented in the Supplementary Tables S1–S3. A comparison of the DMRs at $P < 1e\text{-}06$ demonstrated minimal overlap with a higher level of overlap between the F2 and F3 generations (Fig. 2D). The majority of the alterations in sperm DNA methylation was unique between the generations. A small set of 44 overlapping DMRs between the F2 and F3 generation sperm are presented in the Supplementary Table S4.

The chromosomal locations of the DMRs for each generation are shown in Fig. 3. Nearly all the chromosomes display DMRs as indicated by the red arrowheads and some present clusters of DMRs indicated by black boxes. These different generation DMR clusters are also primarily distinct between the generations with little overlap (Fig. 3D). The CpG density of the DMRs for the F1, F2, and F3 generation sperm is shown in Fig. 4A–C. The CpG density of the DMRs at $P < 1e\text{-}06$ is shown and reveals that the predominant density is one CpG per 100 bp with a range between 1 and 4 CpG. The lengths of the DMRs are presented in Fig. 4D–F and shows that their predominant length is 1 kb and a range of 1–5 kb for each generation DMRs. Thus, the DMRs are associated with CpG deserts with 10–20 CpG within 1 kb [55]. The lists of DMRs with their chromosomal locations, size, and CpG density are presented in the Supplementary Tables S1–S3 for the F1, F2, and F3 generation DMRs, respectively.

Sperm ncRNA Alterations

The differential ncRNA present in sperm between the control versus vinclozolin lineages was determined with NGS using RNA-Seq analysis previously described [40]. The sperm total ncRNA was collected and then sncRNA and lncRNA prepared with appropriate ncRNA extraction and sequencing library procedures described in the Methods section. The read depths of differential ncRNA levels were determined for the F1, F2, and F3 generation sperm with a comparison of the control versus vinclozolin lineage sperm. The lncRNA for each generation with different *P*-value thresholds is compiled in Fig. 5A. The *P*-value used for subsequent analysis selected was $P < 1e\text{-}04$. The sncRNA for each generation with several *P*-value thresholds is shown in Fig. 5B. The *P*-value used for sncRNA analysis selected was $P < 1e\text{-}04$. The lncRNA is higher in number than the sncRNA. For the lncRNA, the F1 generation has a higher number than the F3 generation, and the F3 generation has a lower number than the F2 generation (Fig. 5C). The sncRNA was divided into categories with the piRNA, the miRNA, and the small tRNA being present, as well as a mixture of uncategorized sncRNA (other) (Fig. 5D). Therefore, each generation had differential ncRNA present and they were different between each generation.

The chromosomal locations of the differential ncRNA are presented for lncRNA in Fig. 6. The red arrowheads identify individual lncRNA and regional clusters of lncRNA are shown in black boxes. The F1, F2, and F3 generation lncRNAs are present on all chromosomes (Fig. 6A–C). The analysis of the lncRNA overlap between the generations indicated that the vast majority of differential lncRNA was distinct for each generation (Fig. 6D). The chromosomal locations of the differential ncRNA are shown for sncRNA in Fig. 7A–C. The overlap analysis between the three generations is shown in Fig. 7D. It reveals that the majority of differential sncRNA was unique for each generation. Both the long and small differential ncRNAs were predominantly distinct from the transgenerational F3

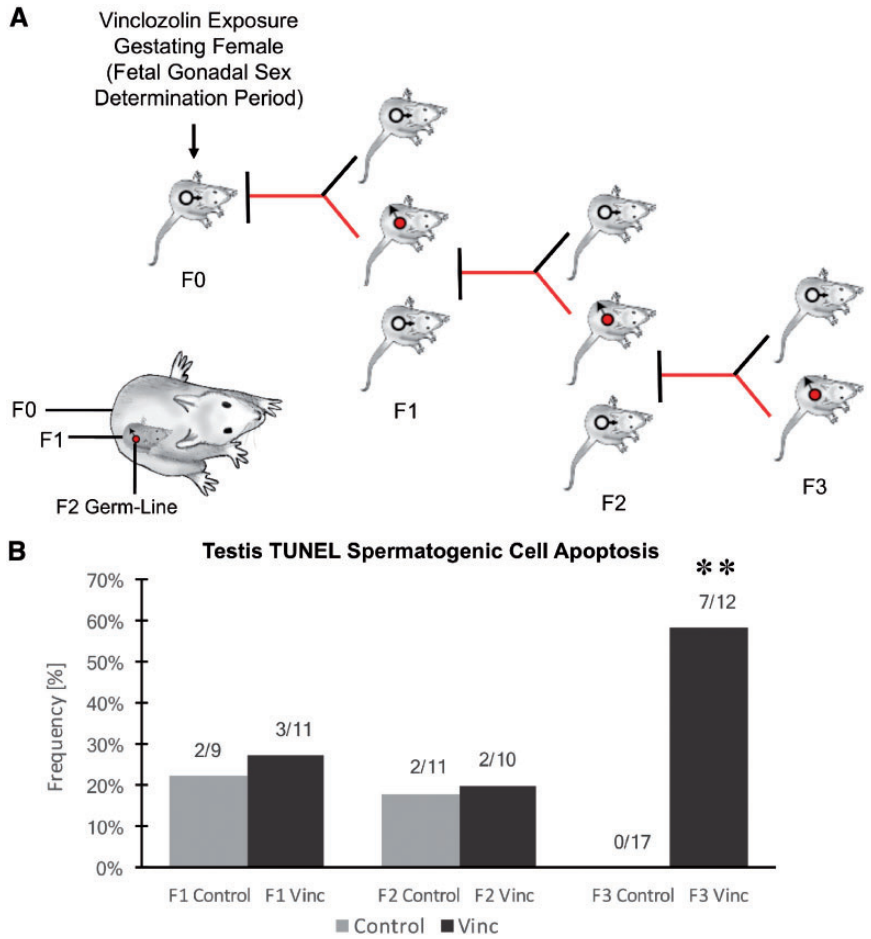

Figure 1: animal breeding scheme and disease. **(A)** Experimental design of F0 generation gestating female exposure then F1, F2, and F3 generations being generated for sperm collection. The direct exposure of the F0 generation female, F1 generation fetus, and F2 generation germline is also shown. **(B)** Testis spermatogenic cell apoptosis as determined with TUNEL analysis of testis histology sections with frequency (%) of apoptosis for each generation and lineage shown. The (**) indicates statistical significance with control with a $P < 0.01$ with a Fishers exact *T*-test

generation ncRNA. The lists of differential ncRNA separated by category for identification, chromosomal location, size, statistics and gene associations are presented in the Supplementary Tables S5–S7 for lncRNA and Supplementary Tables S8–S10 for sncRNA for the F1, F2, and F3 generations, respectively.

Sperm Histones Alterations

A core of histone retention sites have been previously shown in control and vinclozolin lineage rat sperm that are not altered following exposure, but the F3 generation vinclozolin lineage sperm had an increase in the number of histone retention sites [52]. This study examined the sites (DHRs for the F1, F2, and F3 generation control versus vinclozolin lineage sperm with a procedure similar to the DMR analysis. Interestingly, the F1 and F2 generations had negligible DHRs showing no major difference between control and vinclozolin lineages (Fig. 8A and B). However, the F3 generation comparison of the control versus vinclozolin lineage sperm identified an increased number of DHRs (Fig. 8C). The chromosomal locations of these DHRs are represented in Fig. 8D. An overlap analysis of these DHRs between F1, F2, and F3 revealed that each of them was unique (Fig. 8E). DHRs were induced in the F3 generation lineage sperm thus displaying a transgenerational effect whereas a direct exposure did not trigger major alterations. The DHRs are listed with identification, location, size and associated genes in the Supplementary Tables S11–S13 for the F1, F2, and F3 generations, respectively.

Epimutation Gene Associations

The Supplementary Tables S1–S9 provide the lists of DMRs, ncRNAs, and DHRs for all the epigenetic alterations (i.e. epimutations) identified. The known gene associations for these epimutations were determined using genomic location and are also listed. All the associated genes were classified by relevant functions and the functional categories are presented for each generation in Fig. 9A. For this analysis, sncRNA and lncRNA were combined. The top ten gene categories containing multiple genes for F1, F2, and F3 generations are presented for DMRs, ncRNA, and DHRs separately. Epimutations were found predominantly in the metabolism, signaling, and transcription categories. The predominant gene categories for the F1 generation were mostly found with the lncRNA (Fig. 9A). The predominant gene categories for the F3 generation were similar as the F1 generation but found in the DMRs. The ratio of epimutations between the generations was highest for DMRs in the F3 generation, highest for ncRNA in the F1 generation, and negligible DHRs are present in the F1 and F2 generations, but present in the F3 generation (Fig. 10A).

A Control versus vinclozolin F1 generation lineage DMRs

p-value	All Window	Multiple Window
0.001	21869	2434
1e-04	3815	285
1e-05	736	47
1e-06	**170**	**20**
1e-07	52	12

Number of significant windows	1	2	3	4	5	10
Number of DMR	150	15	2	1	1	1

B Control versus vinclozolin F2 generation lineage DMRs

p-value	All Window	Multiple Window
0.001	31185	4239
1e-04	5965	551
1e-05	1270	125
1e-06	**327**	**42**
1e-07	126	24

Number of significant windows	1	2	3	4	6	8
Number of DMR	285	33	5	1	2	1

C Control versus vinclozolin F3 generation lineage DMRs

p-value	All Window	Multiple Window
0.001	46835	11604
1e-04	12240	2534
1e-05	3560	724
1e-06	**1203**	**274**
1e-07	457	123

Number of significant windows	1	2	3	4	5	6	7	8	9	≥10
Number of DMR	929	173	52	20	8	4	5	2	1	9

D Overlap of DMRs

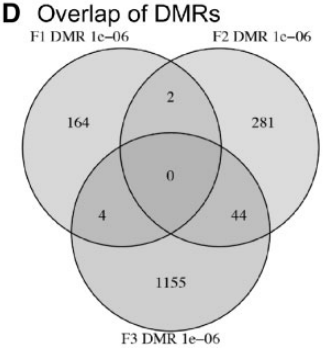

Figure 2: DMR analysis. **(A)** F1 generation control versus vinclozolin lineage DMRs. **(B)** F2 generation control versus vinclozolin lineage DMRs. **(C)** F3 generation control versus vinclozolin lineage DMRs. The number of DMRs found using different *P*-value cutoff thresholds is presented. The All Window column shows all DMRs. The Multiple Window column shows the number of DMRs containing at least two adjacent significant windows. **(D)** The DMR overlap ($P \leq$ 1e-06) for the F1, F2, and F3 generation sperm

The integration of the different epigenetic alterations is suggested in Fig. 9A and B with epimutation-associated genes in specific pathways and gene categories. The majority of the gene categories and pathways observed in the F1 generation was associated with the lncRNAs. The same phenomenon was found in the F3 generation but associated with the DMRs (Fig. 9A and B). Two pathways, axon guidance and pathways in cancer, were selected to investigate the potential overlap with genes involving the lncRNA- and DMR-associated genes (Supplementary Figs. S1 and S2). For the F1 and F3 generation lncRNA and DMRs the pathways were represented by both types of epimutations at independent genes, and few had the same gene involving a lncRNA in the F1 generation and DMR in the F3 generation. In both generations the pathways were affected, but with different types of epimutations.

The Venn diagrams of DMRs, DHRs, and ncRNA suggest negligible overlap between the different types of epimutations within the same generation comparison (Fig. 9C). So, the different epigenetic alterations have different genomic locations and minimal overlap between each other in the same generation. The total list of associated genes with the DMRs, ncRNAs, and DHRs are presented in the Supplementary Tables S1–S13.

Discussion

This study was designed to help understand how three different epigenetic processes in sperm are correlated with vinclozolin-induced epigenetic transgenerational inheritance of disease. A number of transgenerational diseases including testis disease, ovarian disease, kidney pathology, prostate abnormalities, and

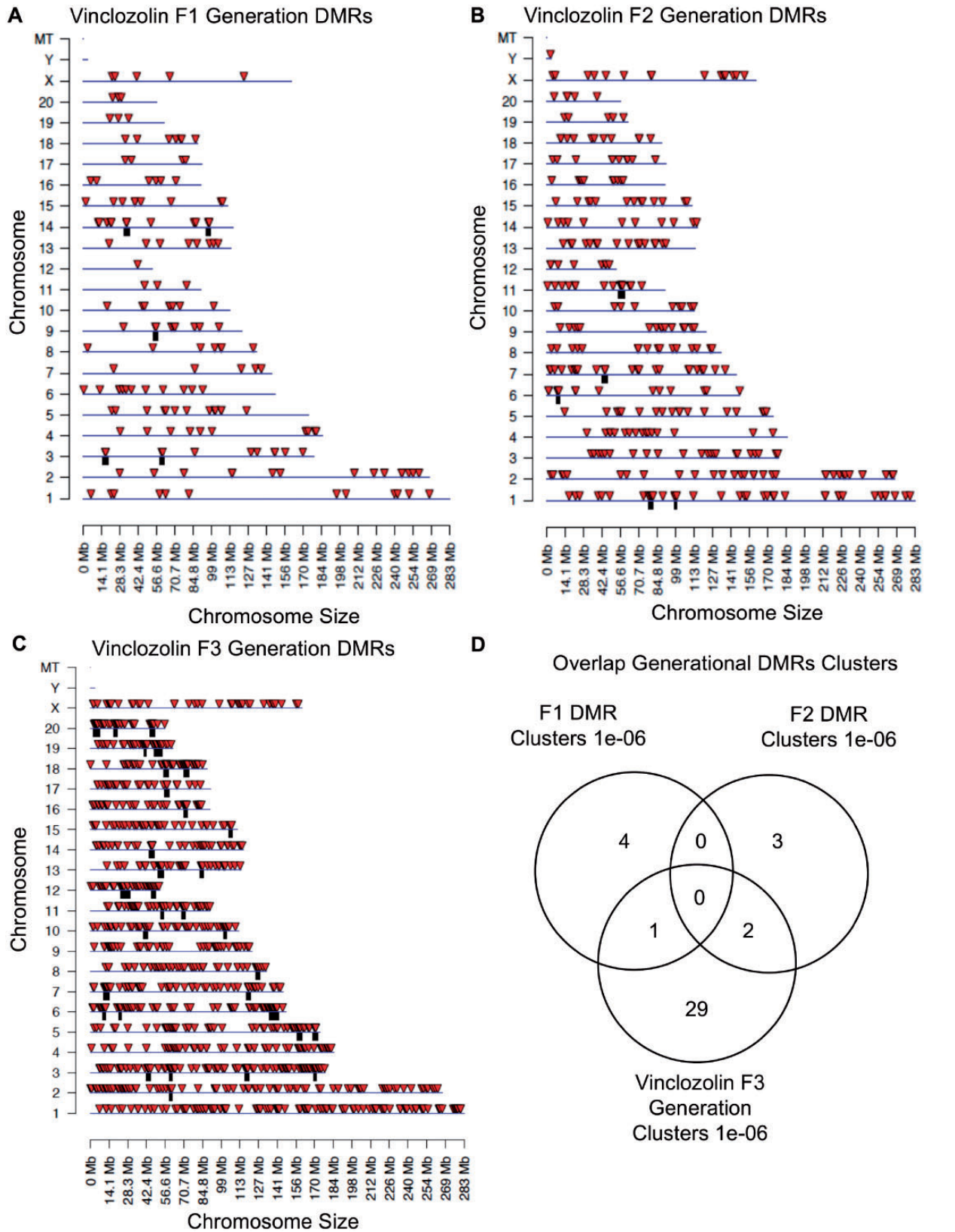

Figure 3: chromosomal locations and overlaps of DMRs. **(A)** Vinclozolin F1 generation DMRs. **(B)** Vinclozolin F2 generation DMRs. **(C)** Vinclozolin F3 generation DMRs. The DMR locations on the individual chromosomes are shown with red arrowheads and clusters of DMRs with black boxes. All window DMRs at a *P*-value threshold of 1e-06 are shown. **(D)** Overlap of the different generations DMR clusters

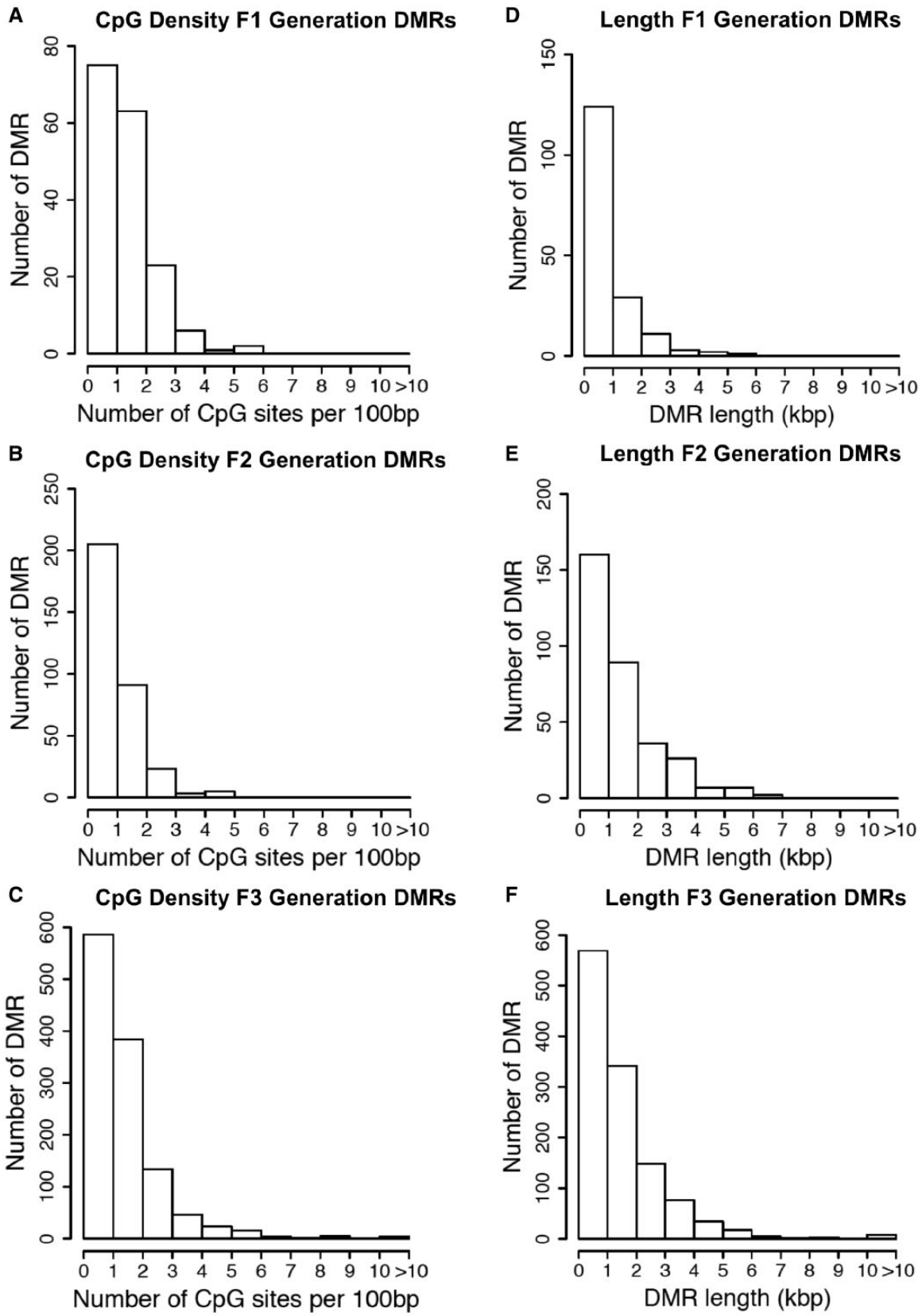

Figure 4: DMR CpG density. **(A)** F1 generation, **(B)** F2 generation, and **(C)** F3 generation. Histograms of the number of DMRs at different CpG densities (CpG/100 bp). All DMRs at a *P*-value threshold of 1e-06 are shown. DMR length (kb) for **(D)** F1 generation, **(E)** F2 generation, and **(F)** F3 generation. Histograms of the number of DMR at different length (kb) are shown

A **Control versus Vinclozolin Lineage Long ncRNA**

P-value	F1	F2	F3
0.001	2031	2255	601
1e-04	**947**	**542**	**400**
1e-05	0	0	0
1e-06	0	0	0
1e-07	0	0	0

B **Control versus Vinclozolin Lineage Small ncRNA**

P-value	F1	F2	F3
0.001	57	23	69
1e-04	**32**	**8**	**34**
1e-05	14	3	16
1e-06	6	0	8
1e-07	4	0	3

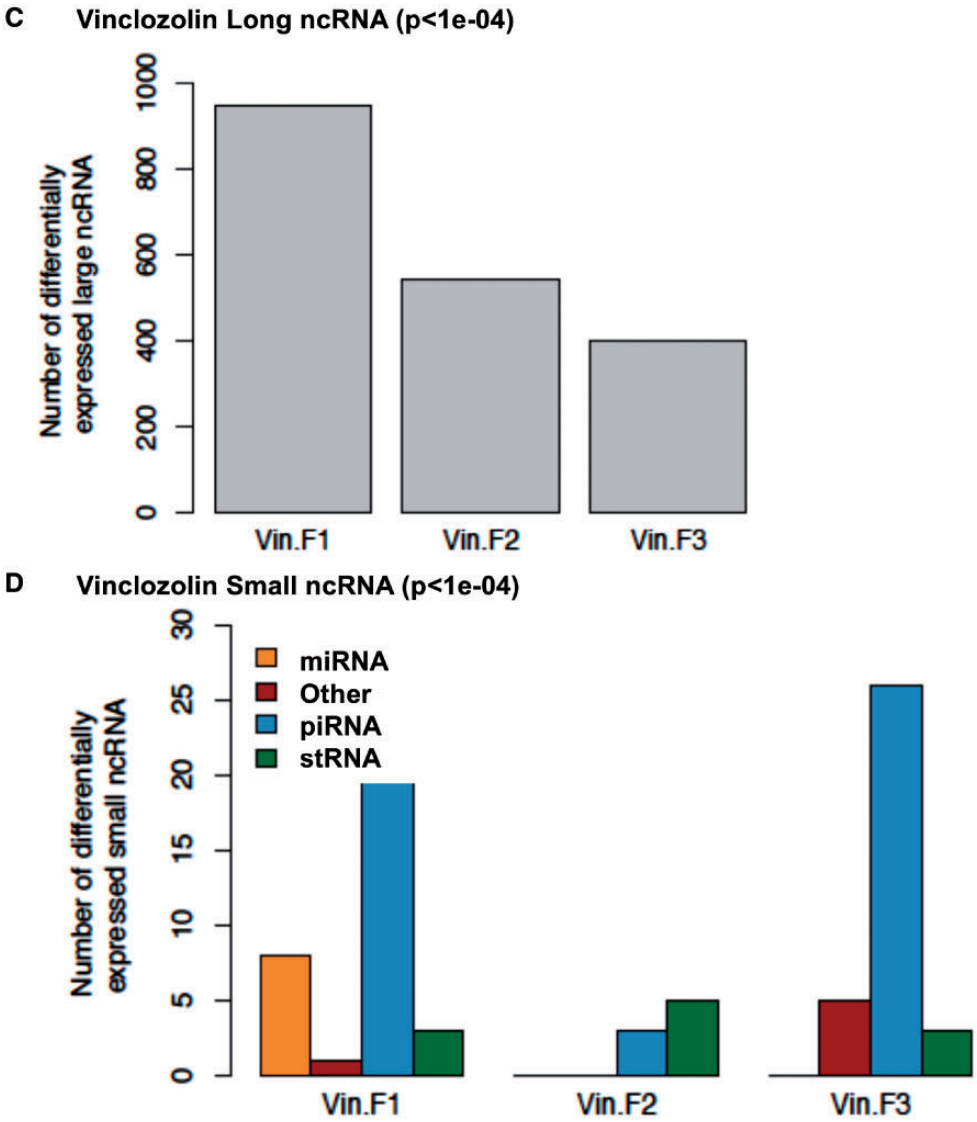

Figure 5: ncRNA differentially regulated in control versus vinclozolin lineage F1, F2, and F3 generation sperm. **(A)** lncRNA and **(B)** sncRNA numbers at different P-value thresholds. **(C)** The number of lncRNA ($P < 1e\text{-}04$) for the F1, F2, and F3 generation correlated to the number of differential lncRNA. **(D)** The number of sncRNA ($P < 1e\text{-}04$) for the F1, F2, and F3 generation correlated to the number of miRNA, piRNA, stRNA, and other sncRNA

anxiety behaviors have been shown to be induced by vinclozolin [37, 56]. Analyzing in parallel DNA methylation, ncRNA content, and histone retention in the same sperm samples from F1, F2, and F3 generation control versus vinclozolin lineage rats provides a broader comprehensive analysis of epigenetic alterations linked with environmentally induced germline epimutations. Classic toxicology studies for risk assessment investigate the direct exposure of the individual only, disregarding the impacts on future generations. However, transgenerational studies on environmental toxicants have shown that even if a

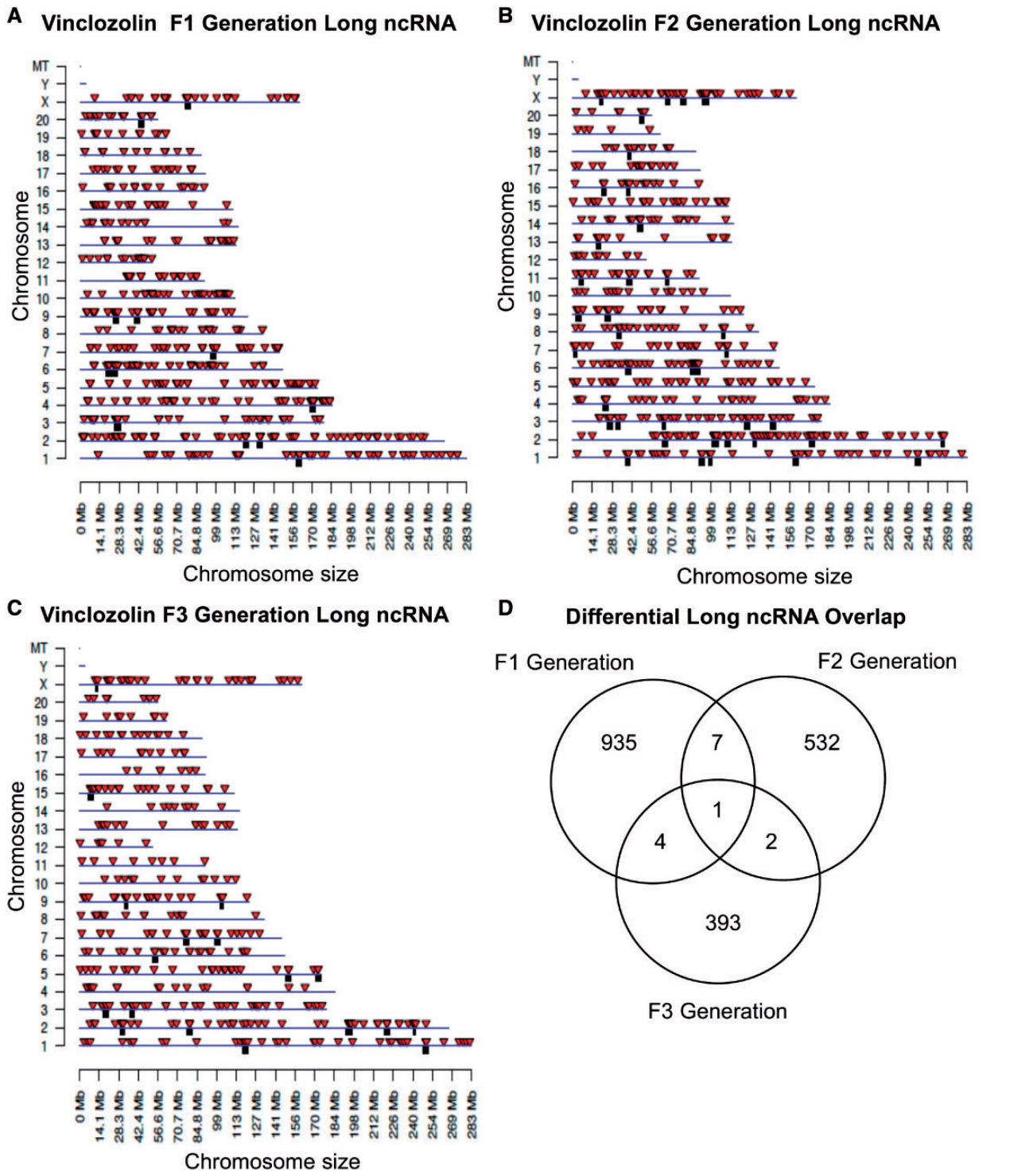

Figure 6: chromosomal locations of lncRNA. **(A)** F1 generation, **(B)** F2 generation, and **(C)** F3 generation sperm. The lncRNA locations on the individual chromosomes are indicated with red arrowheads and clusters with black boxes. The lncRNA at a *P*-value threshold of 10^{-4} is shown. **(D)** The overlap between the lncRNA ($P < 1e\text{-}04$) in the three vinclozolin generations. Overlaps were determined based on common ncRNA names

compound seems safe or has negligible risk from direct exposure mechanisms, it can affect the offspring of future generations [28]. Treatment of a gestating F0 generation female exposes the F1 generation fetus and the germline that will generate the F2 generation (Fig. 1A). Thus, the F1 generation represents a direct exposure, the F2 generation is a mix of direct and generational exposure, and the F3 generation and subsequent generations are considered purely transgenerational. This study investigates and compares the sperm epimutations in each of these generations.

Alterations in DNA methylation patterns were the first epigenetic process shown in F3 generation sperm [16, 57].

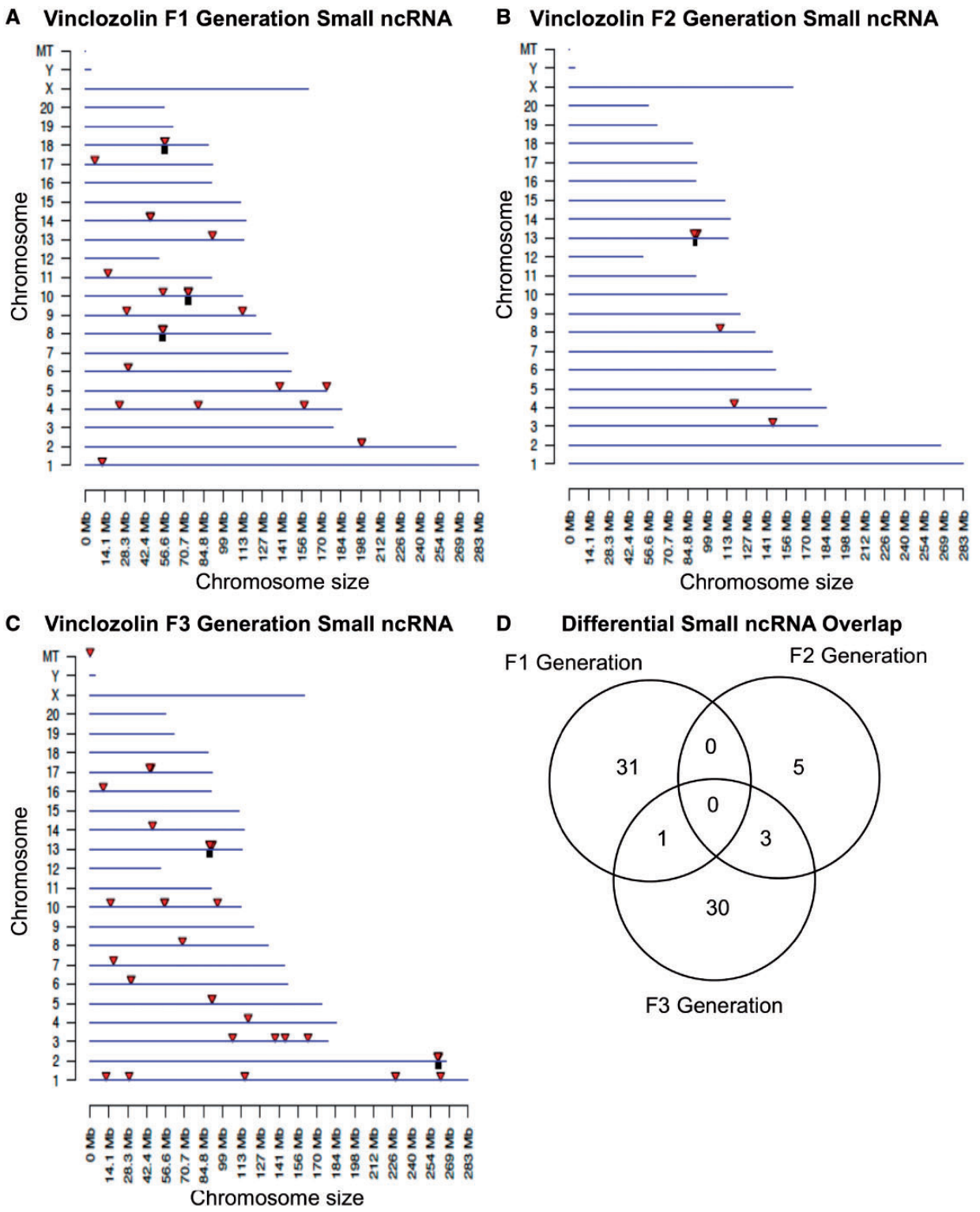

Figure 7: chromosomal locations of small ncRNA. **(A)** F1 generation, **(B)** F2 generation, and **(C)** F3 generation. The sncRNA locations on the individual chromosomes are indicated with red arrowheads and clusters with black boxes. The sncRNA at an FDR-adjusted *P*-value threshold of $P < 1e\text{-}04$ is shown. **(D)** The overlap between the sncRNAs ($P < 1e\text{-}04$) in the three vinclozolin generations. Overlaps were determined based on common RNA names

Therefore, many studies have focused on DNA methylation alterations in the germline and since then numerous chemicals, nutrition or stress exposures have been shown to induced transgenerational phenotypes [21]. A previous study identified a distinct set of DMRs in vinclozolin lineage rat sperm DNA methylation between the F1 and the F3 generation [58]. Most DMRs identified in this study are unique between the F1, F2, and F3 generations. This shows that the direct exposure F1 generation sperm and transgenerational F3 generation sperm DMRs are specific to each generation. Interestingly, we observed

A Vinclozolin F1 Generation DHRs

P-value	All Window	Multiple Window
1e-04	161	3
1e-05	22	2
1e-06	**5**	**0**
1e-07	0	0
1e-08	0	0
Number of significant windows	1	
Number of DHRs	5	

B Vinclozolin F2 Generation DHRs

P-value	All Window	Multiple Window
1e-04	122	3
1e-05	21	1
1e-06	**3**	**0**
1e-07	0	0
1e-08	0	0
Number of significant windows	1	
Number of DHRs	3	

C Vinclozolin F3 Generation DHRs

P-value	All Window	Multiple Window
1e-04	3542	169
1e-05	627	23
1e-06	**99**	**2**
1e-07	19	0
1e-08	5	0
Number of significant windows	1	2
Number of DHRs	97	2

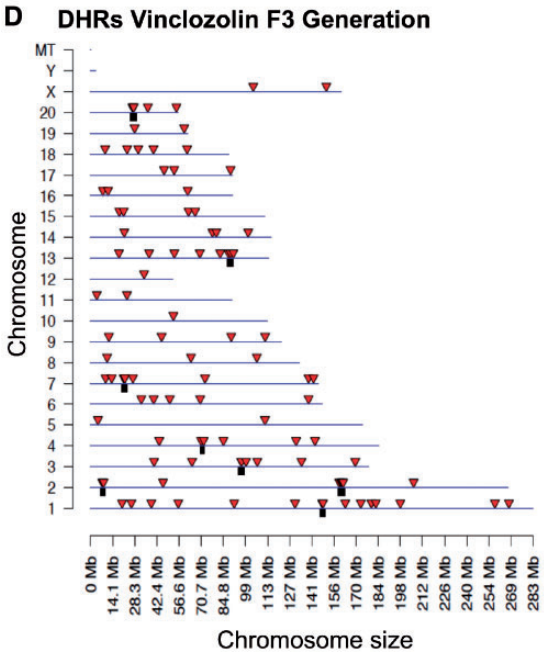

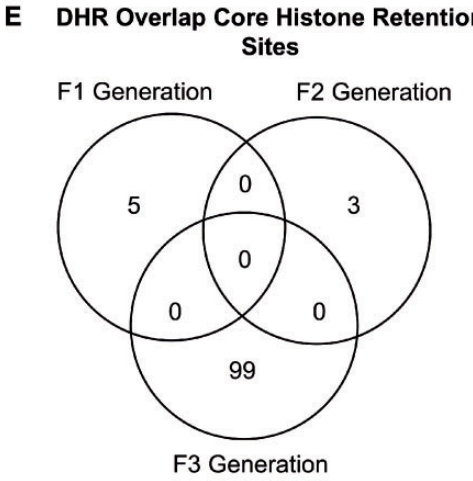

Figure 8: vinclozolin DHRs. **(A)** F1 generation, **(B)** F2 generation, and **(C)** F3 generation. The number of DHRs found using different *P*-value cutoff thresholds. The All Window column shows all DHRs. The Multiple Window column shows the number of DHRs containing at least two significant windows. **(D)** Chromosomal locations of the DHRs in the F3 generation on individual chromosomes are indicated by red arrowheads and DHR clusters with black boxes. All DHRs at a *P*-value threshold of 1e-06 are shown. **(E)** The DHR overlap ($P < 1e\text{-}06$) for the F1, F2, and F3 generation sperm

that the F2 generation seems to have fewer epimutations and has minimal overlap with the F1 and F3 generations. A small set of overlapping DMRs between the F2 and F3 generation sperm are presented in the Supplementary Fig. S4. These represent the potential transgenerational DMR that appear first in the F2 generation. In addition, no known imprinted genes correlated to the DMRs identified. As classic imprinted genes are resistant to environmental alterations in regards to DNA methylation [59], they do not appear in the differential DNA methylation regions observed.

Environmental conditions such as traumatic stress in early life in mice altered miRNA expression and behavioral and metabolic responses in the progeny. Several miRNAs were affected in the serum and brain of the traumatized animals and their progeny when adult. Sperm of traumatized males was also affected. Injection of sperm ncRNAs from these males into fertilized wild-type oocytes reproduced the behavioral and metabolic changes in the resulting offspring. These results suggest that sncRNAs are sensitive to environmental factors in early life and contribute to the inheritance of trauma-induced phenotypes across generations [39]. Vinclozolin-induced epigenetic transgenerational inheritance of disease has also been shown to involve alterations in sperm sncRNA [40]. Transgenerational lncRNA and sncRNA have been proposed to have diverse functions [5]. The sncRNA often targets specific genes through alterations in mRNA metabolism or binding protein [60], whereas the lncRNA regulates the transcriptional machinery and targets multiple distal genes. In this study, the number of lncRNA was much higher than the number of sncRNA. The overlap between each generation was very low or nonexistent. The piRNA was the most common class of sncRNA for the F1 and F3 generations, stRNAs (small tRNA fragments) were the most common for the F2 generation (Fig. 5D). Our results show that concurrent DNA methylation and ncRNA alterations in sperm may be

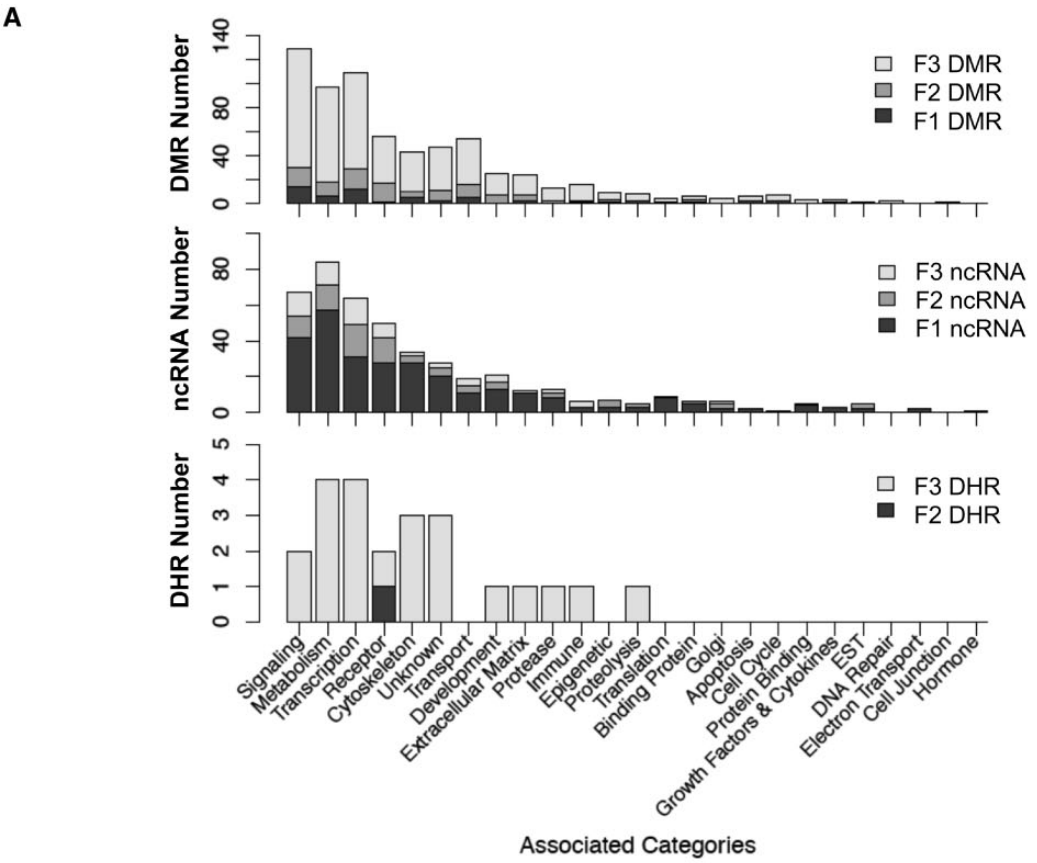

B

Generations / Epimutations	F1 DMRs	F1 lncRNA	F1 sncRNA	F1 DHRs	F2 DMRs	F2 lncRNA	F2 sncRNA	F2 DHRs	F3 DMRs	F3 lncRNA	F3 sncRNA	F3 DHRs
Axon Guidance	5	3			1				10			
Metabolic Pathways		35			4	5			41			
cGMP-PKG Signaling Pathway		6							14			
Human Papillomavirus Infection		6						3	10	3		
Olfactory Transduction		4			5	3			13	5		
Pathways in Cancer		10				3			13	3		
Neuroactive Ligand-Receptor Interaction		3			4				7			
Wnt Signaling Pathway		7							4	3		

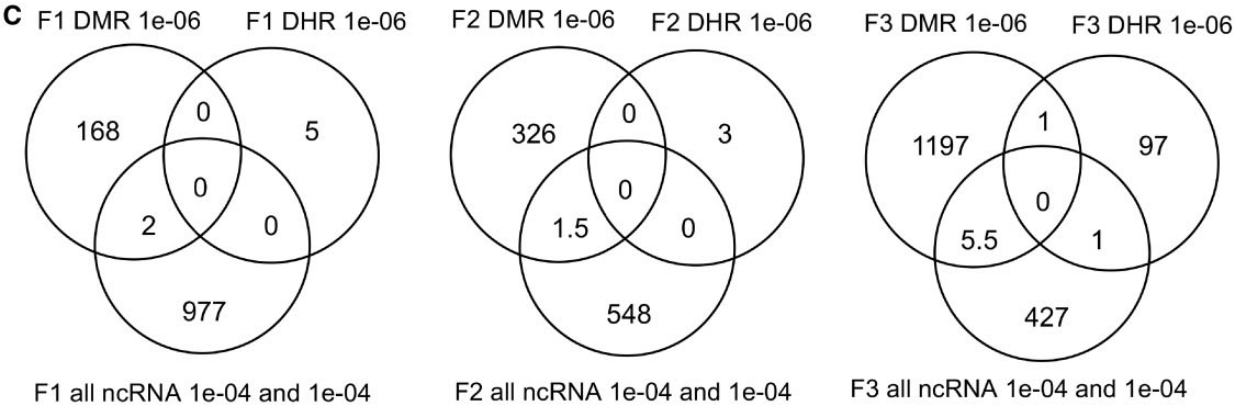

Figure 9: epimutation overlaps and gene associations. **(A)** The number of DMR, ncRNA, and DHR epimutation-associated genes in each gene category for the F1, F2, and F3 generations. **(B)** Gene pathways with epimutation-associated genes for the DMRs, DHRs and ncRNAs in the F1, F2 and F3 generations. The pathways with greater than three associated genes for each epimutation type are listed that were in general common between generations. **(C)** Overlaps of the F1, F2, and F3 generation epimutations between the DMRs, DHRs, and ncRNAs

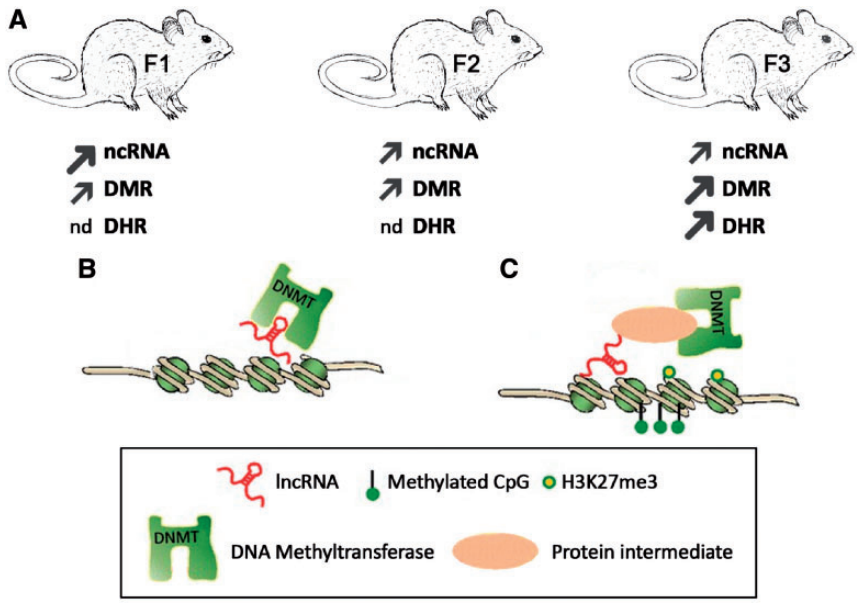

Figure 10: The regulatory mechanisms of DNA methylation by lncRNAs. **(A)** Summary of the different epimutations in the F1, F2, and F3 generation exposed rat sperm with larger/thicker arrows reflecting larger numbers of epimutations than thinner arrows and nd (negligible detected). **(B)** lncRNA/DNMT interaction prevents locus-specific DNA methylation locally *in cis*. **(C)** lncRNA interacts with DNMT1 (methyltransferase 1) indirectly through a protein intermediate. Figure modified from [43]

associated with the epigenetic transgenerational inheritance phenomenon.

Sperm chromatin not only has a unique structure to condense and protect the paternal DNA, but it also provides epigenetic information supporting early embryonic development. The histones and other chromatin proteins remaining are located in structurally and transcriptionally relevant positions in the genome and carry diverse posttranslational modifications relevant to the control of embryonic gene expression. In *Caenorhabditis elegans* and *Drosophila*, inheritance of phenotypes has been associated with histone modifications [13, 61] which has not been reported in mammals. Histone modifications and retentions have been shown to be implicated in male fertility [53, 62]. However, until recently the role of histone retention has not been implicated in transgenerational inheritance studies [52]. At the end of spermatogenesis the histones are removed in many species and the DNA is condensed by protamines forming highly dense nucleoprotamine complexes [63]. Generally, 5–10% of histones are retained and are thought to play a role in the zygotic and early embryonic gene expression [53, 64–67]. In this study, the hypothesis that vinclozolin could alter histone retentions in a transgenerational manner was investigated. In a previous study, control sperm rats were shown to have a highly reproducible core set of histones [52]. This core set of histones generally remained the same in the control animals and the animals exposed to vinclozolin between the F1, F2, and F3 generations. Because of its high reproducibility and consistency between each generation, and despite the treatment with DDT or vinclozolin, these core histone sites are highly conserved and speculated to be critical for early development [52]. The analysis of DHRs revealed that the F1 and the F2 generation control versus vinclozolin lineage sperm had negligible DHRs (Fig. 8). This observation suggests that the direct vinclozolin exposure does not alter histone retention or trigger any changes. However, the F3 generation control versus vinclozolin lineage sperm DHRs increased considerably in comparison to the F1 and F2 generation DHRs. In addition to the DMRs and ncRNAs, alterations in histone retention sites are also associated with the vinclozolin-induced transgenerational F3 generation sperm. Unlike the ncRNAs and DMRs, the F1 and F2 generation histone retention sites were not affected in the exposed animals. The DHR epimutations are all present in the transgenerational F3 generation sperm and therefore might also play a role in mediating the epigenetic transgenerational inheritance phenomenon.

In order to investigate the integration of DMRs, ncRNA, and DHR, the overlap of the different genomic sites between the different epimutations was analyzed. The chromosomal locations of the DMR, ncRNA, and DHR epimutations were distinct with a low number of overlaps. These transgenerational epimutations have chromosomal localizations that are distinct between each other, but generally they are present in regions with similar genomic features (e.g. CpG desert and size). The genome evolving over time develops regions that have very low cytocine (C) levels due to the ability of DNA methylation of the CpG site to promote susceptibility for a C to T conversion point mutation. Over 90% of the known point mutations in the genome are C to T conversions. Therefore, if a cluster of CpG sites with DNA methylation are conserved evolutionarily in these deserts of CpG, they likely are functionally important [55].

The gene associations of the transgenerational epimutations identified two similar categories of genes for the ncRNA and the DMRs involving metabolism, signaling, and transcription. The analysis comparing the F1, F2, and F3 generation epimutation-associated genes showed minimal overlap between the different types of epimutations (Fig. 9C). Each one of them (DMRs, ncRNA, DHRs) appears to associate with different pathways and may be integrated on a functional level. Although the epimutations in sperm can have associated genes, the sperm are transcriptionally silenced due to the compaction of DNA with protamines and complete loss of transcriptional machinery. The epimutations observed will primarily function in the early embryo to impact gene expression and epigenetic programming to alter the embryonic stem cell epigenome and transcriptome. Therefore all somatic cells derived from this stem cell population will have altered epigenomes and transcriptomes, and those sensitive to that will have a susceptibility to develop

disease later in life. Therefore, the epimutation gene associations may be important for later somatic cell development and differentiation, but not relevant to sperm function.

Interestingly, the comparisons in the F1, F2, and F3 generations provide insights into the direct exposure effects to vinclozolin and transgenerational impacts of the exposure. The F1 and F2 generations are exposed directly to vinclozolin (Fig. 1B), whereas the F3 generation is the first transgenerational generation. The effects observed in the F1 and F2 generations were different from the ones observed in the F3 generation. Predominantly, ncRNAs were altered by the direct exposure to vinclozolin in the F1 generation whereas the DNA methylation and histone retention sites were more predominant in the F3 generation. Histone retention did not seem to be affected by a direct exposure of vinclozolin. Therefore, the number of ncRNA was dramatically altered in the F1 generation, but to a lesser extent in the F2 and F3 generations. The altered ncRNA was also distinct between each generation (Fig. 9B). The transgenerational F3 generation alterations in DNA methylation, ncRNAs, and histone retention are distinct from the direct exposure in the F1 and F2 generations.

The analysis of the different epimutations associated gene pathways revealed that the F1 generation ncRNA seemed to be targeted by the direct vinclozolin exposure. However, these ncRNA epimutations (predominantly lncRNA) associated gene pathways disappeared in the F3 generation and similar associated gene pathways were found within the DMRs. The hypothesis is that the ncRNA could be more sensitive to the direct exposure to vinclozolin, then mediate the formation of the other epimutations in the next generation with DNA methylation and histone retention becoming permanent and mediating the epigenetic transgenerational inheritance in the future generations. An emerging hypothesis is the capacity of ncRNAs to modulate gene expression and many of them have been identified to participate in epigenetic control by interacting with various types of proteins involved in histone modification or chromatin remodeling [43]. Although these ncRNA regulations have not been observed in transgenerational animals, lncRNAs appear to be able to modulate DNA and/or histone methylation [43, 68]. Therefore, ncRNA may be the epimutation that helps mediate the formation and actions of the other types of epimutations. Based on Zhao *et al.*, two hypotheses are proposed to explain how lncRNA can interact directly or indirectly with diverse DNMT members (Fig. 10B) [43]. Through recruitment or eviction the lncRNA can either promote or repress DNA methylation *in cis* or *in trans*. The dynamic of the lncRNA repertoire and the ncRNA plasticity to interact with DNA, ncRNA, and protein makes lncRNA a potential mediator to regulate local and sequence-specific DNA methylation or demethylation. Although lncRNA are not as well annotated or functionally linked as sncRNA, as seen in Supplementary Tables S5–S7 nearly a third of those observed have associated genes. These modifications can result in global changes in DNA methylation profile, thus changing how cells can respond to diverse stimuli (Fig. 10). Even though it has not been shown yet, an interplay between lncRNA and histones is likely. Clearly an integration and interplay between the different epigenetic processes will be critical in the epigenetic transgenerational phenomenon and regulation of genome activity.

Studies are in progress to explore the integration of these transgenerational epimutations. One of the possibilities is that the transgenerational epimutations developed in the F1 and F2 generations alter the developmental epigenetic programming of the primordial germ cells (PGCs) which are the stem cells for the germline. This epigenetic alteration in the PGCs development and become permanently established and is transmitted through the germline to the next generation. This germline reprogramming will promote the epigenetic transgenerational inheritance phenomenon. Epigenetic alterations in the transgenerational PGCs have already been observed [32, 69], but further studies are required to better understand the PGCs' transgenerational mechanisms. This study provides new insights into the distinct epigenetic alterations between a direct exposure phenomenon and the transgenerational impact of the exposure. Additional support that vinclozolin is concurrently altering these different types of epimutations comes from similar observations of concurrent alterations following DDT exposure [7].

Further investigation is needed to better understand the integrated mechanisms of the unique transgenerational F3 generation germline epigenetic alterations. It appears that the phenomenon is more complex than just a direct exposure triggering the formation of epimutations that are then simply maintained in the subsequent generations. This study finds concurrent alterations of DNA methylation, ncRNA, and histone retention in the sperm. Observations indicate that all three types of epimutations are involved in the epigenetic transgenerational inheritance phenomenon. The ncRNA have already been shown to act on DNA methylation or histone methylation [43, 68]; so it is not surprising to discover that DNA methylation, ncRNA, and histone retention appear to be integrated to facilitate the epigenetic transgenerational inheritance. The potential impact of these epimutations on disease etiology and other areas in biology requires further investigation and clarification of the mechanisms involved.

Methods

Animal Studies and Breeding

Female and male rats of an outbred strain Hsd: Sprague Dawley SD®™ (Harlan) at about 70 and 100 days of age were fed *ad lib* with a standard rat diet and received *ad lib* tap water for drinking. To obtain time-pregnant females, the female rats in proestrus were pair-mated with male rats. The sperm-positive (Day 0) rats were monitored for diestrus and body weight. On Days 8 through 14 of gestation [36], the females received daily intraperitoneal injections of vinclozolin (100 mg/kg BW/day) or DMSO. The vinclozolin was obtained from Chem Service Inc. (West Chester, PA) and was injected in a 20-µl DMSO vehicle as previously described [70]. Treatment lineages are designated "control" or "vinclozolin" lineages. The treated gestating female rats were designated as the F0 generation. The offspring of the F0 generation rats were the F1 generation. Non-littermate females and males aged 70–90 days from the F1 generation of control or vinclozolin lineages were bred to obtain F2 generation offspring. The F2 generation rats were bred to obtain F3 generation offspring. Individuals were maintained for 12 months and euthanized for sperm collection. The F1–F3 generation offspring were not themselves treated directly with vinclozolin. The control and vinclozolin lineages were housed in the same room and racks with lighting, food, and water as previously described [54, 70, 71]. All experimental protocols for the procedures with rats were pre-approved by the Washington State University Animal Care and Use Committee (IACUC approval # 02568-49).

Testis sections from the males were obtained, fixed for histology, and examined by Terminal Deoxynucleotidyl Transferase-mediated dUTP Nick End Labeling (TUNEL) assay (*in situ* cell death

detection kit, Fluorescein, Sigma, St. Louis, MO) to assess spermatogenic cell apoptosis.

Epididymal Sperm Collection and DNA

The epididymis was dissected free of connective tissue, a small cut made to the cauda and tissue placed in 5 ml of 1× PBS solution for up to 24 h at 4°C. The epididymal tissue was minced and the released sperm was centrifuged at 6000 g, then the supernant removed, and the pellet resuspended in NIM buffer, to be stored at −80°C until further use. One hundred microliters of sperm suspension was sonicated to destroy somatic cells and tissue, spun down at 6000 g, the sperm pellet washed with 1× PBS once, and then combined with 820 µl DNA extraction buffer and 80 µl 0.1 M DTT. The sample was incubated at 65°C for 15 min. Following this incubation 80 µl proteinase K (20 mg/ml) was added and the sample incubated at 55°C for at least 2 h under constant rotation. Then 300 µl of protein precipitation solution (Promega, A7953) was added, the sample mixed thoroughly and incubated for 15 min on ice. The sample was centrifuged at 12 500 g for 30 min at 4°C. One milliliter of the supernatant was transferred to a 2-ml tube and 2 µl of glycoblue and 1 ml of cold 100% isopropanol were added. The sample was mixed well by inverting the tube several times, then left in −20°C freezer for at least 1 h. After precipitation the sample was centrifuged at 12 500 g for 20 min at 4°C. The supernatant was taken off and discarded without disturbing the (blue) pellet. The pellet was washed with 70% cold ethanol by adding 500 µl of 70% ethanol to the pellet and returning the tube to the freezer for 20 min. After the incubation the tube was centrifuged for 10 min at 4°C at 12 500 g and the supernatant discarded. The tube was spun again briefly to collect residual ethanol to the bottom of the tube and then as much liquid as possible was removed with gel loading tip. Pellet was air-dried at RT until it looked dry (about 5 min). Pellet was then resuspended in 100 µl of nuclease free water.

Equal amounts of DNA or ncRNA from each individuals sperm from 3–4 different individuals for the F1 and F2 generations and 4–6 different individuals for the F3 generation were pooled and three different pools generation for each F1, F2, and F3 generation control and vinclozolin lineage males. Therefore, each pool had different individuals and there were three pools for each group. A summary of the pools for the DNA and ncRNA pools is shown in Supplementary Table S14. Two analyses of the same pool were taken, one for DNA and one for ncRNA. Therefore, between 10 and 17 individuals were present in the three pools for the subsequent analysis.

RNA Isolation

The F1–F3 generation vinclozolin and control lineage male epididymal sperm were collected and processed as previously described and stored at −80°C until use [57]. The total RNA (messenger RNA, lncRNA, ribosomal RNA, sncRNA) was isolated using the mirVana miRNA Isolation Kit (Life Technologies) following the manufacturer's instructions with modifications at the lysis stage. In brief, after addition of lysis buffer, the sperm pellets were manually homogenized, followed by a 20-min incubation at 65°C. Samples were then placed on ice, and the default protocol was resumed. For quality control, RNA integrity numbers (RIN) were obtained by RNA 6000 Pico chips run on an Agilent 2100 Bioanalyzer (Agilent). A RIN of 2–4 indicates good sperm RNA quality. Concentration was determined using the Qubit RNA HS Assay Kit (ThermoFisher). Biological replicates of sperm were pooled by equal ncRNA content and were concentrated using Agencourt AMPure XP beads (Beckman Coulter). Some pools had underrepresented replicates due to low concentration. In this case, the maximum RNA content from the replicate was used in the pool and the pool was concentrated. The pools and samples that were underrepresented are as follows: F1 control pool 3, samples 1 and 2; F2 control pool 2, sample 3; and F2 vinclozolin pool 2, sample 3. Equal amounts of each pool were used in the final analysis.

Methylated DNA Immunoprecipitation

MeDIP with genomic DNA was performed as follows: rat sperm DNA pools were generated using the appropriate amount of genomic DNA from each individual for three pools each of control and vinclozolin lineage animals. Genomic DNA was sonicated using the Covaris M220 the following way: the pooled genomic DNA was diluted to 130 µl with TE buffer into the appropriate Covaris tube. Covaris was set to 300-bp program and the program was run for each tube in the experiment. Each sonicated DNA of 10 µl was run on 1.5% agarose gel to verify fragment size. The sonicated DNA was transferred from the Covaris tube to a 1.7-ml microfuge tube and the volume measured. The sonicated DNA was then diluted with TE buffer (10 mM Tris HCl, pH7.5; 1 mM EDTA) to 400 µl, heat-denatured for 10 min at 95°C, then immediately cooled on ice for 10 min. Then 100 µl of 5× IP buffer and 5 µg of antibody (monoclonal mouse anti-5-methyl cytidine; Diagenode #C15200006) were added to the denatured sonicated DNA. The DNA–antibody mixture was incubated overnight on a rotator at 4°C.

The following day magnetic beads (Dynabeads M-280 Sheep anti-Mouse IgG; 11201 D) were pre-washed as follows: the beads were resuspended in the vial, then the appropriate volume (50 µl per sample) was transferred to a microfuge tube. The same volume of Washing Buffer (at least 1 ml PBS with 0.1% BSA and 2 mM EDTA) was added and the bead sample was resuspended. Tube was then placed into a magnetic rack for 1–2 min and the supernatant was discarded. The tube was removed from the magnetic rack and the beads were washed once. The washed beads were resuspended in the same volume of 1× IP buffer (50 mM sodium phosphate ph7.0, 700 mM NaCl, 0.25% TritonX-100) as the initial volume of beads. Fifty microliters of beads was added to the 500 µl of DNA–antibody mixture from the overnight incubation, then incubated for 2 h on a rotator at 4°C.

After the incubation the bead–antibody–DNA complex was washed three times with 1× IP buffer as follows: the tube was placed into magnetic rack for 1–2 min and the supernatant discarded, then washed with 1× IP buffer three times. The washed bead–DNA solution is then resuspended in 250 µl digestion buffer with 3.5 µl Proteinase K (20 mg/ml). The sample was then incubated for 2–3 h on a rotator at 55°C and then 250 µl of buffered phenol–chloroform–isoamylalcohol solution was added to the supe and the tube vortexed for 30 s then centrifuged at 12 500 g for 5 min at room temperature. The aqueous supernatant was carefully removed and transferred to a fresh microfuge tube. Then 250 µl chloroform was added to the supernatant from the previous step, vortexed for 30 s and centrifuged at 12 500 g for 5 min at room temperature. The aqueous supernatant was removed and transferred to a fresh microfuge tube. To the supernatant 2 µl of glycoblue (20 mg/ml), 20 µl of 5 M NaCl and 500 µl ethanol were added and mixed well, then precipitated in −20°C freezer for 1 h to overnight.

The precipitate was centrifuged at 12 500 g for 20 min at 4°C and the supernatant removed, while not disturbing the pellet. The pellet was washed with 500 µl cold 70% ethanol in −20°C freezer for 15 min, then centrifuged again at 12 500 g for 5 min at 4°C and the supernatant was discarded. The tube was spun again briefly to collect residual ethanol to the bottom of the tube and as much liquid as possible was removed with gel loading tip. Pellet was air-dried at RT until it looked dry (about 5 min) then resuspended in 20 µl H_2O or TE. DNA concentration was measured in Qubit (Life Technologies) with ssDNA kit (Molecular Probes Q10212).

ncRNA Sequencing Analysis

LRNA and noncoding RNA were constructed using total RNA with the KAPA Stranded RNA-Seq Library Preparation kit with RiboErase, according to the manufacturer's instructions, with some modifications. The adaptor and barcodes used were from NEBNext Multiplex Oligos for Illumina. Prior to PCR amplification, libraries were incubated at 37°C for 15 min with the USER enzyme (NEB). PCR cycle number was determined using qPCR with the KAPA RealTime Library Amplification kit before final amplification. Size selection (300–700 bp) was performed using Agencourt AMPure XP beads (Beckman Coulter). Quality control was performed using Agilent DNA High Sensitivity chips (Agilent) and Qubit dsDNA high sensitivity assay (ThermoFisher). Libraries were pooled and loaded onto an Illumina NextSeq High Output v2 1x75 chip, and sequenced on an Illumina NextSeq 500 sequencer. Bioinformatics analysis was used to separate mRNA libraries from ncRNA libraries (see ncRNA Bioinformatics section).

Prior to sncRNA library preparation, total sperm RNA samples were enriched for sncRNAs using the miRNA enrichment protocol (Beckman Coulter), and libraries were constructed using the NEBNext Multiplex Small RNA Library Prep Set for Illumina, and barcoded with NEBNext Multiplex Oligos for Illumina. Size selection (135–170 bp) was performed using the Pippin Prep (Sage Science). Quality control was performed using Agilent DNA High Sensitivity chips (Agilent) and Qubit dsDNA high sensitivity assay (ThermoFisher). Libraries were pooled and loaded onto an Illumina NextSeq High Output v2 1x75 chip, and sequenced on an Illumina NextSeq 500 sequencer.

Histone Chromatin Immunoprecipitation ChIP-Seq

Histone chromatin immunoprecipitation with genomic DNA was performed as follows (adapted from [72]): rat sperm pools were generated using a total of 8 million sperm per pool for 3 pools of control and vinclozolin lineage animals. The control pools contained equal amounts of sperm for each of 3–4 individuals for a total of $n = 11$ rats and the vinclozolin pools contained equal amounts of sperm for each of 3 individuals for a total of $n = 9$ rats per exposure group. To remove any somatic cell contamination, sperm samples from each animal were sonicated 10 s using a Sonic Dismembrator Model 300 (Thermo Scientific Fisher, USA) then centrifuged 4000 g for 5 min at 4°C. The supernatant was discarded and the pellet was resuspended and counted individually on a Neubauer counting chamber (Propper Manufacturing Co., Inc., New York, USA) prior to pooling. The sperm pools were reconstituted up to 1 ml with 1× PBS. To reduce disulfide bonds, 50 µl of 1 M DTT was added to each pool and the pools were then incubated for 2 h at room temperature under constant rotation. To quench any residual DTT in the reaction, 120 µl of fresh 1 M NEM (*N*-ethylmaleimide, Thermo Scientific, Rockford, USA) was then added and the samples were incubated for 30 min at room temperature under constant rotation. The sperm cells were pelleted at 2000 g for 5 min at room temperature and the supernatant was discarded. Pellets were resuspended in 1× PBS and then spun again at 2000 g for 5 min at room temperature. The supernatant was discarded. The sperm cell DNA was divided into aliquots of 4 µg of DNA and was then suspended in "complete buffer" [final concentration: 15 mM Tris-HCl (pH 7.5), 5 mM $MgCl_2$, 0.1 mM EGTA; all filtered through a 0.22-µm filter and stored at room temperature; 0.5% tergitol (vol/vol) and 1% DOC (wt/vol), sodium deoxycholate]. A 130 µl of this complete buffer was added to each DNA aliquot. The samples were mixed and incubated for 20 min on ice. These aliquots were sonicated using the Covaris M220 the following way: 4 µg of genomic DNA was resuspended in 130 µl of complete buffer supplemented with tergitol 0.5% and DOC 1%. Covaris was set to a 10-min "Chromatin shearing" program and the program was run for each tube in the experiment.

For each sample 10 µl was run on a 1.5% agarose gel to verify fragment size. Aliquoted samples were pooled back together and centrifuged at 12 500 g for 10 min at room temperature. The supernatant was transferred to a fresh microfuge tube. Sixty-five microliters of protease inhibitor cocktail (1 tablet dissolved in 500 µl, 20× concentrated) (Roche, cat. no. 11 873 580 001) was added to each sample as well as 3 µl of antibody (monoclonal rabbit antihistone H3, Millipore 05-928). The DNA–antibody mixture was incubated overnight on a rotator at 4°C. The following day, magnetic beads (ChIP-Grade protein G magnetic beads, Cell Signaling 9006) were pre-washed as follows: the beads were resuspended in the vial, then 30 µl per sample was transferred to a microfuge tube. The same volume of Washing Buffer (at least 1 ml) was added and the bead sample was resuspended. Tube was then placed into a magnetic rack for 1–2 min and the supernatant was discarded. The tube was removed from the magnetic rack and the beads were washed once. The washed beads were resuspended in the same volume of 1× IP buffer as the initial volume of beads. Thirty microliters of beads was added to each DNA–antibody mixture from the overnight incubation, then incubated for 2 h on a rotator at 4°C. After the incubation, the bead–antibody–DNA complex was washed three times with 1× IP buffer as follows: the tube was placed into a magnetic rack for 1–2 min and the supernatant was discarded, then washed with 1× IP buffer 3 times. The washed bead–antibody–DNA solution was then resuspended in 300 µl of digestion buffer and 3 µl proteinase K (20 mg/ml). The sample was incubated for 3 h on a rotator at 56°C. After incubation the samples were extracted with phenol–chloroform–isoamylalcohol and precipitated with 2 µl of glycoblue (20 mg/ml), a one-tenth volume of 3 M sodium acetate and two volumes of ethanol overnight at −20°C.

The precipitate was centrifuged at 14 000 g for 30 min at 4°C and the supernatant was removed, while not disturbing the pellet. The pellet was washed with 500 µl cold 70% ethanol, then centrifuged again at 14 000 g for 10 min at 4°C and the supernatant was discarded. The tube was spun briefly to collect residual ethanol and as much liquid as possible was removed with a gel loading tip. Pellet was air-dried at RT until it looked dry (about 5 min) then resuspended in 20 µl H20. DNA concentration was measured in the Qubit (Life Technologies) with the BR dsDNA kit (Molecular Probes Q32853).

MeDIP-Seq Analysis

The MeDIP pools were used to create libraries for NGS using the NEBNext® Ultra™ RNA Library Prep Kit for Illumina® (NEB, San

Diego, CA) starting at step 1.4 of the manufacturer's protocol to generate double-stranded DNA. After this step the manufacturer's protocol was followed. Each pool received a separate index primer. NGS was performed at WSU Spokane Genomics Core using the Illumina HiSeq 2500 with a PE50 application, with a read size of ~50 bp and ~100 million reads per pool. Two to three libraries were run in one lane.

Histone ChIP-Seq Analysis

The ChIP pools were used to create libraries for NGS using the NEBNext® Ultra™ II DNA Library Prep Kit for Illumina® (NEB, San Diego, CA). The manufacturer's protocol was followed. Each pool received a separate index primer. NGS was performed at WSU Spokane Genomics Core using Ilumina HiSeq 2500 with a PE50 application, with a read size of ~50 bp and ~35 million reads per pool. Six libraries were run in one lane.

ncRNA Bioinformatics

The sncRNA-Seq data were annotated as follows: reads shorter than 15 nt were discarded by Cutadapt [73]. The remaining reads were matched to known rat sncRNA, consisting of mature miRNA (miRBase, release 21), tRNA (Genomic tRNA Database, rn5), piRNA (piRNABank), rRNA (ENSEMBL, release 76), and mitochondrial RNA (ENSEMBL, release 76) using AASRA pipeline with default parameters [74]. Read counts generated by AASRA were statistically normalized by DESeq2 [75].

The lncRNA data were annotated as follows: trimmomatic was used to remove adaptor sequences and the low-quality reads from the RNA sequencing data [76]. To identify all the transcripts, we used Tophat2 and Cufflinks to assemble the sequencing reads based on the Ensembl_Rnor_6.0 [77]. The differential expression analyses were performed by Cuffdiff. The coding and the noncoding genes were primarily annotated through rat CDS data ensembl_Rnor_6.0. The non-annotated genes were extracted through our in-house script, then analyzed by CPAT, indicating the true ncRNAs [78].

Statistics and Bioinformatics

For the DMR and DHR analyses, the basic read quality was verified using summaries produced by the FastQC program (http://www.bioinformatics.babraham.ac.uk/projects/fastqc/). The raw reads were trimmed and filtered using Trimmomatic. The reads for each MeDIP sample were mapped to the Rnor 6.0 rat genome using Bowtie2 [76] with default parameter options. The mapped read files were then converted to sorted BAM files using SAMtools [79]. To identify DMRs and DHRs, the reference genome was broken into 100-bp windows. The MEDIPS R package [80] was used to calculate differential coverage between control and exposure sample groups. The edgeR *P*-value [81] was used to determine the relative difference between the two groups for each genomic window. Windows with an edgeR *P*-value $<10^{-6}$ were considered DMRs or DHRs. The DMR or DHR edges were extended until no genomic window with a *P*-value <0.1 remained within 1000 bp of the DMR or DHR. CpG density and other information were then calculated for the DMR based on the reference genome.

DMRs, DHRs, and ncRNA were annotated using the biomaRt R package [82] to access the Ensembl database [83]. The genes that fell within 10 kb of the DMR, DHR, or ncRNA edges were then input into the KEGG pathway search [84, 85] to identify associated pathways. The associated genes were then sorted into functional groups by consulting information provided by the DAVID [86], Panther [87], and Uniprot databases incorporated into an internal curated database (www.skinner.wsu.edu under genomic data).

Acknowledgments

We acknowledge Ms Deepika Kubsad and Ms Jayleana Barton for technical assistance and Ms Heather Johnson for assistance in preparation of the manuscript. We thank the Genomics Core Laboratories at WSU and UNR. This study was supported by a John Templeton Foundation (50183) grant to M.K.S. and NIH (ES012974) grant to M.K.S. and NIH grants (HD085506 and GM110767) to W.Y.

Supplementary data

Supplementary data are available at *EnvEpig* online.

Conflict of interest statement. None declared.

References

1. Holliday R. The inheritance of epigenetic defects. *Science* 1987; **238**:163–70.
2. Cosgrove MS, Wolberger C. How does the histone code work? *Biochem Cell Biol* 2005; **83**:468–76.
3. Gray SG, Teh BT. Histone acetylation/deacetylation and cancer: an "open" and "shut" case? *Curr Mol Med* 2001; **1**:401–29.
4. Cao J. The functional role of long non-coding RNAs and epigenetics. *Biol Proced Online* 2014; **16**:11.
5. Yan W. Potential roles of noncoding RNAs in environmental epigenetic transgenerational inheritance. *Mol Cell Endocrinol* 2014; **398**:24–30.
6. Mohammad F, Mondal T, Kanduri C. Epigenetics of imprinted long noncoding RNAs. *Epigenetics* 2009; **4**:277–86.
7. Skinner Mk, Ben Maamar M, Sadler-Riggleman I, Beck D, Nilsson E, McBirney M, Klukovich R, Xie Y, Tang C, Yan W, et al. Alterations in sperm DNA methylation, non-coding RNA and histone retention associate with DDT induced epigenetic transgenerational inheritance of disease. *Epigenetics Chromatin* 2018; **11**:8.
8. Burdge GC, Lillycrop KA, Jackson AA. Nutrition in early life, and risk of cancer and metabolic disease: alternative endings in an epigenetic tale? *Br J Nutr* 2009; **101**:619–30.
9. Jirtle RL, Skinner MK. Environmental epigenomics and disease susceptibility. *Nat Rev Genet* 2007; **8**:253–62.
10. Tang WY, Ho SM. Epigenetic reprogramming and imprinting in origins of disease. *Rev Endocr Metab Disord* 2007; **8**:173–82.
11. Quadrana L, Colot V. Plant transgenerational epigenetics. *Annu Rev Genet* 2016; **50**:467–91.
12. Brookheart RT, Duncan JG. *Drosophila melanogaster*: an emerging model of transgenerational effects of maternal obesity. *Mol Cell Endocrinol* 2016;**435**:20–8.
13. Kelly WG. Transgenerational epigenetics in the germline cycle of *Caenorhabditis elegans*. *Epigenetics Chromatin* 2014;**7**:6.
14. Carvan MJ, Kalluvila TA, Klingler RH, Larson JK, Pickens M, Mora-Zamorano FX, Connaughton VP, Sadler-Riggleman I, Beck D, Skinner MK, et al. Mercury-induced epigenetic transgenerational inheritance of abnormal neurobehavior is correlated with sperm epimutations in zebrafish. *PLoS One* 2017; **12**:e0176155.
15. Leroux S, Gourichon D, Leterrier C, Labrune Y, Coustham V, Rivière S, Zerjal T, Coville J-L, Morisson M, Minvielle F, et al. Embryonic environment and transgenerational effects in quail. *Genet Sel Evol* 2017; **49**:14.

16. Anway MD, Cupp AS, Uzumcu M, Skinner MK. Epigenetic transgenerational actions of endocrine disruptors and male fertility. *Science* 2005; **308**:1466–9.
17. Padmanabhan N, Jia D, Geary-Joo C, Wu X, Ferguson-Smith AC, Fung E, Bieda MC, Snyder FF, Gravel RA, Cross JC, et al. Mutation in folate metabolism causes epigenetic instability and transgenerational effects on development. *Cell* 2013; **155**:81–93.
18. Rassoulzadegan M, Grandjean V, Gounon P, Vincent S, Gillot I, Cuzin F. RNA-mediated non-Mendelian inheritance of an epigenetic change in the mouse. *Nature* 2006; **441**:469–74.
19. Braunschweig M, Jagannathan V, Gutzwiller A, Bee G. Investigations on transgenerational epigenetic response down the male line in F2 pigs. *PLoS One* 2012; **7**:e30583.
20. Northstone K, Golding J, Davey Smith G, Miller LL, Pembrey M. Prepubertal start of father's smoking and increased body fat in his sons: further characterisation of paternal transgenerational responses. *Eur J Hum Genet* 2014; **22**:1382–6.
21. Skinner MK. Endocrine disruptor induction of epigenetic transgenerational inheritance of disease. *Mol Cell Endocrinol* 2014; **398**:4–12.
22. Manikkam M, Tracey R, Guerrero-Bosagna C, Skinner MK. Dioxin (TCDD) induces epigenetic transgenerational inheritance of adult onset disease and sperm epimutations. *PLoS One* 2012; **7**:e46249.
23. Manikkam M, Tracey R, Guerrero-Bosagna C, Skinner M. Pesticide and insect repellent mixture (permethrin and DEET) induces epigenetic transgenerational inheritance of disease and sperm epimutations. *Reprod Toxicol* 2012; **34**:708–19.
24. Tracey R, Manikkam M, Guerrero-Bosagna C, Skinner M. Hydrocarbons (jet fuel JP-8) induce epigenetic transgenerational inheritance of obesity, reproductive disease and sperm epimutations. *Reprod Toxicol* 2013; **36**:104–16.
25. Manikkam M, Tracey R, Guerrero-Bosagna C, Skinner M. Plastics derived endocrine disruptors (BPA, DEHP and DBP) induce epigenetic transgenerational inheritance of adult-onset disease and sperm epimutations. *PLoS One* 2013; **8**:e55387.
26. Skinner MK, Manikkam M, Tracey R, Guerrero-Bosagna C, Haque MM, Nilsson E. Ancestral dichlorodiphenyltrichloroethane (DDT) exposure promotes epigenetic transgenerational inheritance of obesity. *BMC Med* 2013; **11**:228.
27. Manikkam M, Haque MM, Guerrero-Bosagna C, Nilsson E, Skinner MK. Pesticide methoxychlor promotes the epigenetic transgenerational inheritance of adult onset disease through the female germline. *PLoS One* 2014; **9**:e102091.
28. McBirney M, King SE, Pappalardo M, Houser E, Unkefer M, Nilsson E, Sadler-Riggleman I, Beck D, Winchester P, Skinner MK, et al. Atrazine induced epigenetic transgenerational inheritance of disease, lean phenotype and sperm epimutation pathology biomarkers. *PLoS One* 2017; **12**:e0184306.
29. Bayley M, Larsen PF, Baekgaard H, Baatrup E. The effects of vinclozolin, an anti-androgenic fungicide, on male guppy secondary sex characters and reproductive success. *Biol Reprod* 2003; **69**:1951–6.
30. Uzumcu M, Suzuki H, Skinner MK. Effect of the anti-androgenic endocrine disruptor vinclozolin on embryonic testis cord formation and postnatal testis development and function. *Reprod Toxicol* 2004; **18**:765–74.
31. Buckley J, Willingham E, Agras K, Baskin LS. Embryonic exposure to the fungicide vinclozolin causes virilization of females and alteration of progesterone receptor expression in vivo: an experimental study in mice. *Environ Health* 2006; **5**:4.
32. Skinner M, Guerrero-Bosagna C, Haque MM, Nilsson E, Bhandari R, McCarrey J. Environmentally induced transgenerational epigenetic reprogramming of primordial germ cells and subsequent germline. *PLoS One* 2013; **8**:e66318.
33. Nilsson EE, Skinner MK. Environmentally induced epigenetic transgenerational inheritance of disease susceptibility. *Transl Res* 2015; **165**:12–7.
34. Anway MD, Memon MA, Uzumcu M, Skinner MK. Transgenerational effect of the endocrine disruptor vinclozolin on male spermatogenesis. *J Androl* 2006; **27**:868–79.
35. Anway MD, Rekow SS, Skinner MK. Transgenerational epigenetic programming of the embryonic testis transcriptome. *Genomics* 2008; **91**:30–40.
36. Nilsson EE, Anway MD, Stanfield J, Skinner MK. Transgenerational epigenetic effects of the endocrine disruptor vinclozolin on pregnancies and female adult onset disease. *Reproduction* 2008; **135**:713–21.
37. Skinner MK, Anway MD, Savenkova MI, Gore AC, Crews D. Transgenerational epigenetic programming of the brain transcriptome and anxiety behavior. *PLoS One* 2008; **3**:e3745.
38. Guerrero-Bosagna C, Savenkova M, Haque MM, Nilsson E, Skinner MK. Environmentally induced epigenetic transgenerational inheritance of altered Sertoli cell transcriptome and epigenome: molecular etiology of male infertility. *PLoS One* 2013; **8**:e59922.
39. Gapp K, Jawaid A, Sarkies P, Bohacek J, Pelczar P, Prados J, Farinelli L, Miska E, Mansuy IM. Implication of sperm RNAs in transgenerational inheritance of the effects of early trauma in mice. *Nat Neurosci* 2014; **17**:667–9.
40. Schuster A, Skinner MK, Yan W. Ancestral vinclozolin exposure alters the epigenetic transgenerational inheritance of sperm small noncoding RNAs. *Environ Epigenet* 2016; **2**:1–10.
41. Mancini-Dinardo D, Steele SJ, Levorse JM, Ingram RS, Tilghman SM. Elongation of the Kcnq1ot1 transcript is required for genomic imprinting of neighboring genes. *Genes Dev* 2006; **20**:1268–82.
42. Mohammad F, Mondal T, Guseva N, Pandey GK, Kanduri C. Kcnq1ot1 noncoding RNA mediates transcriptional gene silencing by interacting with Dnmt1. *Development* 2010; **137**:2493–9.
43. Zhao Y, Sun H, Wang H. Long noncoding RNAs in DNA methylation: new players stepping into the old game. *Cell Biosci* 2016; **6**:45.
44. Zhao J, Ohsumi TK, Kung JT, Ogawa Y, Grau DJ, Sarma K, Song JJ, Kingston RE, Borowsky M, Lee JT. Genome-wide identification of polycomb-associated RNAs by RIP-seq. *Mol Cell* 2010; **40**:939–53.
45. Cifuentes-Rojas C, Hernandez AJ, Sarma K, Lee JT. Regulatory interactions between RNA and polycomb repressive complex 2. *Mol Cell* 2014; **55**:171–85.
46. Khalil AM, Guttman M, Huarte M, Garber M, Raj A, Rivea Morales D, Thomas K, Presser A, Bernstein BE, van Oudenaarden A, et al. Many human large intergenic noncoding RNAs associate with chromatin-modifying complexes and affect gene expression. *Proc Natl Acad Sci USA* 2009; **106**:11667–72.
47. Rechavi O, Houri-Ze'evi L, Anava S, Goh WSS, Kerk SY, Hannon GJ, Hobert O. Starvation-induced transgenerational inheritance of small RNAs in *C. elegans*. *Cell* 2014;**158**:277–87.
48. Krawetz SA, Kruger A, Lalancette C, Tagett R, Anton E, Draghici S, Diamond MP. A survey of small RNAs in human sperm. *Hum Reprod* 2011; **26**:3401–12.
49. Zhang X, Gao F, Fu J, Zhang P, Wang Y, Zeng X. Systematic identification and characterization of long non-coding RNAs in mouse mature sperm. *PLoS One* 2017; **12**:e0173402.

50. Jodar M, Selvaraju S, Sendler E, Diamond MP, Krawetz SA. The presence, role and clinical use of spermatozoal RNAs. *Hum Reprod Update* 2013; **19**:604–24.
51. Chen Q, Yan W, Duan E. Epigenetic inheritance of acquired traits through sperm RNAs and sperm RNA modifications. *Nat Rev Genet* 2016; **17**:733–43.
52. Ben Maamar M, Sadler-Riggleman I, Beck D, Skinner MK. Epigenetic transgenerational inheritance of altered sperm histone retention sites. *Sci Rep* 2018; **8**:5308.
53. Hammoud SS, Nix DA, Hammoud AO, Gibson M, Cairns BR, Carrell DT. Genome-wide analysis identifies changes in histone retention and epigenetic modifications at developmental and imprinted gene loci in the sperm of infertile men. *Hum Reprod* 2011; **26**:2558–69.
54. Anway MD, Leathers C, Skinner MK. Endocrine disruptor vinclozolin induced epigenetic transgenerational adult-onset disease. *Endocrinology* 2006; **147**:5515–23.
55. Skinner MK, Guerrero-Bosagna C. Role of CpG deserts in the epigenetic transgenerational inheritance of differential DNA methylation regions. *BMC Genomics* 2014; **15**:692.
56. Anway MD, Skinner MK. Transgenerational effects of the endocrine disruptor vinclozolin on the prostate transcriptome and adult onset disease. *Prostate* 2008; **68**:517–29.
57. Guerrero-Bosagna C, Settles M, Lucker B, Skinner M. Epigenetic transgenerational actions of vinclozolin on promoter regions of the sperm epigenome. *PLoS One* 2010; **5**: e13100.
58. Beck D, Sadler-Riggleman I, Skinner MK. Generational comparisons (F1 versus F3) of vinclozolin induced epigenetic transgenerational inheritance of sperm differential DNA methylation regions (epimutations) using MeDIP-Seq. *Environ Epigenet* 2017; **3**:1–12.
59. Tang L, Liu Z, Zhang R, Su C, Yang W, Yao Y, Zhao S. Imprinting alterations in sperm may not significantly influence ART outcomes and imprinting patterns in the cord blood of offspring. *PLoS One* 2017; **12**:e0187869.
60. Dallaire A, Simard MJ. The implication of microRNAs and endo-siRNAs in animal germline and early development. *Dev Biol* 2016; **416**:18–25.
61. Ruden DM, Lu X. Hsp90 affecting chromatin remodeling might explain transgenerational epigenetic inheritance in *Drosophila*. *Curr Genomics* 2008;**9**:500–8.
62. Oliva R, Ballesca JL. Altered histone retention and epigenetic modifications in the sperm of infertile men. *Asian J Androl* 2012; **14**:239–40.
63. Balhorn R. The protamine family of sperm nuclear proteins. *Genome Biol* 2007; **8**:227.
64. Jenkins TG, Carrell DT. The paternal epigenome and embryogenesis: poising mechanisms for development. *Asian J Androl* 2011; **13**:76–80.
65. Hammoud SS, Nix DA, Zhang H, Purwar J, Carrell DT, Cairns BR. Distinctive chromatin in human sperm packages genes for embryo development. *Nature* 2009; **460**:473–8.
66. Hammoud SS, Purwar J, Pflueger C, Cairns BR, Carrell DT. Alterations in sperm DNA methylation patterns at imprinted loci in two classes of infertility. *Fertil Steril* 2010; **94**:1728–33.
67. Zhang X, San Gabriel M, Zini A. Sperm nuclear histone to protamine ratio in fertile and infertile men: evidence of heterogeneous subpopulations of spermatozoa in the ejaculate. *J Androl* 2006; **27**:414–20.
68. Joh RI, Palmieri CM, Hill IT, Motamedi M. Regulation of histone methylation by noncoding RNAs. *Biochim Biophys Acta* 2014; **1839**:1385–94.
69. Miyoshi N, Stel JM, Shioda K, Qu NA, Odahima J, Mitsunaga S, Zhang X, Nagano M, Hochedlinger K, Isselbacher KJ, et al. Erasure of DNA methylation, genomic imprints, and epimutations in a primordial germ-cell model derived from mouse pluripotent stem cells. *Proc Natl Acad Sci USA* 2016; **113**: 9545–50.
70. Manikkam M, Guerrero-Bosagna C, Tracey R, Haque MM, Skinner MK. Transgenerational actions of environmental compounds on reproductive disease and identification of epigenetic biomarkers of ancestral exposures. *PLoS One* 2012; **7**: e31901.
71. Skinner MK, Manikkam M, Guerrero-Bosagna C. Epigenetic transgenerational actions of environmental factors in disease etiology. *Trends Endocrinol Metab* 2010; **21**:214–22.
72. Hisano M, Erkek S, Dessus-Babus S, Ramos L, Stadler MB, Peters AH. Genome-wide chromatin analysis in mature mouse and human spermatozoa. *Nat Protoc* 2013; **8**:2449–70.
73. Martin M. Cutadapt removes adapter sequences from high-throughput sequencing reads. *EMBnet J* 2011; **17**:10–2.
74. Tang C, Xie Y, Yan W. AASRA: an anchor alignment-based small RNA annotation pipeline. bioRxiv. 2017: 132928. doi: https://doi.org/10.1101/132928.
75. Love MI, Huber W, Anders S. Moderated estimation of fold change and dispersion for RNA-seq data with DESeq2. *Genome Biol* 2014; **15**:550.
76. Bolger AM, Lohse M, Usadel B. Trimmomatic: a flexible trimmer for Illumina sequence data. *Bioinformatics* 2014; **30**: 2114–20.
77. Trapnell C, Roberts A, Goff L, Pertea G, Kim D, Kelley DR, Pimentel H, Salzberg SL, Rinn JL, Pachter L, et al. Differential gene and transcript expression analysis of RNA-seq experiments with TopHat and Cufflinks. *Nat Protoc* 2012; **7**:562–78.
78. Wang L, Park HJ, Dasari S, Wang S, Kocher JP, Li W. CPAT: Coding-Potential Assessment Tool using an alignment-free logistic regression model. *Nucleic Acids Res* 2013; **41**:e74.
79. Langmead B, Salzberg Sl. Fast gapped-read alignment with Bowtie 2. *Nat Methods* 2012; **9**:357–9.
80. Lienhard M, Grimm C, Morkel M, Herwig R, Chavez L. MEDIPS: genome-wide differential coverage analysis of sequencing data derived from DNA enrichment experiments. *Bioinformatics* 2014; **30**:284–6.
81. Robinson MD, McCarthy DJ, Smyth GK. edgeR: a Bioconductor package for differential expression analysis of digital gene expression data. *Bioinformatics* 2010; **26**:139–40.
82. Durinck S, Spellman PT, Birney E, Huber W. Mapping identifiers for the integration of genomic datasets with the R/Bioconductor package biomaRt. *Nat Protoc* 2009; **4**:1184–91.
83. Cunningham F, Amode MR, Barrell D, Beal K, Billis K, Brent S, Carvalho-Silva D, Clapham P, Coates G, Fitzgerald S, et al. Ensembl 2015. *Nucleic Acids Res* 2015; **43** (Database issue): D662–9.
84. Kanehisa M, Goto S. KEGG: kyoto encyclopedia of genes and genomes. *Nucleic Acids Res* 2000; **28**:27–30.
85. Kanehisa M, Goto S, Sato Y, Kawashima M, Furumichi M, Tanabe M. Data, information, knowledge and principle: back to metabolism in KEGG. *Nucl Acids Res* 2014; **42**:D199–205.
86. Huang da W, Sherman BT, Lempicki RA. Systematic and integrative analysis of large gene lists using DAVID bioinformatics resources. *Nat Protoc* 2009; **4**:44–57.
87. Mi H, Muruganujan A, Casagrande JT, Thomas PD. Large-scale gene function analysis with the PANTHER classification system. *Nat Protoc* 2013; **8**:1551–66.

Developmental Biology 445 (2019) 280–293

Contents lists available at ScienceDirect

Developmental Biology

journal homepage: www.elsevier.com/locate/developmentalbiology

Developmental origins of transgenerational sperm DNA methylation epimutations following ancestral DDT exposure

Millissia Ben Maamar[a], Eric Nilsson[a], Ingrid Sadler-Riggleman[a], Daniel Beck[a], John R. McCarrey[b], Michael K. Skinner[a,*]

[a] Center for Reproductive Biology, School of Biological Sciences, Washington State University, Pullman, WA 99164-4236, USA
[b] Department of Biology, University of Texas at San Antonio, San Antonio, TX 78249, USA

ARTICLE INFO

Keywords:
Epigenetic
Transgenerational
Primordial germ cells
Spermatogenesis
Sperm
Epimutation
DNA methylation
Testis

ABSTRACT

Epigenetic alterations in the germline can be triggered by a number of different environmental factors from diet to toxicants. These environmentally induced germline changes can promote the epigenetic transgenerational inheritance of disease and phenotypic variation. In previous studies, the pesticide DDT was shown to promote the transgenerational inheritance of sperm differential DNA methylation regions (DMRs), also called epimutations, which can in part mediate this epigenetic inheritance. In the current study, the developmental origins of the transgenerational DMRs during gametogenesis have been investigated. Male control and DDT lineage F3 generation rats were used to isolate embryonic day 16 (E16) prospermatogonia, postnatal day 10 (P10) spermatogonia, adult pachytene spermatocytes, round spermatids, caput epididymal spermatozoa, and caudal sperm. The DMRs between the control versus DDT lineage samples were determined at each developmental stage. The top 100 statistically significant DMRs at each stage were compared and the developmental origins of the caudal epididymal sperm DMRs were assessed. The chromosomal locations and genomic features of the different stage DMRs were analyzed. Although previous studies have demonstrated alterations in the DMRs of primordial germ cells (PGCs), the majority of the DMRs identified in the caudal sperm originated during the spermatogonia stages in the testis. Interestingly, a cascade of epigenetic alterations initiated in the PGCs is required to alter the epigenetic programming during spermatogenesis to obtain the sperm epigenetics involved in the epigenetic transgenerational inheritance phenomenon.

1. Introduction

Numerous environmental factors have been shown to promote the epigenetic transgenerational inheritance of disease such as the agricultural fungicide vinclozolin [1] and the pesticide DDT (dichlorodiphenyltrichloroethane) [2]. Caloric restriction, high fat diets, stress and a variety of different toxicants have also been linked to the transgenerational epigenetic inheritance phenomenon [3–5]. This non-genetic form of inheritance involves epigenetic modifications of the germline (sperm and egg) to pass an altered epigenome to the early embryo that can then impact the transcriptomes and epigenetics of all subsequently derived somatic cells [1,5]. Different epigenetic processes are involved in the transgenerational germline transmission where the environment can impact the health and evolution of species [3,4,6].

Epigenetics is defined as “molecular factors and processes around the DNA that regulate genome activity independent of DNA sequence and that are mitotically stable” [7]. Transgenerational epigenetic inheritance requires the germline transmission of epigenetic information. Different epigenetic processes have been shown to be involved in the transgenerational phenomenon such as DNA methylation [8–10], non-coding RNA [11,12], and histone modifications and retention [10,13,14]. Recently, concurrent alterations in all three of these processes have been observed in transgenerational sperm transmission after exposure to DDT and vinclozolin [15,16]. Most previous studies have been conducted in sperm due to the ability to isolate large numbers of cells and the inability to isolate large numbers of eggs, but experiments have shown that the female germline also has the capacity to transmit epigenetic inheritance [2,17]. The current study investigated the transgenerational sperm transmission of DNA methylation alterations after DDT exposure.

The primordial germ cells (PGCs), which give rise to spermatogenic (or oogenic) cells, develop and migrate down the genital ridge to colonize the indifferent gonad [18]. Upon sex determination and depending on the chromosomal sex, the PGCs differentiate into the

* Corresponding author.
E-mail address: skinner@wsu.edu (M.K. Skinner).

https://doi.org/10.1016/j.ydbio.2018.11.016
Received 5 September 2018; Received in revised form 1 November 2018; Accepted 26 November 2018
Available online 27 November 2018

male or female germline lineage [19]. In the rat gonad, the early developing testis germ cells will become prospermatogonia cells during the male gonadal sex determination period by embryonic day 16 (E16) [20,21]. By postnatal day 10 (P10) the germline develops into spermatogonia. Following the onset of puberty the initial wave of spermatogenesis begins in the testis where the spermatocytes, including the meiotic stage of pachytene spermatocytes, develop. After meiosis the round spermatid stage differentiates, then in the final spermatozoa stage the cells are released into the lumen of the seminiferous tubules [22], Fig. 1A. After entering the caput region of the epididymis the spermatozoa undergo further differentiation. During the transit in the epididymis the spermatozoa mature. When the spermatozoa reach the final caudal stage of the epididymis, the sperm have developed the capacity for motility and fertility [23,24]. Prior to ejaculation or degradation the mature caudal epididymal sperm will be stored in the vas deferens. In the current study we used several male germline developmental periods (E16 prospermatogonia, P10 spermatogonia, adult pachytene spermatocytes, round spermatids, caput epididymal spermatozoa, and caudal epididymal sperm), Fig. 1A, to investigate the developmental origins of the transgenerational sperm DMRs following DDT exposure in the F0 generation.

Epigenetic programming occurs during these male germline developmental periods. The migrating PGCs have an erasure of DNA methylation that then re-methylate during gonadal sex determination to create the male germline and prospermatogonia [25]. In the adult testis, during spermatogenesis some epigenetic programming events occur [26,27]. The first examples of this male germline epigenetic programming were observed with imprinted genes [28,29]. Imprinted genes can develop either early in the embryonic period or develop during spermatogenesis. Although previous studies have discussed the

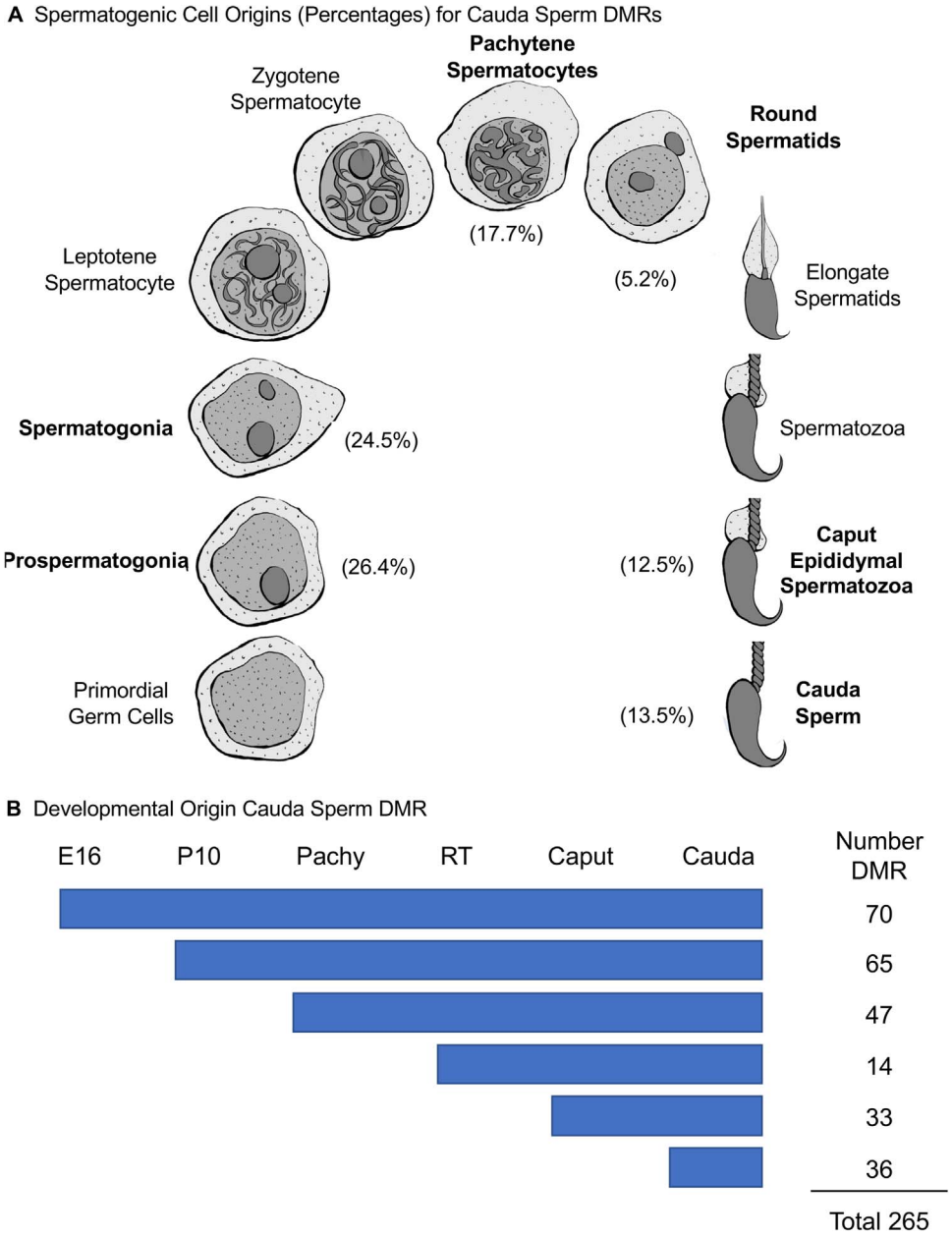

Fig. 1. Sperm DMR developmental origins. (A) Spermatogenic cell origin percentages for cauda sperm DMRs. The schematic of each developmental cell morphology listed during gametogenesis and spermatogenesis and epididymal maturation. The percentage DMR in brackets is presented for the developmental stages analyzed. (B) Developmental origins of cauda sperm DMRs for each stage of development with number DMRs at specific stages listed. The prospermatogonia (E16), spermatogonia (P10), pachytene spermatocytes (Pachy), round spermatids (RT), caput spermatozoa (Caput) and cauda sperm (Cauda) are presented.

germline developmental origins of epigenetic inheritance [5,30–34], none of these studies identified the developmental programming origins of the transgenerational epigenetic alterations observed in sperm.

The current study was designed to investigate the developmental origins of the DDT induced transgenerational sperm DMRs termed epimutations. The hypothesis tested is that a cascade of epigenetic changes occurs during development such that the majority of DMRs develop throughout gametogenesis and spermatogenic stages. It has been previously demonstrated that epigenetic alterations occur in the PGC [35]. However, due to this being the earliest stem cell stage of the germline, the PGCs DMRs were found to be different from the epimutations observed in sperm [35]. These observations suggest that the epimutations in sperm develop at later stages of epigenetic programming. The present study shows the majority of sperm DMRs originate during spermatogonia development and spermatogenesis, but some also do originate during epididymal maturation. This is one of the first genome-wide analyses of epigenetic programming during gametogenesis for transgenerational sperm epimutations [36].

2. Results

F3 generation control and DDT lineage male rats were used in this experimental design to isolate various germ cell stages for epigenetic analysis. The F0 generation gestating female rats at 90 days of age were transiently exposed to DDT or a vehicle control during gestational days 8–14. This stage of fetal development corresponds to when the PGCs migrate to colonize the indifferent gonad through the early stage of gonadal sex determination as previously described [18,25,35]. The F1 generation offspring were obtained and when they reached 90 days of age they were bred within the control and DDT lineages to generate the F2 generation (grand offspring) which were then bred at 90 days of age to obtain the transgenerational F3 generation for each control and DDT lineage. No cousin or sibling breedings were used to avoid any inbreeding artifacts. Only the F0 generation gestating females were exposed to DDT, which also directly exposed the F1 generation fetus and the germline within the F1 generation fetus that will generate the F2 generation. Therefore, the F3 generation is the first transgenerational generation not directly exposed [37] and was used to study the developmental origins of the transgenerational sperm epimutations. The F3 generation control and DDT lineage male rats were aged to the embryonic day 16 (E16) fetal stage for prospermatogonia cell isolation, to postnatal day 10 (P10) for spermatogonial cell isolation, and to 120 days of age for pachytene spermatocyte isolation, round spermatid isolation, caput spermatozoa isolation, and cauda epididymal sperm isolation. A gravity sedimentation StaPut protocol, as described in the Methods [38,39], was used to isolate the prospermatogonia, spermatogonia, pachytene spermatocytes and round spermatids cells. Three different pools each with different individual sets of animals from different litters were obtained with 5–6 males per pool for the E16 stage, 6–7 males per pool for the P10 stage, 3 adult males per pool for the adult stages. Therefore, 3–7 different males were used in the analysis within each of the three different pools analyzed for both the control and DDT lineages. Genomic DNA was isolated from each purified germ cell stage pool and from individual animals for epididymal caput spermatozoa and cauda sperm [8,13] and then three pools generated for subsequent epigenetic analysis.

The analysis of differential DNA methylation regions (DMRs) was performed with a methylated DNA immunoprecipitation (MeDIP) procedure followed by next generation sequencing for an MeDIP-Seq protocol described in the Methods [8]. The F3 generation control versus DDT lineage pools were compared to identify the DMRs at each developmental stage of the male germline. The DMRs at various p-value thresholds are presented at each developmental stage in Fig. 2. An EdgeR p-value of $p < 1e-05$ was selected at all stages for further analysis of the DMRs. This correlated with an FDR (false discovery rate) value of < 0.1 for all except the E16 prospermatogonia which was more variable. The All Windows is all DMRs with at least one 100 bp region (window) with statistical significance and the Multiple Windows being ≥2 significant 100 bp windows. The number of DMRs with multiple windows is also presented in Fig. 2. Most developmental stages showed approximately 100–300 DMRs. The epigenetic alterations were higher at the pachytene spermatocyte and round spermatid stages which showed more than 300 DMRs. The chromosomal locations of the DMRs at each developmental stage are presented in Fig. 3. The red arrowheads indicate the location of a DMR with the black boxes indicating clusters of DMRs. In most stages, all the chromosomes, except the Y and mitochondrial DNA (MT), were found to contain DMRs. The genomic features of the DMRs at each stage of development were investigated. The CpG density of the DMRs at all stages was 1–5 CpG per 100 bp with 1 CpG per 100 bp being predominant, Fig. 4. This is characteristic of a low density CpG desert [40] which has been observed with previous transgenerational DMRs. The length of the DMRs at all the developmental stages were between 1 and 4 kb with 1 kb length being predominant, Fig. 5. Therefore, the DMRs are generally 1 kb in size with around 10 CpGs as previously observed [40]. The overlap between the various developmental stage DMRs was investigated and is presented in Fig. 6A. The DMRs were found to be primarily stage specific with a very low number of DMRs overlapping between the stages with a $p < 1e-05$. The cauda sperm and the caput spermatozoa had the highest level of overlap with 88 DMRs, Fig. 6B and S7 Table, comprising over 45% of the caput epididymal spermatozoa DMRs. These observations suggest a cascade of epigenetic programming occurs throughout male germline development.

The DNA methylation alterations of the DMRs at each stage of development were investigated. For the developmental time-course the top 100 statistically significant DMRs at each stage of development were examined regarding the scaled mean read depth between the control versus DDT lineage DMR data. The scaled mean read depths at each DMR was separated into control greater than DDT data (i.e. decrease in DNA methylation) and DDT greater than control data (i.e. increase in DNA methylation) which is presented as a scaled mean read depth, Figs. 7 and 8. The E16 prospermatogonia DMRs had 28 DMR with a decrease in methylation and 72 DMR with an increase in methylation, Figs. 7A & 8A. For both data sets the DMR methylation alterations generally dropped by the P10 spermatogonia stage and became mixed with no distinct patterns in later stages. Although a few of both populations stayed elevated, the majority had an alteration in DNA methylation at later stages of development. The P10 spermatogonia DMRs had 38 DMRs with a decrease in methylation and 62 with an increase in methylation in regard to % mean read depth, Figs. 7B & 8B. A dramatic change in methylation between the prospermatogonia to spermatogonia stage and from the spermatogonia to later stages of development were observed. Therefore, the E16 prospermatogonia and P10 spermatogonia stage DMRs are for the most part unique at these stages of development. The pachytene spermatocyte DMRs had predominantly a decrease in methylation with 63 DMRs and 37 DMRs with an increase, Figs. 7C & 8C. Therefore, DNA methylation was primarily decreased in the pachytene spermatocyte DMRs. The round spermatid DMRs had a higher number of 72 DMR with an increase and 28 DMR with a decrease, Figs. 7D & 8D. The caput epididymal spermatozoa DMRs had 46 DMR with a decrease and 54 DMR with an increase in methylation, Figs. 7E & 8E. The cauda epididymal sperm DMRs had 49 DMR with a decrease and 51 DMR with an increase, Figs. 7F & 8F. The caput spermatozoa and cauda epididymal sperm have relatively consistent DNA methylation characteristics for both data sets. Therefore, the cauda sperm show more consistent DNA methylation profiles during spermatogenesis and epididymal sperm maturation, but are distinct in the spermatogonial stem cell stages.

Genes associated with the DMRs were identified and compared at each of the developmental stages. The DMRs that had a gene within 10 kb distance, so the promoter is considered, were identified and the

A Prospermatogonia (E16)

P-value	All Window	Multiple Window
0.001	4011	265
1e-04	522	25
1e-05	**94**	**11**
1e-06	27	5
1e-07	12	4

Number Windows	1	2	3	4	5
Number of DMR	83	7	2	1	1

B Spermatogonia (P10)

P-value	All Window	Multiple Window
0.001	4728	464
1e-04	722	107
1e-05	**195**	**47**
1e-06	86	32
1e-07	48	19

Number Windows	1	2	3	4	5	20
Number of DMR	148	35	4	5	2	1

C Pachytene Spermatocytes

P-value	All Window	Multiple Window
0.001	11776	891
1e-04	1917	78
1e-05	**340**	**13**
1e-06	71	5
1e-07	20	2

Number Windows	1	2	3
Number of DMR	327	9	4

D Round Spermatids

P-value	All Window	Multiple Window
0.001	11006	1276
1e-04	1816	131
1e-05	**323**	**17**
1e-06	60	0
1e-07	7	0

Number Windows	1	2
Number of DMR	306	17

E Caput Epididymal Spermatozoa

P-value	All Window	Multiple Window
0.001	6644	616
1e-04	1146	148
1e-05	**284**	**72**
1e-06	117	52
1e-07	74	38

Number Windows	1	2	3	4	≥5
Number of DMR	212	39	13	5	15

F Cauda Sperm

P-value	All Window	Multiple Window
0.001	4611	478
1e-04	809	143
1e-05	**265**	**82**
1e-06	140	55
1e-07	87	40

Number Windows	1	2	3	4	≥5
Number of DMR	183	39	20	10	13

Fig. 2. DMR identification and numbers. The number of DMRs found using different p-value cutoff thresholds. The All Window column shows all DMRs. The Multiple Window column shows the number of DMRs containing at least two significant windows (100 bp each). The number of DMRs with the number of significant windows (100 bp per window) at a p-value threshold of 1e-05 is presented. (A) E16 prospermatogoina. (B) P10 spermatogonia. (C) Pachytene spermatocytes. (D) Round Spermatids. (E) Caput Spermatozoa. (F) Cauda Sperm.

associated genes and gene functional categories determined, S1–S6 Tables. The DMRs with a p < 1e-05 were used in this analysis at all the developmental stages. The number of genes associated with specific gene functional categories is presented in Fig. 9A. Each of the developmental stages are presented to compare the major gene categories. The signaling, metabolism, transcription and receptor gene categories were the major categories present in the different developmental stages. Additional categories were cytoskeleton, development, transport and immune system, that were present in all the developmental stages, Fig. 9A. The DMR associated genes at each developmental stage were also used in a gene pathway analysis applying the KEGG pathway association as described in the Methods. The number of DMR associated genes involved with the major pathways is presented in Fig. 9B. The most predominant pathways present in at least two different developmental stages are shown. The E16 prospermatogonia, round spermatids, caput spermatozoa and cauda sperm had DMR associated genes in the metabolic pathways. The E16 prospermatogonia, P10 spermatogonia, pachytene spermatocytes had DMR associated genes in the pathways in cancer in common. Therefore, the only pathways that were present in nearly all the stages are metabolism and pathways in cancer. The caput epididymal spermatozoa and cauda sperm were more consistent than the others which were more distinct.

The final aspect of the study involved an investigation of the developmental origins of the cauda sperm DMRs, meaning when the differential DNA methylation alterations appeared within the developmental stages examined. In the cauda sperm there are 265 DMRs at p < 1e-05. For the analysis of developmental origins the 265 DMRs were examined individually with a reduced statistical stringency of p < 0.05 to see the first stage the DMR appears or originates. Fig. 1B demonstrates 70 DMRs were developed in the E16 prospermatogonia stage, 65 DMRs in the P10 spermatogonia stage, 47 DMRs in the spermatocyte stage, 14 DMRs in the round spermatid stage, 33 DMRs in the caput epididymal spermatozoa stage, and 36 DMRs in the cauda sperm stage, S8 Table. The cauda sperm had a total of 265 DMRs at p < 1e-05 with the majority of DMRs originating in the prospermatogonia and spermatogonia. Fewer were observed in the round spermatids and caput epididymal spermatozoa stages, Fig. 1B. The percentage of the total DMR origins and schematic of the different

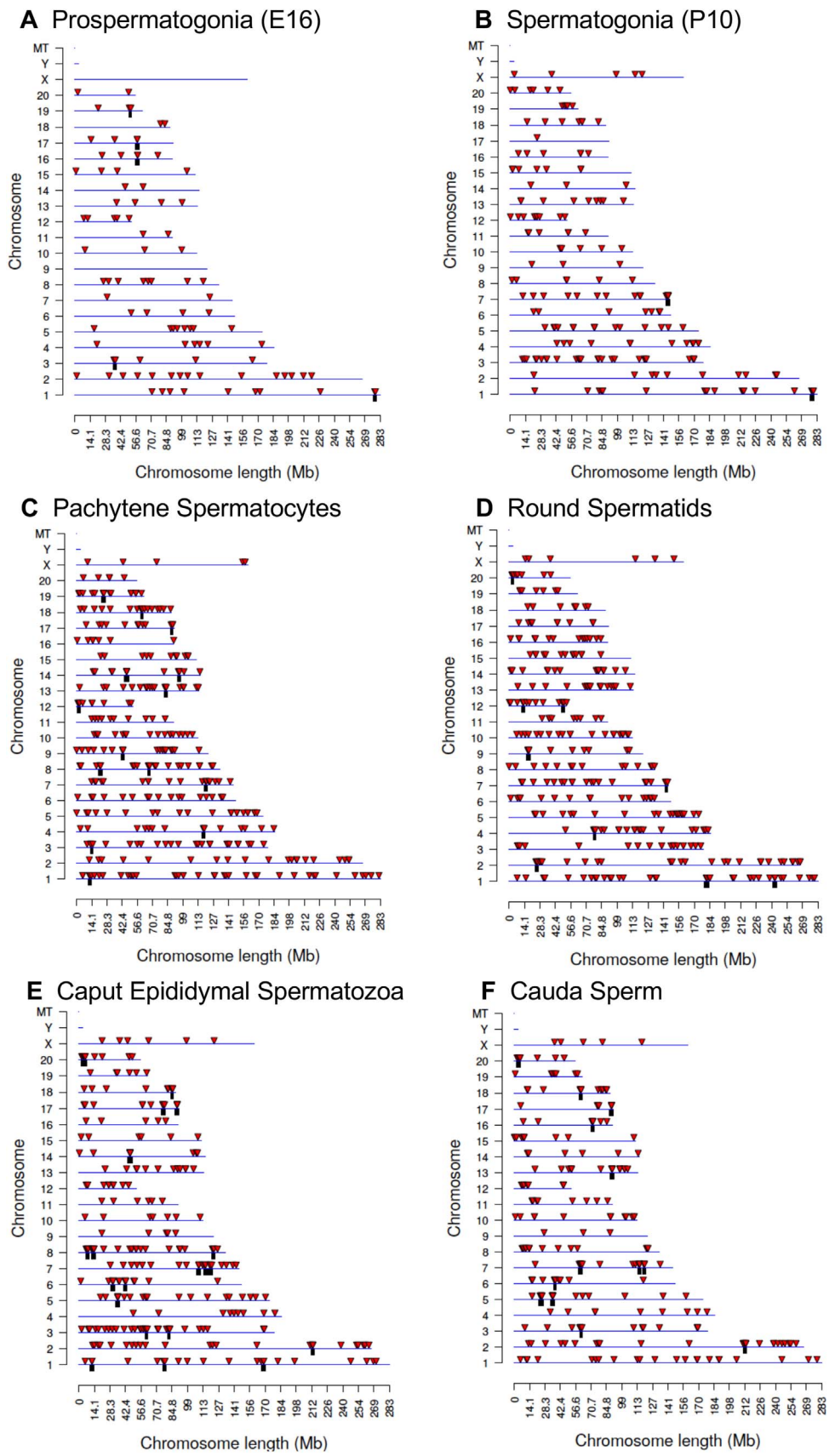

Fig. 3. DMR chromosomal locations. The DMR locations on the individual chromosomes is represented with an arrowhead and a cluster of DMRs with a black box. All DMRs containing at least one significant window at a p-value threshold of 1e-05 are shown. (A) E16 prospermatogoina. (B) P10 spermatogonia. (C) Pachytene spermatocytes. (D) Round Spermatids. (E) Caput Spermatozoa. (F) Cauda Sperm.

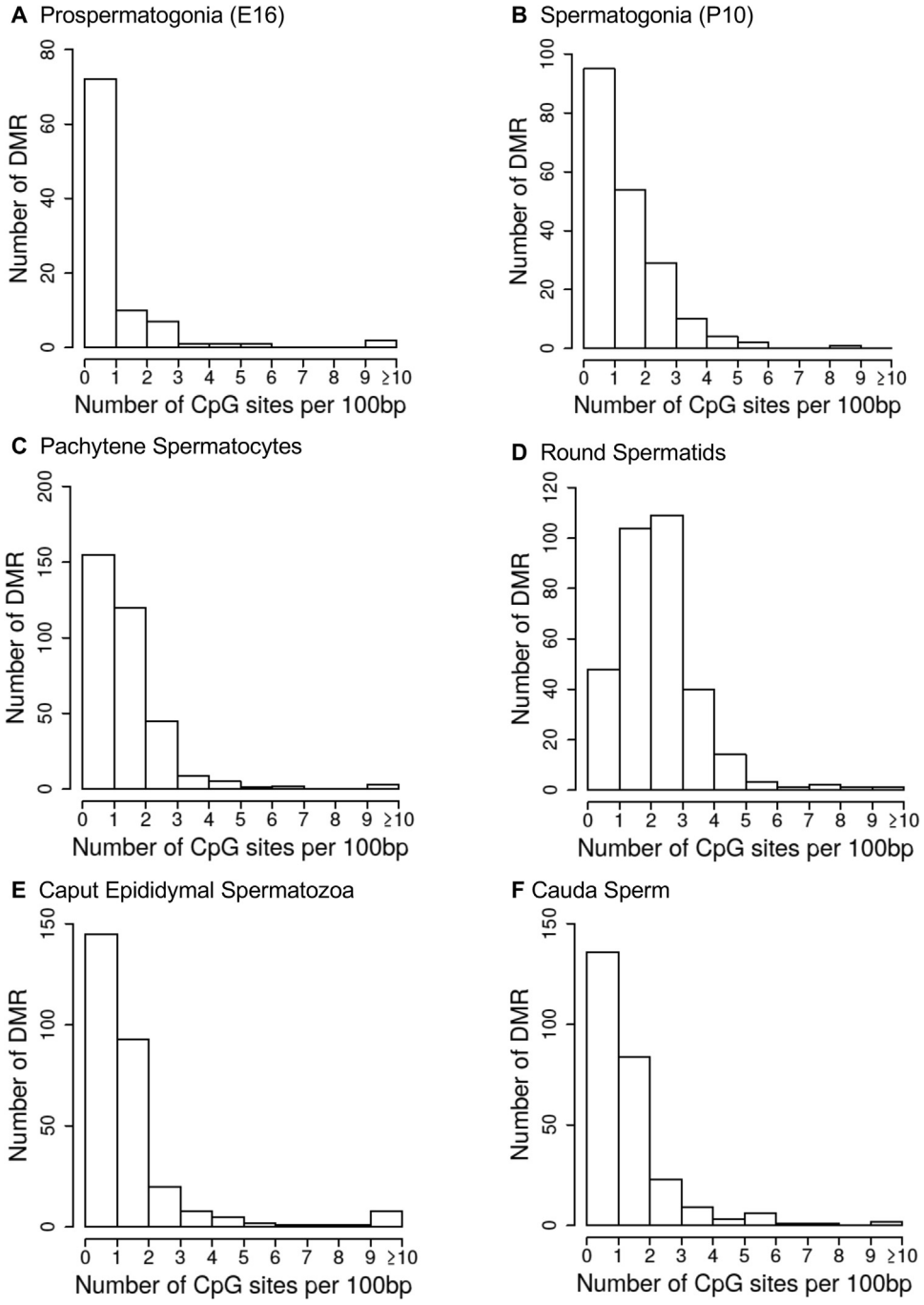

Fig. 4. DMR genomic features. The number of DMRs at different CpG densities. All DMRs at a p-value threshold of 1e-05 are shown. (A) E16 prospermatogoina. (B) P10 spermatogonia. (C) Pachytene spermatocytes. (D) Round Spermatids. (E) Caput Spermatozoa. (F) Cauda Sperm.

stage cells during development is presented in Fig. 1A. Therefore, the majority of the transgenerational sperm DMRs were developed during the prospermatogonia and spermatogonia stages with a small number developed in the epididymal maturation stages. This correlated to a cascade of epigenetic and transcriptome changes during these stages of male germline development to generate the transgenerational sperm epimutations, Fig. 1A.

3. Discussion

The aim of the current study was to identify the developmental origins of the cauda sperm transgenerational DMRs that transmit the epigenetic transgenerational inheritance of disease and phenotypic variation. During embryonic day 8–14 in the rat, when the primordial germ cells (PGCs) migrate to colonize the indifferent fetal gonad, the F0 generation gestating female exposure to DDT was performed [18,25,35]. Five different stages of male germ cell development were investigated: E16 prospermatogonia, P10 spermatogonia, and adult pachytene spermatocytes, round spermatids, caput epididymal spermatozoa and cauda sperm, Fig. 1A. The functional considerations of these cell populations involve the prospermatogonia precursor stem cell population, spermatogonia stem cell population in the testis, the meiotic pachytene spermatocyte cell population, the post-meiotic spermatid population and the spermatozoa present in the caput epididymis, and mature sperm in the cauda epididymis. The caput spermatozoa and cauda epididymal sperm were directly isolated as described in the Methods then sonicated and washed to remove any contaminating somatic cells, so are pure sperm cell preparations. For

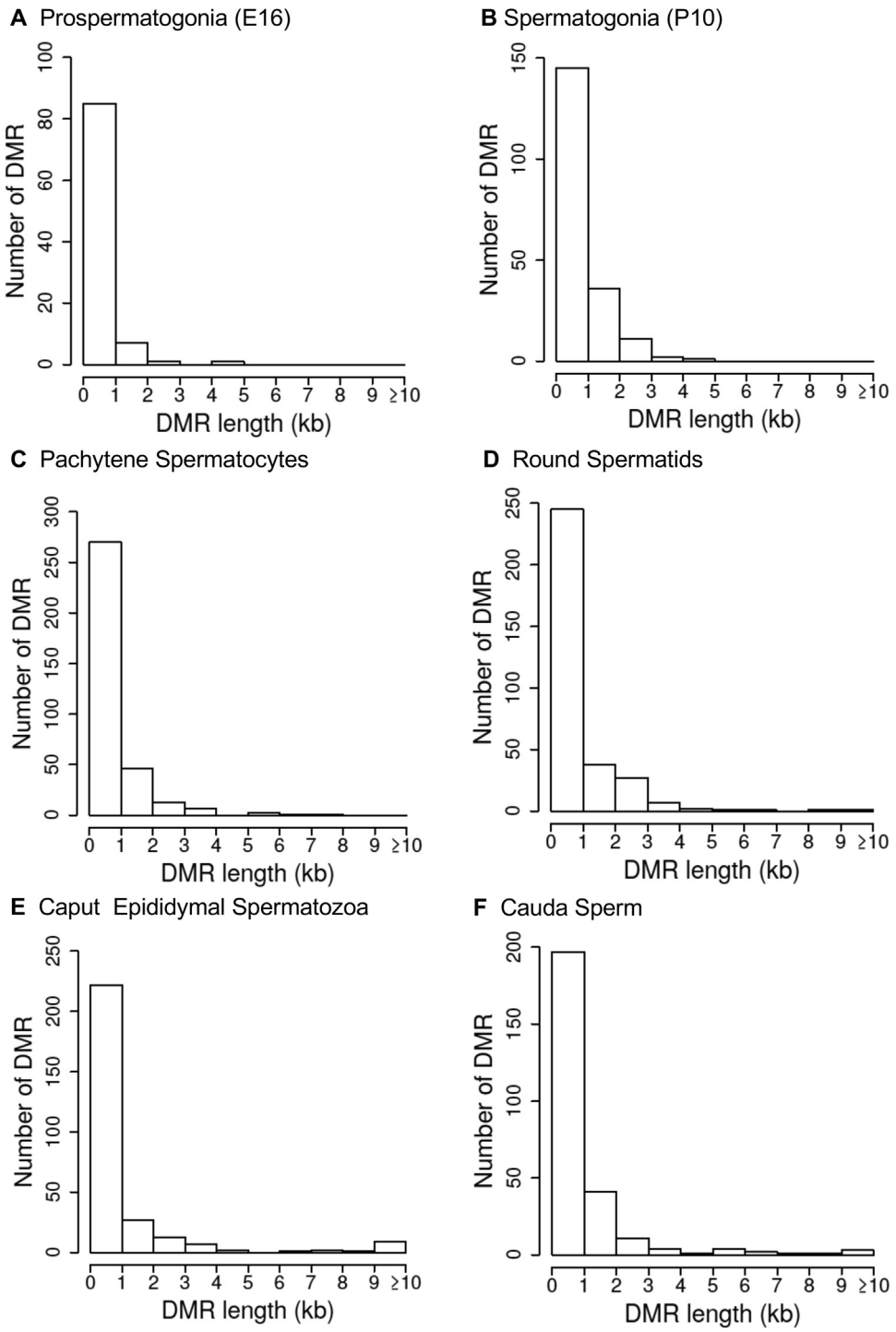

Fig. 5. DMR lengths. All DMRs at a p-value threshold of 1e-05 are shown. (A) E16 prospermatogoina. (B) P10 spermatogonia. (C) Pachytene spermatocytes. (D) Round Spermatids. (E) Caput Spermatozoa. (F) Cauda Sperm.

the other cell populations a gravity sedimentation on a StaPut apparatus procedure was used to isolate the specific cell populations as previously described [39,40]. The E16 prospermatogonia and P10 spermatogonia were found to have a greater than 85% purity. The pachytene spermatocytes were greater than 95% spermatocytes with two-thirds of these cells pachytene spermatocytes and one-third other spermatocyte stages. This is due to the longer developmental life span or developmental period of pachynema compared to the other stages of first meiotic prophase [41] and to the efficiency of the StaPut gradient protocol. For the isolated round spermatids 95% of them were spermatids with 90% of them being round spermatids and 10% being elongate spermatids and other spermatogenic cell stages [42]. Despite obtaining a high purity for these developmental stage male germline cell populations, cell purity needs to be considered in the data interpretations. The embryonic day 16 (E16) prospermatogonia were isolated from the fetal gonad, the postnatal day 10 (P10) from the early pubertal age, the pachytene spermatocytes, round spermatids, caput epididymal spermatozoa and cauda sperm were all isolated from postnatal day 120 (P120) age adult male rats. DDT has been previously shown to induce transgenerational inheritance of disease between 6 and 12 months of age [5]. Therefore, by choosing the postnatal day 120 or earlier with negligible disease present, no disease artifacts are

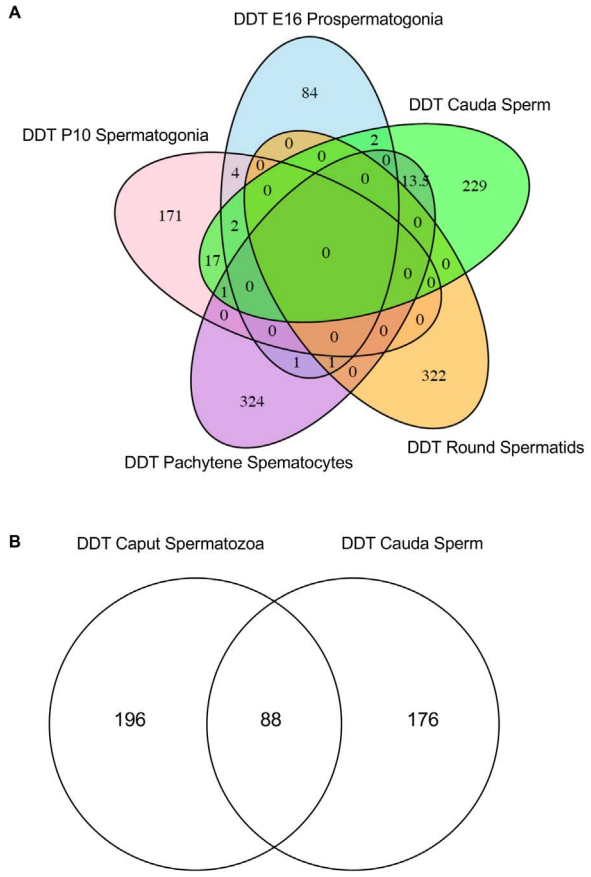

Fig. 6. Developmental stage DMR overlaps. (A) Different developmental stage DMRs overlap. (B) Epididymal caput spermatozoa and caudal sperm DMR overlap.

anticipated in the current study. This is consistent with the primary objective of the study to investigate the developmental origins of the sperm DMR, but future studies can now consider disease correlations.

The transgenerational F3 generation control and DDT lineage germline samples were compared at each of the developmental stages. The F1 and F2 generations have somatic cell and germline epigenetic alterations due to the F1 generation fetal direct exposure and F1 generation fetal germline direct exposure that will generate the F2 generation. Therefore, the F3 generation is the first transgenerational generation not having any direct exposures, so was the focus of the current study [37]. A comparison of the F1 generation direct exposure sperm DMR development with the transgenerational F3 generation observations will be an interesting future study to consider. All F3 generation developmental samples had differential DNA methylation regions (DMRs). Excluding the caput spermatozoa and cauda epididymal sperm with common DMRs, all the other stage DMRs were found to be primarily distinct from each other, Fig. 6. The majority of the epigenome was not altered (i.e. potentially millions of CpG regions) and the current study focused on the transgenerational alterations at each stage of development. The distinct DMRs at each stage indicate a cascade of epigenetic changes occur to program the sperm transgenerational epigenome.

A comparison of the different developmental stage germline populations was conducted in regard to DNA methylation alterations for the top 100 most statistically significant DMRs at each developmental stage separately. Analysis of these DNA methylation alterations for the different developmental stage DMRs revealed that the E16 prospermatogonia and P10 spermatogonia presented distinct patterns of DNA methylation compared to the other stages, Figs. 7 and 8. The statistically significant top 100 DMRs at both these developmental stages altered greatly with adjacent stages and often lost their statistical significance. In contrast, the pachytene spermatocytes, round spermatids, caput epididymal spermatozoa and caudal sperm were more consistent between each other regarding the DMRs maintaining similar DNA methylation alterations and statistical significance, Figs. 7 and 8. This suggests that the developing stem cells and spermatogonia have principally unique DNA methylation profiles associated with the cascade of epigenetic programming of the cells. When the spermatogonia initiate the spermatogenesis process there is a cascade of epigenetic programming and DNA methylation observed between the spermatogenic cell populations, as well as between spermatozoa undergoing epididymal maturation. Observations suggest a dynamic epigenetic programming of the male germline in the testis and epididymis. Epididymal maturation has been shown to promote structural and molecular alterations in the developing sperm, which also appear to be involved in the transgenerational sperm DMR programming [32].

Significant epigenetic reprogramming in the primordial germ cells (PGCs) has already been described. DNA methylation erasure during migration and colonization of the fetal gonad has been shown to occur [18]. This process enables the germline stem cell population to facilitate the generation of the male or female germ lines following gonadal sex determination [18,25]. A stable epigenetic cascade of events occurs to produce the spermatogonial stem cell population in the adult testis. Studies have shown that environmental toxicants have the ability to promote epigenetic DNA methylation alterations in the PGCs and prospermatogonia [35]. These transgenerational DMRs observed in the PGCs were found to be distinct from the caudal epididymal sperm DMRs [35]. The current study supports this observation and determines that sperm DMRs not only originate in the fetal period, but trigger a cascade of epigenetic alterations that eventually impact the mature sperm epigenome, Fig. 1B. Therefore, the developmental cascade of epigenetic programming initiated by fetal exposure induces a number of DMRs that are also maintained throughout development.

In the cauda sperm, the origins of the DMRs were identified. The majority of them originate throughout the development of prospermatogonia, spermatogonia and spermatocytes, Fig. 1B and S9 Table. A smaller number of DMRs also arose in the round spermatids and cauda epididymal sperm. The highest number of DMRs was observed in the prospermatogonia, the stage of development during which the initial F0 generation gestating female and F1 generation developing fetus were exposed. The DMRs in the cauda sperm originated in all the earlier developmental spermatogenic stages and through epididymal maturation. These observations correlated with the DNA methylation alteration data for DMRs between the different developmental stages shown in Figs. 7 and 8. Thus, the primary origin of the transgenerational sperm DMR epimutations/DMRs does not occur during early PGC development or in the embryonic stem cell population, but throughout development and spermatogenesis in the testis, as well as during epididymal maturation. Although the induction of a cascade of epigenetic programming in the PCGs is critical as previously suggested [7,35], there is a continual cascade of epigenetic alterations throughout spermatogenesis to give rise to the transgenerational sperm DMRs, Fig. 1A. Another recent study investigating vinclozolin induced sperm DMR origins found similar observations, but the highest level of DMRs were developed at the pachytene spermatocyte stage [36]. Therefore, an exposure specificity may exist in the developmental epigenetics observed.

The DMRs associated genes were identified for DMRs at $p < 1e\text{-}05$ at each stage of development. The analysis of associated gene functional categories identified signaling, transcription, metabolism and receptor as the major categories at all stages of development. The pathway analysis also identified a number of stage specific pathways with negligible overlap except in metabolism and pathways in cancer. Gene pathways more specific to testis development such as meiosis or the pyruvate pathway did not contain more than a few DMR associated

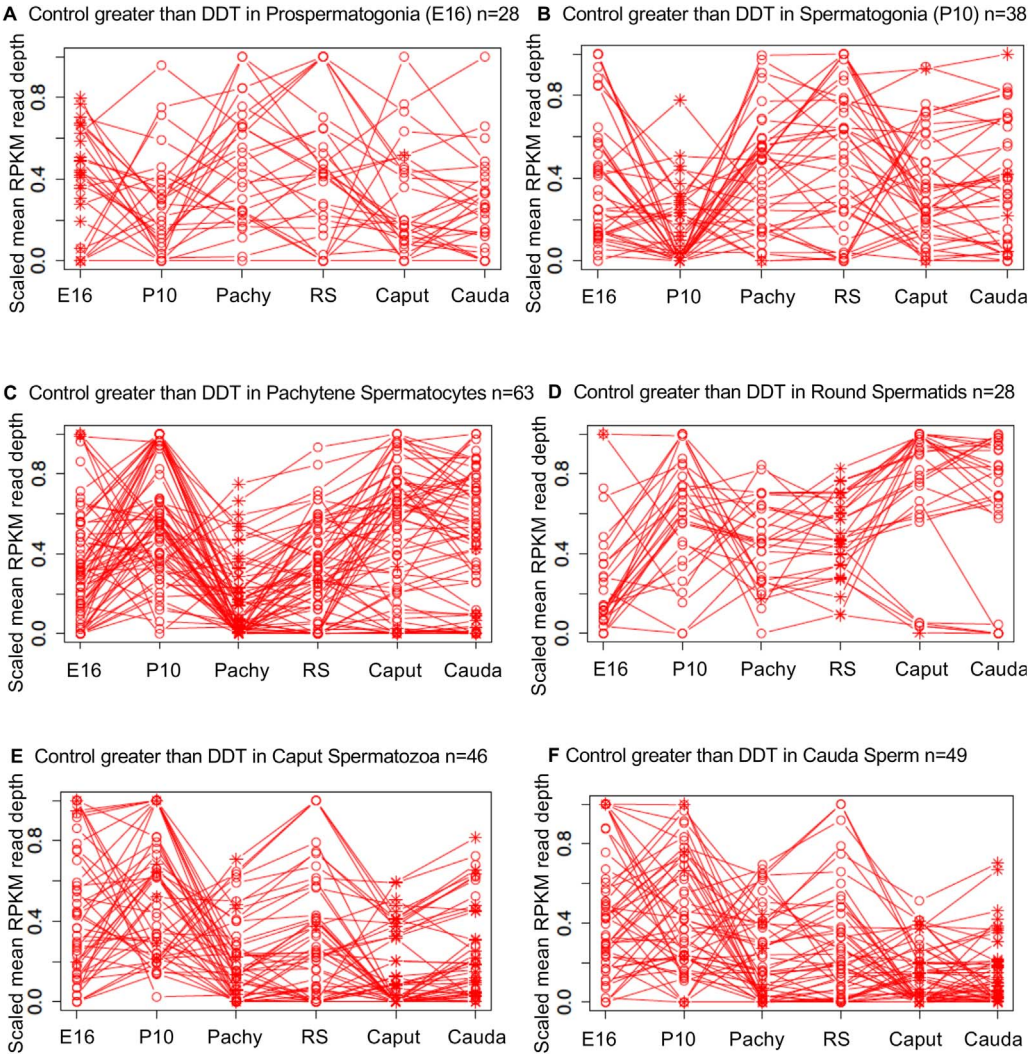

Fig. 7. Timeline DMR development. Top 100 statistically significant DMR developmental alterations for control greater than DDT in read depths (decrease in DNA methylation). Genomic windows with an edgeR p-value < 10^{-5} are indicated by astrisks and windows separated showing only those with an RPKM read depth elevated in the control. (A) E16 prospermatogoina. (B) P10 spermatogonia. (C) Pachytene spermatocytes. (D) Round spermatids. (E) Caput spermatozoa. (F) Cauda sperm.

genes. Therefore, for all the stages of development for the DMR-associated genes involved similar gene categories, but different pathways. Future studies are needed to correlate the DMRs with data identified from transcriptome and altered non-coding RNA expression to provide a better understanding as to how the DMRs may regulate genome activity.

The caput epididymal spermatozoa displayed unique DMRs and others that were in common with the cauda sperm. Interestingly, the cauda epididymal sperm did acquire DMRs that were not present in earlier stages of development. Even though the majority of the cauda epididymal sperm DMRs were obtained during prior developmental stages, 36 DMRs were acquired at the cauda epididymal sperm stage of maturation only, S7 and S8 Tables. Two studies have previously suggested that epididymal maturation (epididymosomes) may be involved with transgenerational sperm maturation regarding epigenetic alterations, but no direct data have been provided [43–45]. The current study supports a role for epididymal maturation altering sperm DMRs. However, the majority of DMRs originated during earlier developmental stages and spermatogenesis in the testis and not the epididymis, Fig. 1B. A combination of early development, spermatogenesis and epididymal mutation appears to be involved in the development of the transgenerational sperm epimutations. Further investigation is needed to elucidate the molecular mechanisms in the epididymis that alter sperm epigenetics.

4. Conclusions

The current study was designed to investigate the developmental origins of transgenerational sperm DMRs induced by the pesticide DDT. Results show that each stage of male germ cell development examined, including the E16 prospermatogonia, P10 spermatogonia, pachytene spermatocytes, round spermatids, caput epididymal spermatozoa and cauda sperm, has distinct and unique DMRs when the DDT lineage and control lineage F3 generation samples are compared. Both the prospermatogonia and spermatogonia display unique DNA methylation alterations in comparison with later stages that are more consistent. The origins of the cauda sperm DMRs developed throughout the earlier developmental stages with the highest number during prospermatogonia, spermatogonia and pachytene spermatocytes, and fewer originating during epididymal maturation. In conclusion, a developmental cascade of epigenetic programming occurs from the PGCs to the sperm with epimutations developing throughout the different stages of development, Fig. 1A. The initial speculation that the DMRs may develop in the PGCs is not the case, even though the developmental cascade initiated is important. Recently, sperm carrying transgenerational epimutations were found to have alterations in DNA methylation, ncRNAs and histone retention, such that all epigenetic factors are involved in the epigenetic transgenerational inheritance phenomenon [15,16]. Future studies will now need to investigate these

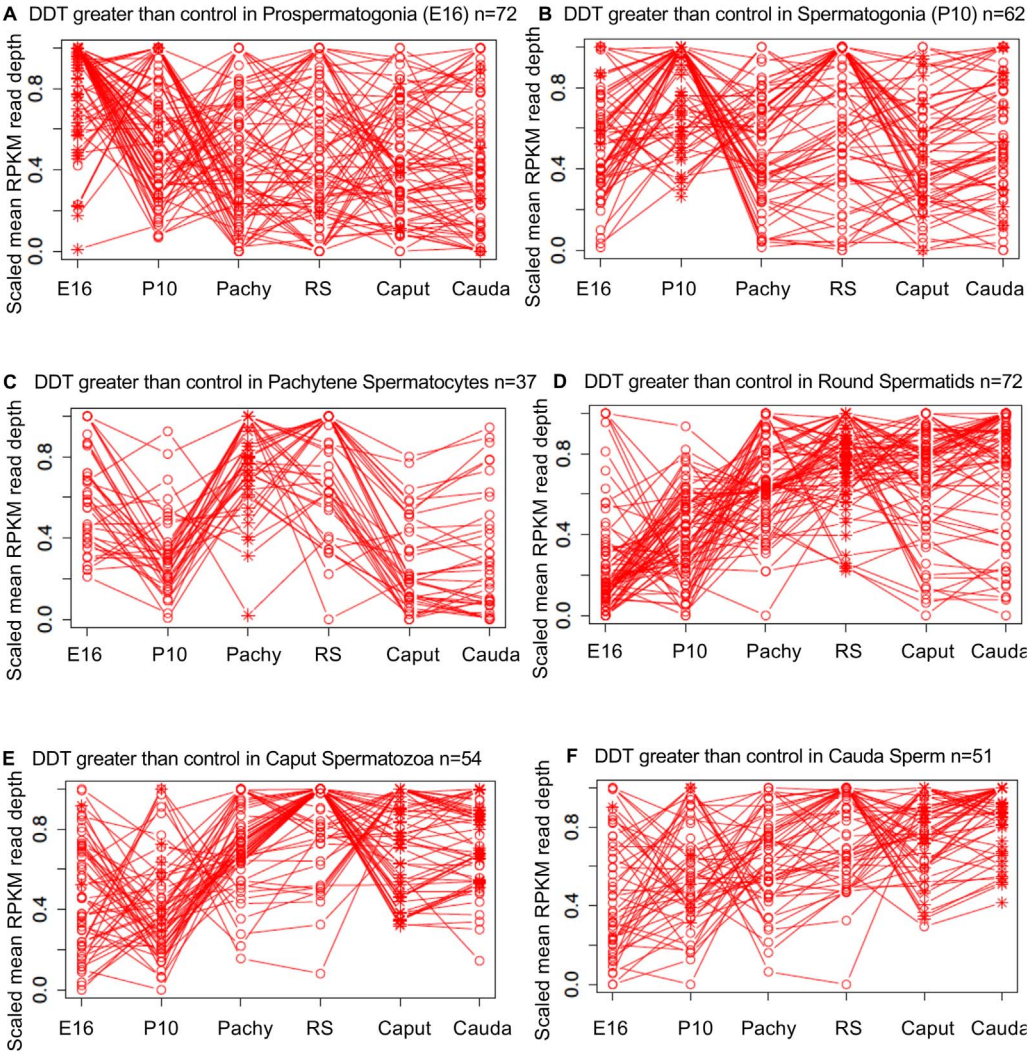

Fig. 8. Timeline DMR development. Top 100 statistically significant DMR developmental alterations for DDT greater than control in read depths (increase in DNA methylation). Genomic windows with an edgeR p-value < 10^{-5} are indicated by astrisks and windows separated showing only those with an RPKM read depth elevated in the DDT over control. (A) E16 prospermatogoina. (B) P10 spermatogonia. (C) Pachytene spermatocytes. (D) Round spermatids. (E) Caput spermatozoa. (F) Cauda sperm.

other epigenetic processes and correlated gene expression to develop a more systems biology assessment of the molecular mechanism involved.

5. Methods

5.1. Animal studies and breeding

Female and male rats of an outbred strain Hsd: Sprague Dawley®™SD®™ obtained from Harlan/Envigo (Indianapolis, IN) at about 70–100 days of age were maintained in ventilated (up to 50 air exchanges/hour) isolator cages (cages with dimensions of 10 ¾″ W×19 ¼″ D×10 ¾″ H, 143 square inch floor space, fitted in Micro-vent 36-cage rat racks; Allentown Inc., Allentown, NJ) containing Aspen Sani chips (pinewood shavings from Harlan) as bedding, and a 14 h light: 10 h dark regimen, at a temperature of 70 F and humidity of 25–35%. The mean light intensity in the animal rooms ranged from 22 to 26 ft-candles. Rats were fed ad lib with standard rat diet (8640 Teklad 22/5 Rodent Diet; Harlan) and ad lib tap water for drinking. To obtain time-pregnant females, the female rats in proestrus were pair-mated with male rats. The sperm-positive (i.e. sperm plug present) (day 0) rats were monitored for diestrus and body weight. On days 8 through 14 of gestation [46], the females received daily intraperitoneal injections of DDT (25 mg/kg body weight/day) or dimethyl sulfoxide (DMSO). The DDT (dichlorodiphenyltrichloroethane) was obtained from Chem Service Inc. (West Chester, PA) and reported to have a purity of 98.2%. DDT were dissolved and injected in DMSO vehicle as previously described [47]. Treatment lineages are designated 'control' or 'DDT' lineages. The treated gestating female rats were designated as the F0 generation. The offspring of the F0 generation rats were the F1 generation. Non-littermate females and males aged 70–90 days from the F1 generation of control or DDT lineages were bred to obtain F2 generation offspring. The F2 generation rats were bred to obtain F3 generation offspring. The F1–F3 generation offspring were not themselves treated directly with DDT. The control and DDT lineages were housed in the same room and racks with lighting, food and water as previously described [47–49]. All experimental protocols for the procedures with rats were pre-approved by the Washington State University Animal Care and Use Committee (IACUC approval # 6252).

5.2. Epididymal sperm collection and DNA isolation

Testis and epididymis were collected from 12 month old rats for germ cell collection. The epididymis was dissected free of connective tissue and divided into caput and cauda halves with a cut in the mid-corpus. A small cut made to the cauda and to the caput and each half was placed in 3 ml of PBS for up to 2 h at 4 °C. Caput and cauda epididymal tissue were each coarsely minced and the liquid with the

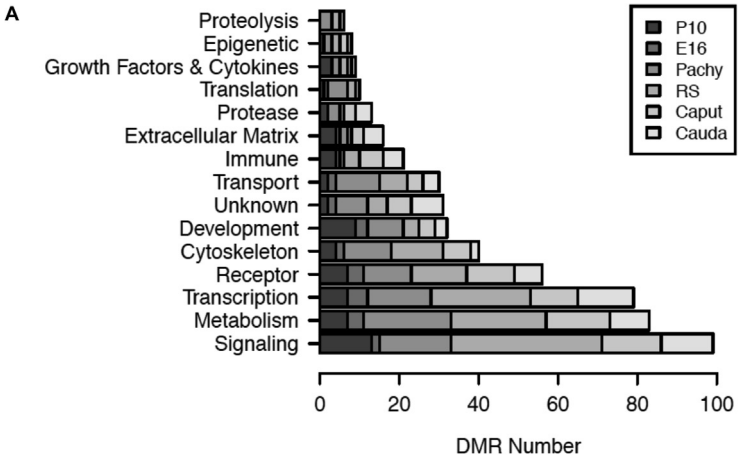

B DMR Gene Association Pathways

DDT Prospermatogonia E16
rno05160 Hepatitis C (2)
rno04913 Ovarian steroidogenesis (2)
rno04217 Necroptosis (2)
rno04976 Bile secretion (2)
rno01100 Metabolic pathways (2)

DDT Spermatogonia (P10)
rno05200 Pathways in cancer (6)
rno05224 Breast cancer (4)
rno05226 Gastric cancer (4)
rno04928 Parathyroid hormone synthesis, secretion and action (3)
rno04380 Osteoclast differentiation (3)

DDT Pachytene Spermatocytes
rno01100 Metabolic pathways (10)
rno04014 Ras signaling pathway (6)
rno05206 MicroRNAs in cancer (6)
rno05200 Pathways in cancer (6)
rno05165 Human papillomavirus infection (6)

DDT Round Spermatids
no01100 Metabolic pathways (11)
rno05200 Pathways in cancer (8)
rno04010 MAPK signaling pathway (7)
rno04360 Axon guidance (6)
rno04151 PI3K-Akt signaling pathway (6)
rno04144 Endocytosis (6)

DDT Caput Spermatozoa
rno05168 Herpes simplex infection (9)
rno04514 Cell adhesion molecules (CAMs) (9)
rno04612 Antigen processing and presentation (8)
rno05165 Human papillomavirus infection (8)
rno01100 Metabolic pathways (7)

DDT Cauda Sperm
rno01100 Metabolic pathways (5)
rno04514 Cell adhesion molecules (CAMs) (4)
rno04650 Natural killer cell mediated cytotoxicity (4)
rno04145 Phagosome (4)
rno04510 Focal adhesion (4)

Fig. 9. Sperm DMR associated gene categories and pathways. (A) DMR associated gene functional categories for each stage (color insert) versus DMR number. (B) DMR associated gene pathways for each stage of development with number of DMR associated genes in pathway in brackets. Bolded pathways show overlap in at least three developmental stages.

released sperm collected. For each sample the released sperm was centrifuged at 6000×*g*, then the supernatant removed, and the pellet resuspended in NIM buffer, to be stored at −80 °C until further use. One hundred µl of sperm suspension was sonicated to destroy somatic cells and tissue, spun down at 6000×*g*, the sperm pellet washed with 1x PBS once, and then combined with 820 µl DNA extraction buffer and 80 µl 0.1 M DTT. The sample was incubated at 65 °C for 15 min. Following this incubation 80 µl proteinase K (20 mg/ml) was added and the sample incubated at 55 °C for at least 2 h under constant rotation. Then 300 µl of protein precipitation solution (Promega, A7953) was added, the sample mixed thoroughly and incubated for 15 min on ice. The sample was centrifuged at 12,500×*g* for 30 min at 4 °C. One ml of the supernatant was transferred to a 2 ml tube and 2 µl of glycoblue and 1 ml of cold 100% isopropanol were added. The sample was mixed well by inverting the tube several times then left in −20 °C freezer for at least one hour. After precipitation the sample was centrifuged at 12,500×*g* for 20 min at 4 °C. The supernatant was taken off and discarded without disturbing the (blue) pellet. The pellet was washed with 70% cold ethanol by adding 500 µl of 70% ethanol to the pellet and returning the tube to the freezer for 20 min. After the incubation the tube was centrifuged for 10 min at 4 °C at 12,500×*g* and the supernatant discarded. The tube was spun again briefly to collect residual ethanol to bottom of tube and then as much liquid as possible was removed with gel loading tip. Pellet was air-dried at RT until it looked dry (about 5 min). Pellet was then resuspended in 100 µl of nuclease free water.

5.3. Developing germ cell stage isolation and DNA preparation

Harlan Sprague-Dawley rats (Harlan Inc., Indianapolis IN) were used for all experiments. The rats were kept in a temperature controlled environment and given food and water ad libitum. Estrous cycles of female rats were monitored by cellular morphology from vaginal smears. Rats in early estrus were paired with males overnight and mating confirmed by sperm-positive smears, denoted day 0 of pregnancy. Pregnant rats were euthanized at embryonic day 16 (E16) of gestation, and fetal gonads were collected for germ cell preparations. Sex was determined on the basis of gonadal morphology. Germ cells were isolated exclusively from males.

Purified populations of male PGCs type T1 prospermatogonia (at E16) were prepared using a mini StaPut gradient method as previously described [50,51]. Briefly, fetal testes were pooled and dissociated by incubation in 0.25% trypsin-EDTA (Sigma) with vigorous pipetting using a 1000 microliter pipette tip, and the resulting cell solution was filtered through 100 µm nylon mesh to yield a single cell suspension. This cell suspension was then loaded onto a 50 ml 2–4% bovine serum albumen (BSA) gradient prepared in KREBS buffer, and the cells were allowed to sediment at unit gravity at 4 °C for two hours as described [50,51]. The gradient was then fractionated and aliquots of the fractions were examined under phase optics to identify those enriched for the appropriate cell types on the basis of morphological characteristics. The enriched fractions were pooled to yield the final sample which was ≥85% pure for the desired male germ cell type in each case.

Three pools of prospermatogonia were prepared for each treatment group, with each pool derived from testes of 5–6 rats from different litters.

A similar mini StaPut gradient method [50,51] was used to isolate spermatogonia from testes of 10-day old rats, with the addition of incubation of the testes in 0.5 mg/ml collagenase (Sigma C1639) at 33 °C for 20 min with agitation to dissociate the seminiferous tubules. Three pools of spermatogonia from 10-day old rats were prepared for each treatment group, with each pool derived from testes of 6–7 rats from different litters.

To isolate pachytene spermatocytes and round spermatids, testes were collected from 12 month old rats suspended in F-12 culture medium (Gibco-Life Technologies, USA. Ref 11765-054) and shipped overnight on ice to Dr. John McCarrey. A StaPut gradient method was used to isolate the developing germ cell stages as previously described [50,51]. Three pools of cells of each cell type were prepared for each treatment group, with each pool derived from testes of three rats from different litters. DNA was isolated from prospermatogonia, spermatogonia, pachytene spermatocytes and round spermatids using the same procedure as was used for sperm, with the omission of sonication and DTT treatments.

5.4. Methylated DNA immunoprecipitation MeDIP

Methylated DNA Immunoprecipitation (MeDIP) with genomic DNA was performed as follows: rat DNA pools were generated using the appropriate amount of genomic DNA from each individual for 3 pools each of control and DDT lineage animals. Genomic DNA pools were sonicated using the Covaris M220 the following way: the pooled genomic DNA was diluted to 130 µl with TE buffer into the appropriate Covaris tube. Covaris was set to 300 bp program and the program was run for each tube in the experiment. 10 µl of each sonicated DNA was run on 1.5% agarose gel to verify fragment size. The sonicated DNA was transferred from the Covaris tube to a 1.7 ml microfuge tube and the volume measured. The sonicated DNA was then diluted with TE buffer (10 mM Tris HCl, pH7.5; 1 mM EDTA) to 400 µl, heat-denatured for 10 min at 95 °C, then immediately cooled on ice for 10 min. Then 100 µl of 5X IP buffer and 5 µg of antibody (monoclonal mouse anti 5-methyl cytidine; Diagenode #C15200006) were added to the denatured sonicated DNA. The DNA-antibody mixture was incubated overnight on a rotator at 4 °C.

The following day magnetic beads (Dynabeads M-280 Sheep anti-Mouse IgG; 11201D) were pre-washed as follows: The beads were resuspended in the vial, then the appropriate volume (50 µl per sample) was transferred to a microfuge tube. The same volume of Washing Buffer (at least 1 ml PBS with 0.1% BSA and 2 mM EDTA) was added and the bead sample was resuspended. Tube was then placed into a magnetic rack for 1–2 min and the supernatant discarded. The tube was removed from the magnetic rack and the beads washed once. The washed beads were resuspended in the same volume of IP buffer (50 mM sodium phosphate ph7.0, 700 mM NaCl, 0.25% TritonX-100) as the initial volume of beads. 50 µl of beads were added to the 500 µl of DNA-antibody mixture from the overnight incubation, then incubated for 2 h on a rotator at 4 °C.

After the incubation the bead-antibody-DNA complex was washed three times with IP buffer as follows: The tube was placed into magnetic rack for 1–2 min and the supernatant discarded, then washed with IP buffer 3 times. The washed bead-DNA solution is then resuspended in 250 µl digestion buffer with 3.5 µl Proteinase K (20 mg/ml). The sample was then incubated for 2–3 h on a rotator at 55 °C and then 250 µl of buffered Phenol-Chloroform-Isoamylalcohol solution was added to the supe and the tube vortexed for 30 s then centrifuged at 12,500×*g* for 5 min at room temperature. The aqueous supernatant was carefully removed and transferred to a fresh microfuge tube. Then 250 µl chloroform were added to the supernatant from the previous step, vortexed for 30 s and centrifuged at 12,500×*g* for 5 min at room temperature. The aqueous supernatant was removed and transferred to a fresh microfuge tube. To the supernatant 2 µl of glycoblue (20 mg/ml), 20 µl of 5 M NaCl and 500 µl ethanol were added and mixed well, then precipitated in −20 °C freezer for 1 h to overnight.

The precipitate was centrifuged at 12,500×*g* for 20 min at 4 °C and the supernatant removed, while not disturbing the pellet. The pellet was washed with 500 µl cold 70% ethanol in −20 °C freezer for 15 min then centrifuged again at 12,500×*g* for 5 min at 4 °C and the supernatant discarded. The tube was spun again briefly to collect residual ethanol to bottom of tube and as much liquid as possible was removed with gel loading tip. Pellet was air-dried at RT until it looked dry (about 5 min) then resuspended in 20 µl H2O or TE. DNA concentration was measured in Qubit (Life Technologies) with ssDNA kit (Molecular Probes Q10212).

5.5. MeDIP-Seq analysis

The MeDIP pools were used to create libraries for next generation sequencing (NGS) using the NEBNext® Ultra™ RNA Library Prep Kit for Illumina® (NEB, San Diego, CA) starting at step 1.4 of the manufacturer's protocol to generate double stranded DNA. After this step the manufacturer's protocol was followed. Each pool received a separate index primer. NGS was performed at WSU Spokane Genomics Core using the Illumina HiSeq. 2500 with a PE50 application, with a read size of approximately 50 bp and approximately 30 million reads per pool. Five to six libraries were run in one lane.

5.6. Statistics and bioinformatics

For the DMR analyses, the basic read quality was verified using summaries produced by the FastQC program http://www.bioinformatics.babraham.ac.uk/projects/fastqc/. The raw reads were trimmed and filtered using Trimmomatic. The reads for each MeDIP sample were mapped to the Rnor 6.0 rat genome using Bowtie2 [52] with default parameter options. The mapped read files were then converted to sorted BAM files using SAMtools [53]. To identify DMRs, the reference genome was broken into 100 bp windows. Genomic windows with no CpG or ambiguous base within 1000 bp were identified in the reference genome and used as control genes to perform RUVg normalization [54]. The MEDIPS [55] and edgeR [56] R packages were used to calculate differential coverage between control and exposure sample groups. The edgeR p-value was used to determine the relative difference between the two groups for each genomic window. Windows with an edgeR p-value less than 10–5 were considered DMRs. The FDR adjusted p-values were also calculated. The DMR edges were extended until no genomic window with an edgeR p-value < 0.1 remained within 1000 bp of the DMR. CpG density and other information was then calculated for the DMR based on the reference genome. DMRs were annotated using the biomaRt R package [57] to access the Ensembl database [58]. The genes that fell within 10kbp of the DMR edges were then input into the KEGG pathway search [59,60] to identify associated pathways. The associated genes were then sorted into functional groups by consulting information provided by the DAVID [61], Panther [62], and Uniprot databases incorporated into an internal curated database (www.skinner.wsu.edu under genomic data). All molecular data has been deposited into the public database at NCBI (GEO # GSE121585).

Acknowledgments

We acknowledge Ms. Margaux McBirney, Ms. Deepika Kubsad and Mr. Ryan Thompson for technical assistance and Ms. Heather Johnson for assistance in preparation of the manuscript. We thank Ms. Stephanie E. King for generating the germ cell schematics in Fig. 9. We thank the Genomics Core laboratory at WSU Spokane. This study was supported by a John Templeton Foundation, USA (50183)

(https://templeton.org/) grant to MKS and NIH, USA (ES012974) (https://www.nih.gov/) grant to MKS. The funders had no role in study design, data collection and analysis, decision to publish, or preparation of the manuscript

Declaration of interests

The authors declare no competing interests.

CRediT authorship contribution statement

Millissia Ben Maamar: Writing - original draft, Writing - review & editing, Formal analysis, Investigation, **Eric Nilsson:** Writing - review & editing, Formal analysis, Investigation, **Ingrid Sadler-Riggleman:** Writing - review & editing, Formal analysis, Investigation, Validation, **Daniel Beck:** Writing - review & editing, Data curation, Investigation, Validation, **John R. McCarrey:** Writing - review & editing, Investigation, Supervision, **Michael K. Skinner:** Writing - original draft, Writing - review & editing, Conceptualization, Funding acquisition, Investigation, Project administration, Supervision

Appendix A. Supporting information

Supplementary data associated with this article can be found in the online version at doi:10.1016/j.ydbio.2018.11.016.

References

Anway, M.D., Cupp, A.S., Uzumcu, M., Skinner, M.K., 2005]. Epigenetic transgenerational actions of endocrine disruptors and male fertility. Science 308 (5727), 1466–1469.

Skinner, M.K., Manikkam, M., Tracey, R., Guerrero-Bosagna, C., Haque, M.M., Nilsson, E., 2013]. Ancestral dichlorodiphenyltrichloroethane (DDT) exposure promotes epigenetic transgenerational inheritance of obesity. BMC Med. 11 (1–16), 228.

Soubry, A., 2015]. Epigenetic inheritance and evolution: a paternal perspective on dietary influences. Prog. Biophys. Mol. Biol. 118 (1–2), 79–85.

Vaiserman, A.M., Koliada, A.K., Jirtle, R.L., 2017]. Non-genomic transmission of longevity between generations: potential mechanisms and evidence across species. Epigenetics Chromatin 10 (1), 38.

Nilsson, E., Sadler-Riggleman, I., Skinner, M.K., 2018]. Environmentally induced epigenetic transgenerational inheritance of disease. Environ. Epigenetics 4 (2), 1–13, (dvy016).

Skinner, M.K., 2015]. Environmental epigenetics and a unified theory of the molecular aspects of evolution: a Neo-Lamarckian concept that facilitates Neo-Darwinian evolution. Genome Biol. Evol. 7 (5), 1296–1302.

Skinner, M.K., 2011]. Environmental epigenetic transgenerational inheritance and somatic epigenetic mitotic stability. Epigenetics 6 (7), 838–842.

Beck, D., Sadler-Riggleman, I., Skinner, M.K., 2017]. Generational comparisons (F1 versus F3) of vinclozolin induced epigenetic transgenerational inheritance of sperm differential DNA methylation regions (epimutations) using MeDIP-seq. Environ. Epigenetics 3 (3), 1–12, (dvx016).

Quadrana, L., Colot, V., 2016]. Plant transgenerational epigenetics. Annu. Rev. Genet. 50, 467–491.

Sharma, U., Rando, O.J., 2017]. Metabolic inputs into the epigenome. Cell Metab. 25 (3), 544–558.

Gapp, K., Jawaid, A., Sarkies, P., Bohacek, J., Pelczar, P., Prados, J., Farinelli, L., Miska, E., Mansuy, I.M., 2014]. Implication of sperm RNAs in transgenerational inheritance of the effects of early trauma in mice. Nat. Neurosci. 17 (5), 667–669.

Yan, W., 2014]. Potential roles of noncoding RNAs in environmental epigenetic transgenerational inheritance. Mol. Cell Endocrinol. 398 (1–2), 24–30.

Ben Maamar, M., Sadler-Riggleman, I., Beck, D., Skinner, M.K., 2018]. Epigenetic transgenerational inheritance of altered sperm histone retention sites. Sci. Rep. 8, 5308, (1-10).

Furuhashi, H., Kelly, W.G., 2010]. The epigenetics of germ-line immortality: lessons from an elegant model system. Dev. Growth Differ. 52 (6), 527–532.

Skinner, M.K., Ben Maamar, M., Sadler-Riggleman, I., Beck, D., Nilsson, E., McBirney, M., Klukovich, R., Xie, Y., Tang, C., Yan, W., 2018]. Alterations in sperm DNA methylation, non-coding RNA and histone retention associate with DDT-induced epigenetic transgenerational inheritance of disease. Epigenetics Chromatin 11 (1), 1–24, (8).

Ben Maamar, M., Sadler-Riggleman, I., Beck, D., McBirney, M., Nilsson, E., Klukovich, R., Xie, Y., Tang, C., Yan, W., Skinner, M.K., 2018]. Alterations in sperm DNA methylation, non-coding RNA expression, and histone retention mediate Vinclozolin induced epigenetic transgenerational inheritance of disease. Environ. Epigenetics 4 (2), 1–19, (dvy010).

Manikkam, M., Haque, M.M., Guerrero-Bosagna, C., Nilsson, E., Skinner, M.K., 2014]. Pesticide methoxychlor promotes the epigenetic transgenerational inheritance of adult onset disease through the female germline. PLoS One 9 (7), 1–19, (e102091).

Seisenberger, S., Andrews, S., Krueger, F., Arand, J., Walter, J., Santos, F., Popp, C., Thienpont, B., Dean, W., Reik, W., 2012]. The dynamics of genome-wide DNA methylation reprogramming in mouse primordial germ cells. Mol. Cell 48 (6), 849–862.

Jost, A., Vigier, B., Prepin, J., Perchellet, J.P., 1973]. Studies on sex differentiation in mammals. Recent Prog. Horm. Res. 29, 1–41.

McCarrey, J.R., 2013]. Toward a more precise and informative nomenclature describing fetal and neonatal male germ cells in rodents. Biol. Reprod. 89 (2), 47.

McCarrey, J.R., 2012]. The epigenome as a target for heritable environmental disruptions of cellular function. Mol. Cell Endocrinol. 354 (1–2), 9–15.

Dym, M., Fawcett, D.W., 1971]. Further observations on the numbers of spermatogonia, spermatocytes, and spermatids connected by intercellular bridges in the mammalian testis. Biol. Reprod. 4 (2), 195–215.

Orgebin-Crist, M.C., Danzo, B.J., Cooper, T.G., 1976]. Re-examination of the dependence of epididymal sperm viability on the epididymal environment. J. Reprod. Fertil. Suppl. 24 suppl, 115–128.

Cornwall, G.A., 2009]. New insights into epididymal biology and function. Hum. Reprod. Update 15 (2), 213–227.

Tang, W.W., Kobayashi, T., Irie, N., Dietmann, S., Surani, M.A., 2016]. Specification and epigenetic programming of the human germ line. Nat. Rev. Genet. 17 (10), 585–600.

Ku, H.Y., Gangaraju, V.K., Qi, H., Liu, N., Lin, H., 2016]. Tudor-SN interacts with Piwi antagonistically in regulating spermatogenesis but synergistically in silencing transposons in drosophila. PLoS Genet. 12 (1), e1005813.

La Salle, S., Oakes, C.C., Neaga, O.R., Bourc'his, D., Bestor, T.H., Trasler, J.M., 2007]. Loss of spermatogonia and wide-spread DNA methylation defects in newborn male mice deficient in DNMT3L. BMC Dev. Biol. 7, 104.

Mann, J.R., 2001]. Imprinting in the germ line. Stem Cells 19 (4), 287–294.

Barlow, D.P., Bartolomei, M.S., 2014]. Genomic imprinting in mammals. Cold Spring Harb. Perspect. Biol. 6 (2), 1–21.

Hanson, M.A., Skinner, M.K., 2016]. Developmental origins of epigenetic transgenerational inheritance. Environ. Epigenetics 2 (1), 1–9, (dvw002).

Soubry, A., Hoyo, C., Jirtle, R.L., Murphy, S.K., 2014]. A paternal environmental legacy: evidence for epigenetic inheritance through the male germ line. Bioessays 36 (4), 359–371.

Boskovic, A., Rando, O.J., 2018]. Transgenerational epigenetic inheritance. Annu. Rev. Genet. 52, (p. Epub ahead of print).

Soubry, A., Hoyo, C., Butt, C.M., Fieuws, S., Price, T.M., Murphy, S.K., Stapleton, H.M., 2017]. Human exposure to flame-retardants is associated with aberrant DNA methylation at imprinted genes in sperm. Environ. Epigenetics 3 (1), dvx003.

del Mazo, J., Prantera, G., Torres, M., Ferraro, M., 1994]. DNA methylation changes during mouse spermatogenesis. Chromosome Res. 2 (2), 147–152.

Skinner, M., Guerrero-Bosagna, C., Haque, M.M., Nilsson, E., Bhandari, R., McCarrey, J., 2013]. Environmentally induced transgenerational epigenetic reprogramming of primordial germ cells and subsequent germline. PLoS One 8 (7), 1–15, (e66318).

Skinner, M.K., Nilsson, E., Sadler-Riggleman, I., Beck, D., McCarrey, J.R., 2018]. Developmental origins of transgenerational sperm DNA methylation epimutations Following ancestral vinclozolin exposure. Pending.

Skinner, M.K., 2008]. What is an epigenetic transgenerational phenotype? F3 or F2. Reprod. Toxicol. 25 (1), 2–6.

Ariel, M., McCarrey, J., Cedar, H., 1991]. Methylation patterns of testis-specific genes. Proc. Natl. Acad. Sci. USA 88 (6), 2317–2321.

Hermann, B.P., Mutoji, K.N., Velte, E.K., Ko, D., Oatley, J.M., Geyer, C.B., McCarrey, J.R., 2015]. Transcriptional and translational heterogeneity among neonatal mouse spermatogonia. Biol. Reprod. 92 (2), 54.

Skinner, M.K., Guerrero-Bosagna, C., 2014]. Role of CpG deserts in the epigenetic transgenerational inheritance of differential DNA methylation regions. BMC Genom. 15 (1), 692.

Ventela, S., Ohta, H., Parvinen, M., Nishimune, Y., 2002]. Development of the stages of the cycle in mouse seminiferous epithelium after transplantation of green fluorescent protein-labeled spermatogonial stem cells. Biol. Reprod. 66 (5), 1422–1429.

Suresh, R., Aravindan, G.R., Moudgal, N.R., 1992]. Quantitation of spermatogenesis by DNA flow cytometry: comparative study among six species of mammals. J. Biosci. 17 (4), 413–419.

Sharma, U., Conine, C.C., Shea, J.M., Boskovic, A., Derr, A.G., Bing, X.Y., Belleannee, C., Kucukural, A., Serra, R.W., Sun, F., Song, L., Carone, B.R., Ricci, E.P., Li, X.Z., Fauquier, L., Moore, M.J., Sullivan, R., Mello, C.C., Garber, M., Rando, O.J., 2016]. Biogenesis and function of tRNA fragments during sperm maturation and fertilization in mammals. Science 351 (6271), 391–396.

Rompala, G.R., Mounier, A., Wolfe, C.M., Lin, Q., Lefterov, I., Homanics, G.E., 2018]. Heavy chronic intermittent ethanol exposure alters small noncoding RNAs in mouse sperm and epididymosomes. Front. Genet. 9, 32.

Ariel, M., Cedar, H., McCarrey, J., 1994]. Developmental changes in methylation of spermatogenesis-specific genes include reprogramming in the epididymis. Nat. Genet. 7 (1), 59–63.

Nilsson, E.E., Anway, M.D., Stanfield, J., Skinner, M.K., 2008]. Transgenerational epigenetic effects of the endocrine disruptor vinclozolin on pregnancies and female adult onset disease. Reproduction 135 (5), 713–721.

Manikkam, M., Guerrero-Bosagna, C., Tracey, R., Haque, M.M., Skinner, M.K., 2012]. Transgenerational actions of environmental compounds on reproductive disease and identification of epigenetic biomarkers of ancestral exposures. PLoS One 7 (2), 1–12, (e31901).

Skinner, M.K., Manikkam, M., Guerrero-Bosagna, C., 2010]. Epigenetic transgenerational actions of environmental factors in disease etiology. Trends Endocrinol. Metab. 21 (4), 214–222.

Anway, M.D., Leathers, C., Skinner, M.K., 2006]. Endocrine disruptor vinclozolin

induced epigenetic transgenerational adult-onset disease. Endocrinology 147 (12), 5515–5523.
McCarrey, J.R., Berg, W.M., Paragioudakis, S.J., Zhang, P.L., Dilworth, D.D., Arnold, B.L., Rossi, J.J., 1992]. Differential transcription of Pgk genes during spermatogenesis in the mouse. Dev. Biol. 154 (1), 160–168.
Kafri, T., Ariel, M., Brandeis, M., Shemer, R., Urven, L., McCarrey, J., Cedar, H., Razin, A., 1992]. Developmental pattern of gene-specific DNA methylation in the mouse embryo and germ line. Genes Dev. 6 (5), 705–714.
Bolger, A.M., Lohse, M., Usadel, B., 2014]. Trimmomatic: a flexible trimmer for Illumina sequence data. Bioinformatics 30 (15), 2114–2120.
Langmead, B., Salzberg, S.L., 2012]. Fast gapped-read alignment with Bowtie 2. Nat. Methods 9 (4), 357–359.
Risso, D., Ngai, J., Speed, T.P., Dudoit, S., 2014]. Normalization of RNA-seq data using factor analysis of control genes or samples. Nat. Biotechnol. 32 (9), 896–902.
Lienhard, M., Grimm, C., Morkel, M., Herwig, R., Chavez, L., 2014]. MEDIPS: genome-wide differential coverage analysis of sequencing data derived from DNA enrichment experiments. Bioinformatics 30 (2), 284–286.
Robinson, M.D., McCarthy, D.J., Smyth, G.K., 2010]. edgeR: a Bioconductor package for differential expression analysis of digital gene expression data. Bioinformatics 26 (1), 139–140.
Durinck, S., Spellman, P.T., Birney, E., Huber, W., 2009]. Mapping identifiers for the integration of genomic datasets with the R/Bioconductor package biomaRt. Nat. Protoc. 4 (8), 1184–1191.
Cunningham, F., Amode, M.R., Barrell, D., Beal, K., Billis, K., Brent, S., Carvalho-Silva, D., Clapham, P., Coates, G., Fitzgerald, S., Gil, L., Giron, C.G., Gordon, L., Hourlier, T., Hunt, S.E., Janacek, S.H., Johnson, N., Juettemann, T., Kahari, A.K., Keenan, S., Martin, F.J., Maurel, T., McLaren, W., Murphy, D.N., Nag, R., Overduin, B., Parker, A., Patricio, M., Perry, E., Pignatelli, M., Riat, H.S., Sheppard, D., Taylor, K., Thormann, A., Vullo, A., Wilder, S.P., Zadissa, A., Aken, B.L., Birney, E., Harrow, J., Kinsella, R., Muffato, M., Ruffier, M., Searle, S.M., Spudich, G., Trevanion, S.J., Yates, A., Zerbino, D.R., Flicek, P., 2015]. Ensembl 2015. Nucleic Acids Res. 43, D662–D669.
Kanehisa, M., Goto, S., 2000]. KEGG: kyoto encyclopedia of genes and genomes. Nucleic Acids Res. 28 (1), 27–30.
Kanehisa, M., Goto, S., Sato, Y., Kawashima, M., Furumichi, M., Tanabe, M., 2014]. Data, information, knowledge and principle: back to metabolism in KEGG. Nucleic Acids Res. 42, D199–D205.
Huang da, W., Sherman, B.T., Lempicki, R.A., 2009]. Systematic and integrative analysis of large gene lists using DAVID bioinformatics resources. Nat. Protoc. 4 (1), 44–57.
Mi, H., Muruganujan, A., Casagrande, J.T., Thomas, P.D., 2013]. Large-scale gene function analysis with the PANTHER classification system. Nat. Protoc. 8 (8), 1551–1566.